1-1-2014

Effects of Mix Design Using Chloride-Based Accelerator on Concrete Pavement Cracking Potential

Daniel Aaron Buidens
University of South Florida, dbuidens@mail.usf.edu

Effects of Mix Design Using Chloride-Based Accelerator on Concrete Pavement Cracking Potential

by

Daniel A. Buidens

A thesis submitted in partial fulfillment
of the requirements for the degree of
Master of Science in Civil Engineering
Department of Civil and Environmental Engineering
College of Engineering
University of South Florida

Major Professor: Abla Zayed, Ph.D.
Kyle A. Riding, Ph.D.
Rajan Sen, Ph.D.

Date of Approval:
October 15, 2014

Keywords: Autogenous shrinkage, Stress relaxation, Free-shrinkage, Restraint, Chemical admixtures

DEDICATION

This work is dedicated to my wife. The love, support and encouragement that you have provided me has kept me motivated and given me the drive to keep working hard and to not give up. Your patience through this thesis process is truly amazing, I owe you a lifetime of attention, and I will never forget the things you have given up so that I could write this document.

ACKNOWLEDGMENTS

I want to thank my parents for giving me the support that I needed to continue attending college when income was low and tuition costs were high. Mom, without the financial help that you gave me I could not afford the keep attending. Michael, your public speaking, has given me the courage to present and defend my thesis. Dad, your drive to never give up has taught me to never give up. Terry, your will to survive has been inspirational. Tim, the guidance and work ethic that you taught me has made me into the man I am today and I am proud to call you Dad. Sue, your success has been inspirational in my life, and I could always talk to you.

I want to acknowledge and give a special thanks to my coworkers: Tom, Natalya, Phil, Victor, Anthony, Andre, and Reza. THANK YOU for the help you provided me and the knowledge that you shared with me. Every one of you has something special to offer and I will remember you all forever. Dr. Zayed, you have taught me so many things about concrete, research, and life. I want to thank you for the persistent pushing that you did to make me into a more productive engineer. You are a strong individual and you demand respect when enter a room, I aspire to be more like you some day. Dr. Riding, I have learned many things from you, you are truly a wealth of knowledge, thank you for your contributions of time and energy to help me with this research. You have been a crucial component to this research group and to my success and I am honored to have worked with you. Dr. Sen, your advice is priceless. You have taught me many valuable things about design, repairs, and life. Working with you both in and outside of the class room has been a privilege.

I want to thank the structures team, Danny Winters, Kevin Johnson, Liz Mitchell, Vince Depianta, Zuly Garcia, Jeff Vomacka, Tony Benitez, and Dr. Mullins, for all their help. Tony & Chester and the USF machine shop were crucial components to my success, for the precision machine work that went into both the free shrinkage frame and the rigid cracking frame.

Thomas Meagher, your help and craftsmanship was paramount to the construction of the cracking frame. Also, you were essential to carrying out the cracking frame experiments, helping with the mixing, preparation and placement of concrete. Natalya Shanahan, your knowledge and advice are unmatched. For your assistance with mix design, I am truly grateful. Victor, you are a computer whiz, and I am appreciative of all the help that you have provided me in the short time that we worked together. Andre Bien-Aime, your help in the lab and on the computer is greatly appreciated. You taught me the ropes when I joined the team and I am very much appreciative of the time that we spent together. Ahmadreza Sedaghat, you generosity and willingness to help and teach are unmatched and I will be forever grateful for your help. You have so many skills, and I hope that someday you get the chance to teach others. Phillip Hittepole, your help with equipment set up and calibration was very helpful and necessary. I admire your attention to detail when it comes to pretty much anything. Thank you for all your help with testing and creating awesome spreadsheets.

A special thanks to the Florida Department of Transportation for funding part of the research project. I am very grateful for the opportunity to participate in this research project and I have worked hard to meet the expectations of the project. I am honored to be a part of your team. Thank you to CEMEX, Vulcan, and W.R. Grace for material donations and delivery assistance. Your generosity has enabled us to conduct this research that is very important to me and my research team.

TABLE OF CONTENTS

LIST OF TABLES

LIST OF FIGURES

ABSTRACT

Cracked pavement slabs lead to uncomfortable and eventual unsafe driving conditions for motorists. Replacement of cracked pavement slabs can interrupt traffic flow in the form of lane closures. In Florida, the traffic demands are high and pavement repairs need to be carried out swiftly typically using concrete with high cement contents and accelerators to create rapid setting and strength gain. The concrete used in these pavement replacements is usually accompanied by a high temperature rise, making the replaced slabs susceptible to cracking. Cracking is a result of developed tensile stresses in the concrete, which exceed the concrete's tensile strength capacity. This research is being conducted to determine the risk of cracking for pavement slabs with varying dosages of chloride based accelerator used to promote high early strength. To analyze the effect of the accelerator, five different concrete mixtures including a control were assessed in a series of tests with varying accelerator dosages. Experiments included: mortar cube testing, concrete cylinder testing, autogenous deformation measured with a free-shrinkage frame, and restrained stress analysis using a rigid cracking frame.

The findings indicate that accelerators are necessary to meet the strength requirements, and that the higher the accelerator dose, the higher the early shrinkage in the first 24 hours determined from the free shrinkage frame. Accidental overdose of the chloride-based accelerator results in the highest cracking potential and the highest shrinkage when tested under field generated temperature profiles.

CHAPTER 1: INTRODUCTION

Badly cracked pavement slabs require replacement to keep roadways safe. High traffic demands force these types of repairs to be executed quickly with high performance materials at times when traffic demands are lighter. Faster setting concrete reduces construction time for highway pavement slab replacements; however, this can be problematic because of the risk of the concrete cracking due to associated high heat generation. Minimum strength requirements need to be met before the pavement is opened to traffic, and because of that, these pavement projects warrant the use of concrete accelerators to meet the minimum strength requirements in the short time frames available. There is no maximum strength limitation in place for replacement slabs. The accelerators allow for these repairs to be quickly performed, because they speed up cement hydration, but there can be consequences in terms of larger temperature gradients that develop when using the accelerators. To complicate the process, the mixtures use high amounts of cement heated water and sun warmed materials creating higher concrete temperatures than normal concrete delivery temperatures [1]. These "hot mixes" typically have shorter workability times and generally have a higher tendency to crack at early ages. The fresh concrete temperature is typically approaching 100°F before the accelerator is added.

The goal of this study was to determine if cracking potential increased with accidental increase in accelerator dosage? The motivation of the research conducted was to determine the effect that an accidental accelerator overdose has on the cracking sensitivity of pavement slabs in these rapid slab replacement projects.

The expectation is that the strength will be higher at early ages in the mixtures that contain accelerator but consequently lower at later ages. The accelerator will increase the temperature of the concrete and is expected to result in higher thermal strains. These strains can lead to stresses if the concrete is restrained and can lead to higher cracking potentials. Additionally, it has been documented that $CaCl_2$ generally increases volumetric change in concrete either under moist curing or drying conditions [2]. Hydration will be accelerated from the use of the $CaCl_2$ accelerator resulting in faster autogenous shrinkage. The principal reason for using $CaCl_2$ is to produce high early strength, required to permit early removal of formwork.

The higher temperatures that these mixtures experience are responsible for higher thermal volumetric changes. Chemical, drying and plastic shrinkage are also sources of volume change that can affect a young concrete element. Chemical shrinkage due to cement hydration is a source of volumetric change and through self-desiccation, it leads to autogenous shrinkage. Drying shrinkage is unavoidable, but it can be postponed through the use of adequate curing techniques. In Equation 1, it can be seen that the total strain that a young concrete can experience is a function of thermal, autogenous, and drying strains.

$$\varepsilon_{TOTAL} = \varepsilon_{THERMAL} + \varepsilon_{AUTOGENOUS} + \varepsilon_{DRYING} \quad \text{Equation 1}$$

where,

ε_{TOTAL} = total unrestrained strain

$\varepsilon_{THERMAL}$ = thermal strain

$\varepsilon_{AUTOGENOUS}$ = autogenous strain

ε_{DRYING} = drying shrinkage strain

Autogenous shrinkage is approximated to begin between 9 and 24 hours [3]. In this research, autogenous shrinkage is expected to start much sooner, in-fact, immediately after final

set for the mixtures tested. This study aims to quantify the effect of accelerator overdose on the cracking potential using a free shrinkage frame, and a rigid cracking frame. Five different concrete mixtures with variable accelerator dosage were prepared for each of the frames. The free shrinkage frame is used to measure free deformations caused by thermal strain and autogenous shrinkage under zero restraint conditions in a temperature controlled lubricated formwork. The rigid cracking frame is used to quantify the stresses developed from strain induced by thermal and autogenous shrinkage when the ends of the concrete are partially restrained. Modulus of elasticity and tensile splitting strength of concrete cylinders as well as compressive strength testing were also performed to provide data on concrete mechanical properties evolution under isothermal curing conditions. The data was collected from the cylinders which were prepared at 23°C and cured in isothermal curing tanks maintained at 23°C. The cylinders were prepared so that maturity curves could be generated for the purpose of mechanical property estimates of the concrete in the frames at different ages and temperatures to increase the relevance of comparisons.

CHAPTER 2: LITERATURE REVIEW

2.1 Construction Methods

Advancements in concrete admixtures over the last decade have led to an increase in the use of high early strength-lower water/cement ratio (w/c) concrete. These concrete mixtures have been widely used in concrete pavement replacements as they usually allow the road to be opened to traffic 6 hours after placement. These high performance mixes are frequently referred to as Rapid Strength Concrete (RSC) [4] or Early-Open-to-Traffic concrete (EOT) ([1]). However, since the w/c is low, RSC are particularly sensitive to the use of proper construction practices and environmental conditions such as air temperature and humidity levels and placement time. The California Department of Transportation (Caltrans) has had extensive experience with pavement cracking research. Over the years, it has been concluded that the main causes leading to early pavement cracking are inadequate saw depths, late sawing, restraint stresses from shrinkage or temperature change, stresses from curling or warping, and opening pavement to traffic before adequate strength has been achieved (Caltrans 2008). The performance of the replacement slabs greatly depends on the elastic modulus of the concrete and whether it has enough early developed tensile strength to resist the tensile stresses induced from the high temperatures generated [5]

There are nationwide common practices for Portland cement concrete (PCC) pavement construction; however, due to regional weather conditions and available materials, each state also has their own practices. Different repairs are carried out for different types of cracked pavement slabs. If the damage is from spalling near a joint, and not to the full depth of the slab, a partial

depth repair can be made. When transverse or longitudinal cracks extend through a slab, the concrete near the crack needs to be cut to the full depth and removed. In some cases, a practice known as stitching or dowel bar retrofitting can be implemented to repair transverse cracks [6]. Corner cracks and shattered slabs also require full depth replacement. Standard practices described in the Integrated Manual for Construction Practices (IMCP) require that cracked slabs are diamond-blade saw-cut to the full pavement depth down to the sub-base and removed. These cuts are made up to existing construction joints or repair boundaries, such as transverse and longitudinal joints, which run perpendicular and parallel to the flow of traffic, respectively [7].

Caution needs to be taken to not disturb the sub-base or damage it during the slab removal, and restrictions are in place to prevent the sub-base from being cut more than to a depth of ½ inch [8]. The slabs are first cut into large pieces and then lifted out and trucked off site. Any sub-base material that is removed should be repaired following slab removal with compaction of the base material, as well as proper moisture content preparations [9]. Currently, Florida requires that the subgrade be within 2 percent of its optimum moisture content before concrete is placed to reduce water consumption by aggregates [9]. California uses treated base under the pavement slab, which if damaged during excavation requires repair with rapid setting concrete and needs time to harden before the top slab is placed. Rigid treated base has been used in Florida in the past; however, unbound base is more commonly used in new pavements. When pavement repairs are placed over an existing rigid base, asphalt concrete is used as a bond breaker between the base and slab to minimize the degree of restraint provided by the base [10]. In California, plastic sheeting is used as a bond breaker [11].

After the sub-base has been prepared, dowel bars are installed into the existing slab typically 12 inches on center to half the slab depth in the longitudinal direction to provide load

transfer between slabs. The dowels are anchored into the existing slab and greased with a bond breaker substance applied to the free end to prevent the concrete from bonding to the dowel. This is done to prevent any restraint on the new slab that would result in tensile stresses on the new concrete. In Florida, greasing of the bars or a zinc coating serves as the bond breaker. While thirty other states polled in the American Concrete Pavement Association ACPA survey allow epoxy coatings on the dowel bars, Florida does not allow epoxy coatings on dowel bars or tie-rods. Drilling the holes for the dowels is typically done using a gang drill (several drills mounted parallel to a rigid frame), if enough space is available. A minimum of 4 holes can be drilled with the gang drill, and is preferred over single mounted drills or hand held drills [12]. Misalignment of dowels is a large contributing factor to premature cracking because misaligned dowels prevent lateral movement of the slab during thermal volume changes thus generating stresses in the slab [4]. Chen and Won also observed that improperly installed dowels were not able to relieve the environmental restraints, and were a contributing cause to cracking [13]. Tie-bars, which are not the same thing as dowel bars are not used to provide load transfer between slabs but instead to prevent longitudinal movement between lanes. Bond breaker is also applied to the vertical faces of the adjacent slabs to reduce restraint on the pavement repair slab.

A minimum slab replacement length of 6 feet and full lane width are recommended; half lane repairs are not permitted by any of the surveyed agencies [4], [11]. Most agencies have concluded that if two repairs are close in proximity, it is more cost effective to repair the full width and length of the entire slab than it is to make additional saw-cuts to repair multiple smaller areas [11].

2.2 Construction Requirements

Minimum strength requirements and specific construction requirements are in place to ensure that the work performed meets the traffic demand so that the repair can be opened to traffic. Construction requirements for rapid concrete repairs in Florida include: minimum target compressive strength of 2,200 psi at 6 hours and 3,000 psi at 24 hours, slump of 1.5 to 4 inches, entrained air of 1-6% and a maximum concrete temperature of 100°F before placement and after to the addition of accelerators. The compressive strength is verified by cylinder testing as well as maturity testing as specified in ASTM 1074. Additionally, temperature sensors can be installed in-place if designated by the Engineer on site for purposes of monitoring temperature and performing maturity tests [9].

California uses 3 different variations for rapid strength concrete (RSC) based on available lane closure times and strength requirements. The first type of RSC contains specialty or proprietary cement mixtures and can meet strength requirements within 2-4 hours. The second type of RSC uses Type III cements with non-chloride accelerator, and a high-range water-reducer (HRWR) admixture. This second mixture can meet opening strength requirements within 4-6 hours. The third type of mixture uses a lower dosage of non-chloride accelerator and can meet opening requirements within 12 to 24 hours. The use of each of these three RSC mixtures is determined based on the available lane closure times [11]. California has the following opening-to-traffic requirements: 2,000 psi compressive strength, 400 psi flexural strength, 300 psi modulus of rupture from center point loading, or a 250 psi third point loading [11]. NCHRP Report 540 [1] documented Early Open to Traffic (EOT) concrete strength requirements for 11 states utilizing 6-8 hour EOT mixes and 20-24 hour EOT mixes. The required range for compressive strength before opening in the report was between 2,500 and 3,500 psi, which is

higher than required in Florida, and between 300 and 600 psi for flexural strength. Currently, there is no requirement for flexural strength in the FDOT pavement specifications; for bridge decks and pre-cast slabs, the requirements are 550 psi minimum flexural strength or the minimum compressive strength specified in the plans [9]. Some states (Maryland, Missouri, and Ohio) have the same criterion for both 6-8 hour EOT strengths and 20-24 hour strengths. Others (Michigan and Arkansas) have higher strength requirements for the 20-24 hours EOT Concrete. Georgia uses 3 different mixes that allow the roads to be opened to traffic in 4 hours, 12 hours or 24 hours.

2.3 Concrete Placement for Repair Slabs

The Florida Department of Transportation (FDOT) requirements specify that placement of concrete from ready-mix trucks should take place quickly and be evenly distributed into the repair areas to limit over-working with shovels. Vibration should follow placement for good compaction especially around dowel bars and the patch perimeter. Finishing should be accomplished through the use of vibratory screeds or straightedges, and match the surrounding surface profile with a maximum tolerance for difference in height of only ± $1/8^{th}$ in from the adjacent slab. Texturing the surface similar to the surrounding pavement and then taking the appropriate steps to cure the fresh slab as soon as possible is key to avoid stress on the fresh concrete from drying shrinkage [9]. In addition to placement specifications, California requires that the concrete truck drivers are trained on how to retard a mix that is setting [11]. Florida prohibits the addition of accelerator, which is added at the job site, to pavement replacement concrete that is more than 60 minutes old [9].

Weather during construction is an important factor that affects the potential for cracking. Adverse environmental conditions that can increase cracking potential include high winds,

extreme low and high temperatures and low humidity. IMCP specification states that concrete should not be placed during periods of high evaporation, unless evaporation retarder films, sun shades, wind breaks, and fogging are used to prevent excessive evaporation from the slab surface [7]. Some agencies do not permit replacement slabs to be constructed during the daytime hours, as casting at night significantly reduces cracking. For example, California as well as Georgia only permit concrete placement in the evening between 10:00 p.m. and 2:00 a.m. Placing at night provides the benefit of lower air temperatures and higher humidity levels. Meadows indicates that lowering the placement temperature reduces the cracking tendency [14]. When compared to a placement temperature of 95°F, placement temperatures of 50°F and 73°F produce a reduced stress to strength ratio prior to cooling. This indicates that cooling the fresh concrete prior to placement in hot weather conditions will reduce the strength reduction due to thermal effects [14]. Florida does not currently specify the timing of concrete slab placement. In this respect placement temperature is the temperature of the concrete at placement. The temperature of the concrete can be determined or monitored at different times in the process. The environmental temperature is the air temperature.

Inadequate curing is often blamed as a major cause of cracking. Well-timed curing and good quality curing compounds are essential, since moisture is essential for proper hydration, especially in EOT concretes. Drying shrinkage is a major concern for a concrete slab especially in hotter climates. Texas DOT points out that high temperatures generated from rapid-setting concrete can encourage rapid evaporation of water from the surface leading to cracking problems and that curing must start as soon as possible [6]. Section 925 of the FDOT Standard specifications for road and bridge construction lists: wet burlap, membrane curing compounds and sheet materials such as waterproof paper, polyethylene film and white burlap-polyethylene

sheets, as acceptable curing methods [9]. Sprayable curing compounds are also frequently used as curing methods by many agencies. The membrane curing compounds should be suitable for spraying at temperatures prevalent at the time of construction and should form a continuous, uniform film. The methods for curing replacement slabs currently in place are to evenly spray the curing compound, then cover the surface and exposed area with 2 layers of white burlap-polyethylene curing blanket conforming to the FDOT Standard specifications for road and bridge construction section 925 or insulating blankets approved by the engineer. The goal is to cover the slab with the curing material as soon as the surface is hard enough to resist marring and to continue curing the slab until the required 6-hour strength is achieved [9]. California also only uses power-operated curing compound application to ensure even coating of repair slabs [11].

Saw cutting of pavement is a significant step in the installation of new pavement and replacement pavements. Transverse cracks can be controlled through the implementation of shorter panel lengths and more saw cuts [11]. The joint spacing or distance between cuts should be "chosen to limit stress caused by restraint to movements from creep, shrinkage, and temperature effects" [15]. ACI 224.3R-95 recommends that transverse joint spacing "should not be more than 24 times the slab thickness (typically 21 times for stabilized bases and 24 times for non-stabilized), and not farther than 20 feet apart regardless of thickness"[16]. The depth of initial cut should be at least 0.25 times the slab thickness to ensure crack formation at the joint and 1/3 of the slab thickness for stabilized-base pavements. Florida requires the maximum spacing between the joints to be limited to 15 feet. The Federal Highway Administration (FHWA) advises that repairs made for slabs longer than 10 to 13 feet should be constructed with an intermediate joint to prevent cracking [11]. Longitudinal joints are also of importance in concrete pavement construction and are used to prevent cracking along the pavement centerline

as they help to alleviate the effects of curling [16]. FDOT limits the spacing between longitudinal joints to a maximum 14 feet [17]. Saw-cutting operations should begin as soon as the concrete is able to support the weight of the saw-cutting equipment and operator [16]. The FDOT puts a lot of emphasis on timely cutting of joints to prevent uncontrolled cracks. Transverse joints need to be made as soon as the concrete is hard enough to resist raveling from the cut, and before excessive shrinkage cracking occurs. The initial cut for transverse joints has to be made within the first 12 hours. The initial cut should be $1/8^{th}$ inch wide and to a depth of $1/3^{rd}$ of the thickness. The second cut is then to be made to plan specifications. For longitudinal joints, the saw-cutting should be completed as soon as possible and in no case in more than 72 hours after any pavement placement [9]. In California, timely saw-cutting is also identified as a crucial step in a successful pavement replacement. Caltrans states that cutting joints too early can lead to spalling and cutting too late can lead to random cracking in the repaired area [11].

2.4 Material Requirements

California only uses Type III cements for RSC concrete pavements, and a specialty cement in ultra-fast repairs [11]. Georgia uses either Type I or III depending on the construction time frame [18]. All of the 11 states in the NCHRP report require the use of Type I, II, or III Portland cement for the 20-24 hour EOT concrete mixtures, and the specified minimum cement content varied from 564-846 lb/yd^3. Texas specifies a minimum cement content of 658 lb/yd^3 for Type I cement versus 564 lb/yd^3 for Type III cement [1].

Michigan, Georgia and Illinois specified that calcium chloride accelerator be used in cold weather, for instance, if the temperature is below 65°F [9]. California does not allow the use of chloride containing accelerators. It has been concluded that the use of chloride-containing accelerators doubles the amount of shrinkage experienced by concrete compared to shrinkage

with no accelerator [11]. As far as retarders, if the air temperature is higher than 96°F, the use of a retarder may not be effective; instead, it is recommended that a slower setting concrete mixture should be used [11].

Supplementary cementitious materials (SCM) are not typically used in rapid concrete pavement repair. However, some states do allow their use as partial cement replacement. Indiana allows 10% fly ash or 15% ground granulated blast furnace slag additions for 20-24 hour EOT concrete [1]. Florida also allows the use of SCMs for new concrete pavement [9].

Typically a No. 57 or No. 67 stone blend is selected in Florida for replacement slabs [9], and these same aggregate sizes are used by Texas and Wisconsin as well [8]. The aggregate specifications used are agency-specific. The maximum aggregate size used in pavements is 2 inches, and are utilized in: Idaho, Nevada, Michigan, Missouri, and Utah. The smallest max coarse aggregates used in pavement are 0.75 inches, in Kansas with limestone mixtures, and 1.0 inch in Wyoming, South Carolina, Oklahoma, Indiana and Montana [19]. Section 901 of the FDOT code specifies the requirements for coarse aggregates used by the FDOT for a variety of different applications. Coarse aggregates should consist of naturally occurring materials crushed from parent rock into gravel typically of the lime rock variety. Aggregate selection for pavement replacements should be based on the aggregate reactivity and a low coefficient of thermal expansion and mix design are subject to departmental approval. The maximum aggregate size allowed in Florida pavement construction is 1-1/2 inches. Section 902 of the FDOT Standard Specification for Road and Bridge Construction specifies that the fine aggregates shall consist of natural silica sand and can be from local similar inert and unreactive hard, strong, durable particles. Variation in fineness modulus in sand from a single source should not be greater than 0.2 in either direction of the target FM [9].

It has been observed that rough textured or crushed amorphous aggregates lead to higher tensile strengths over smoother aggregates, especially at early ages [20]. Micro-cracking originates at the interfacial transition zone (ITZ), and cracking develops as load is applied. These ITZ's are the weak links in the concrete where the potential for cracking originate. The other main potential for cracking associated with aggregate lies in the aggregate's coefficient of thermal expansion (CTE). Aggregates need to be selected on the basis of having as close a CTE to the cement paste as possible to reduce cracking potential.

Florida allows the use of Type I, IS, II, and III cements for pavement slabs, in accordance with AASHTO M85 and M240. Florida requires 451 to 790 lb/yd^3 of cement for new pavement slab mixture designs. The rapid-strength mixtures containing more cement are subjected to approval by the department and demonstration slabs may be required [9]. For example, FDOT mix 353-094 uses 900 lb/yd^3 of cement, and also utilizes $CaCl_2$ accelerator. Section 353 of the FDOT Standard Specifications for Road and Bridge Construction states that "for concrete pavement slab replacement, the use of pozzolans and slag is optional" [9]. The specification, however, does not provide guidance for percent replacement of cement specifically for concrete pavement slab replacement. For new pavement, Florida allows fly ash replacement of 18-22% by weight of cement, while for slag, 25-70% replacement by weight of cement is allowed.

The use and acceptance of chemical admixtures is found in section 924-2 of the Florida code, where a qualified "Products List" of the allowed admixtures can be found. The Department maintains a list of qualified admixtures including: air-entraining, water-reducing (Type A), accelerating 850 (Type C), water-reducing and retarding (Type D), water-reducer and accelerating admixture containing calcium chloride (Type E), high-range water reducer (Type F) and high-range water-reducer and retarder (Type G), high-range water-reducer (Type I -

Plasticizing and Type II - Plasticizing and retarding) in producing flowing concrete, in addition to corrosion inhibitors. Type B admixtures, which are classified as retarding admixtures are not allowed [9].

2.5 Early-Age Cracking in Concrete Pavement

ACI report 231R-10 on early-age cracking identifies thermal- and moisture-related concrete volume changes as the causes of early-age concrete cracking. The report "defines "early age" as the period after final setting, during which properties are changing rapidly." The early age period is generally approximated to be 7 days [21]. The magnitude of volume changes determines the magnitude of the stresses generated for a given degree of restraint. Both magnitude and timing of these stresses with respect to concrete mechanical properties development should be considered to be the determining factors of the concrete cracking potential [22]. The total strain that develops in a young concrete can be defined that any combinations of thermal, autogenous or shrinkage strains compose the total strain.

2.5.1 Shrinkage

2.5.1.1 Autogenous Shrinkage and Volume Change

Autogenous shrinkage is the bulk volume change that results from the consumption of capillary pore water during hydration. Autogenous shrinkage is a result of chemical shrinkage that leads to self-desiccation, which is the internal volume change that occurs during hydration. due to the fact that the hydration products occupy less volume than the anhydrous cement and water [23]. The mechanisms that lead to autogenous and drying shrinkage are essentially the same in that they both are due to redistribution of water within the concrete microstructure. Whether autogenous shrinkage or drying to the surrounding environment, ACI 224R-01 points out the need to separate these phenomena [16]. The loss of water, whether internal or external,

generates compressive stresses on the pore walls through cohesion and capillary action, reducing the pore volume, resulting in the bulk volume reduction. Neville states that the loss of capillary water, "causes little or no shrinkage", and volume change results from the loss of adsorbed water which is physically bound to the gel particles [24]. If concrete is restrained, this shrinkage will lead to development of internal tensile stresses. If the shrinkage is significant enough to cause the stresses to exceed the tensile strength of the concrete, cracking is likely to occur.

Autogenous shrinkage has received a lot of attention with respect to early-age cracking of high performance concretes (HPC). These mixtures have low w/cm ratios below 0.39 and high cementitious material content. The literature indicates that autogenous shrinkage is considered to be negligible in concretes with w/cm ratios above 0.4 [1] or 0.42 [25].

At the time that initial setting is occurring, all the capillary pores in the concrete are saturated with water. As the water in the existing pores is consumed and new pores are created during the hydration process, the pore water is redistributed by the capillary forces, which draws the water out of the larger pores into the smaller ones [26]. Now the small pores are saturated, and the large partially filled pores with both water and air, resulting in a drop in the relative humidity (RH). The RH is generally assumed to be 100% at saturation; however, Lura et al. reported values of 98% RH at saturation [27]. This is explained by the presence of salts in the pore solution, which lowers the RH by 1-3% [28]. These salts are a byproduct the accelerator leaves in the pore solution after about 24 hours [28].

The total autogenous deformation or shrinkage can be summarizes with Equation 2 and consists of 3 basic components; namely, early age plasticity, which is active before an initial network of cement particles has formed that could resist early age deformation, elastic deformation, and viscoelastic deformation represented by creep. In the last few decades, since

low water to cement rations have been used, deformation induced by self-desiccation capillary forces, have been the major source of autogenous shrinkage. However, new results indicate that differences between measured and calculated autogenous deformations are becoming more pronounced in the first 24 hours after mixing. Indicating that creep has an important role in early age autogenous deformation of hydrating paste, especially in the first 7 days, when strength and elastic modulus are still developing [29].

$$\varepsilon_T = \varepsilon_p + \varepsilon_e + \varepsilon_c \qquad \text{Equation 2}$$

where,

ε_T = total autogenous shrinkage

ε_p = early age plasticity

ε_e = elastic deformation

ε_c = visco-elastic deformation represented by creep

Several factors can affect the magnitude and rate of autogenous deformation beyond just the w/c ratio. Some materials can increase autogenous shrinkage more than others even at equivalent level of hydration [30]. Silica fume for example does not necessarily lead to smaller pore sizes, but instead it subdivides pores, refining the pore structure [31]. Smaller pore sizes cause the water menisci to have a smaller radius of curvature which results in higher exerted stresses on the pore walls during drying. As mentioned, the menisci cause contraction on the pore walls, compressive stresses develop on the pore walls as the paste is drawn inward causing the concrete member to shrink [31]. The shrinking will affect the global volume and if restrained, the shrinkage will lead to tensile stresses.

In this regard, chemical admixtures such as calcium chloride which is a widely used accelerator for cement, can also affect measured autogenous shrinkage. This accelerator is most

active in the first day, and is known to increase the rate of C-S-H formation [32]. Riding et al. go on further to say that not only is more C-S-H gel produced, but its morphology is also changed and it leads to increased surface area. Consumption of pore solution places compressive stresses on the pore walls and they contract faster than normal concretes as a result. Because the accelerator speeds up the hydration reaction, much higher autogenous shrinkage results in the first day. Young found that when 1% $CaCl_2$ was added to tricalcium silicate (C_3S) paste, the volume of finer pores increased compared to C_3S paste without accelerator additions [33]. Suryavanshi, Scantlebuy, and Lyon found that the addition of $CaCl_2$ caused a decrease in total pore volume in mortar specimens at $CaCl_2$ content of 1.75%. The addition of $CaCl_2$ increased the pore volume for finer pores, and it decreased the number of coarse pores, which was attributed to a change in morphology of C-S-H gel from a fibrous to a dense morphology [34].

2.5.1.2 Drying Shrinkage

Drying shrinkage generally refers to hardened concrete volume change due to the loss of moisture to the environment, and it represents the shrinkage strain induced by the loss of water from the hardened material [25]. Drying shrinkage is big a problem, especially if inadequate allowances for the shrinkage induced strain are not made during design. If the concrete is restrained the shrinkage can lead to tensile stresses which will ultimately result in cracking.

2.5.1.3 Plastic Shrinkage

Plastic shrinkage occurs while concrete, still in the plastic stage, is exposed to atmospheric drying where the drying rate of water from the surface of the concrete exceeds the bleed rate. Plastic shrinkage is most common in horizontal surfaces of pavements and slabs due to rapid evaporation from the large surface area. The problem is increased in the presence of wind, low humidity, high air temperatures and especially high concrete temperatures [7].

2.5.2 Thermal Effects in Concrete Pavement

There can be many thermal stresses the concrete will experience after placement, some can be beneficial, and some can be harmful. Thermal induced stresses in concrete are a function of: the coefficient of thermal expansion of the hardening concrete, the level of restraint, the temperature rise from the time of placement, and the creep adjusted modulus of elasticity. Fresh concrete temperatures can influence the stresses that develop, and efforts should be made to ensure that the placement temperature is similar to the concrete environment temperature. Hot formwork can be problematic, and can raise concrete temperatures. Accelerators can quickly raise concrete temperature due to rapid cement reactions, and dosage amount should be considered based on fresh concrete temperature. Efforts should be made to lower the placement temperature of the concrete and to lower the temperature of the formwork if possible. Shading a placement site or nighttime placements can be effective to keep formwork temperatures generally lower. The reason that temperature and heat transfer to and from the environment is so important, is to not develop extreme temperature differentials or large temperature changes that are restrained because they can certainly cause cracks. Heat generation from the hydration reaction leads to high early concrete temperatures, which can go higher if accelerators are used. This heat generation can be a catalyst for some reactions, but it can also lead to stress differentials developing from an increasing temperature difference from heat generation and dissipation. This stress differential stems from the concrete surface cooling while heat generation is still occurring on the interior. In essence, one part of the concrete is expanding from heat generation while another is contracting from cooling. The size of the element and the temperature of the environment can compound the effect of this temperature differential, and for larger elements the allowable temperature differential is restricted. Some Departments of

Transportation have placed limits of a 35°F temperature differential for mass concrete elements between the core of the concrete element and the surface. This limitation indicates that thermally induced strains from temperature differentials are bad for concrete and too large of a temperature gradient can lead to a crack. It should be noted that this should be applied to concrete possessing low coefficients of thermal expansion, and the limit on the temperature differential should be based on a per mixture basis.

Concrete in a plastic or hardened state is just like many other materials and it will expand when heated and contract when cooled. The coefficient of thermal expansion develops as the concrete matures and is typically higher in early age, due to the water present in the fresh concrete. The deformation that results from these temperature fluctuations induces stresses if the concrete is restrained. As discussed previously, restraint can come from the temperature differential that occurs between the cooler outer surface of the concrete and higher internal concrete temperature gradient. This differential is problematic because of heat dissipation causing the outer surface to be cooling and contracting because of the lower temperature, while the core is expanding due to the heat generation.

The differences between the aggregate and paste coefficients of thermal expansion can also be a source of restraint. In pavements, subgrade, adjacent slabs and dowels can be sources of restraint, so it is important to reduce the restraint if possible. The level of restraint can be reduced by using aggregates with low coefficients of thermal expansion or by reducing the temperature differential. Thielen and Hintzen [34], point out that the behavior of early age concrete is dependent on the degree of restraint and the temperature rise during hydration. The degree of compressive stresses experienced during hydration due to early expansion from heat generation is small compared to the tensile stresses developed when the concrete cools because

the concrete modulus increases with time. If restraint is reduced, the tendency for cracking will also be reduced. In the study performed by Thielen and Hintzen, it was found that if the restraint factor is reduced, the temperature difference that leads to cracking, increases linearly [35]. Restraint, temperature difference from placement, and elastic modulus are all components contributing to the magnitude of the induced thermal stresses, as illustrated in Equation 3. As one of the components of the equation is reduced, the concrete cracking potential is reduced. Since the equation describes the change in stress, the equation can be used to represent the stress at different times as the stress develops. For example, as the temperature changes or as the restraint changes, the equation can provide a snapshot of the stress at any time that is of interest, 2 hours after mixing, 24 hours, etc. The temperature difference from placement until the time of interest as well as some other factors such as creep, coefficient of thermal expansion, modulus of elasticity and the degree of restraint, all play a role in how much thermal stress develops. The level of stress developed can be expressed by Equation 3 [36].

$$\Delta\sigma_{Thermal} = \Delta T * \alpha(t) * E_{cr}(t) * K_r \qquad \text{Equation 3}$$

where,

$\Delta\sigma_{Thermal}$ = change in concrete stress from a thermal influence (psi)

ΔT = change in concrete temperature from the time of placement to the time of interest (°F)

$\alpha(t)$ = coefficient of thermal expansion for concrete at the time of interest. (in/in/°F)

$E_{cr}(t)$ = creep adjusted modulus of elasticity at a given time (t) (psi)

K_r = restraint factor ranges from 0 unrestrained to 1.0 fully restrained (unit-less)

It can be seen that to reduce stress in Equation 3, that a reduction in temperature change or a reduction in the level of restraint would lead to less changes in stress. Additionally, slower developing modulus and low CTE are also ways to reduce stress induced by thermal effects. The

concrete will experience tensile stresses at temperatures higher than the placement temperature simply from the fact that the setting takes place at a higher temperature than the placement temperature. Tensile stresses are also possible at temperatures above the setting temperature due to the fact that the stiffness is increasing over time [14]. Compressive and tensile stresses will result from temperature increases and decreases, respectively. It should be noted that the coefficient of thermal expansion and the creep adjusted modulus are time dependent. To be able to accurately compute the thermal stress, a thorough understanding of these variables is critical.

2.6 Stress and Strain Differentiation

In this section, developed strain and the resulting compressive and tensile stresses developed during testing are considered here and will be identified and described as to why they are of interest to this research. From Nam et al, the time dependent deformation of concrete is broken down into components of stress described by the following:

- Stress dependent strain - which is produced by stress in the concrete – sum of elastic strain and creep strain
- Stress independent strain – which is not related to stress – is the sum of the thermal strain and the shrinkage strain
- The total strain – sum of both stress-dependent and stress-independent strains

These components can be described with a simple example. If a specimen were prepared and unrestrained, stress independent strain would develop, and it would be the only strain developed. The strain with no stress would develop. If the specimen was fully restrained at both ends, there would be no strain but internal stress would develop. The stress, be it tensile or compressive, could be quantified as equal to the stress independent strain multiplied by the elastic modulus of the specimen at a given time. In an event that there is some strain permitted,

the stress dependent strain in the specimen will be the difference between the total strain and the stress independent strain. In this last example the stress can be calculated by multiplying the difference between the bars total strain and the stress independent strain by the elastic modulus at the time of measurement [37].

Consider a concrete element that is fully restrained in a uniaxial stress state. Take for example a newly mixed batch of concrete, and place it in the cracking frame. In the early stages of hydration, heat will be generated and released due to the exothermic reaction between cement and water. The amount of heat generated is dependent on the type of cement, cement fineness, water to cement ratio, the fresh concrete placement temperature, and the size of the element. When the cement in the concrete starts to hydrate, there will be a rise in temperature that will cause the concrete to expand from the thermal effects of the hydration. The effects of the rapid gain in stiffness coupled with the high temperatures, forces the concrete into a state of compression. During this development of compressive stresses the young concrete is mitigating these stresses due to a high level of relaxation [14]. As the heat of hydration subsides, there is a decrease in heat generation, the concrete can begin to cool and the rate of cooling is dependent on the size and geometry of the element and the temperature of the surroundings, in this example the temperature of the formwork. It is during this phase that the concrete is at risk of cracking if the tensile strength or capacity is exceeded by the tensile stresses that develop during this cooling.

The total strain in the specimen is basically the sum of the temperature strain and shrinkage strain. The temperature induced strain is a product of the thermal history of the concrete, while the shrinkage strain is the result of autogenous and drying shrinkage. In mixtures with low water to cement ratios, there is not enough water to hydrate all the cement and any

small amounts of available pore solution are quickly used up. When the pore solution starts to get consumed pore water moves from larger pores to capillary pores and a drop in humidity inside the pores takes place. The drop in humidity causes an increase in hoop stress and pores become smaller due to capillary action on the pore walls [14]. These small volumetric changes add up to account for a total volumetric change, all due to autogenous shrinkage.

It should be noted that the strains produced by autogenous shrinkage, thermal effects and drying shrinkage do not cause stresses in the concrete unless these strains are restrained; if that is the case, then, restraint stresses are developed. As mentioned earlier, sources of restraint can come from different mechanisms, for this particular example and explanation of Equation 3, it will be assumed that there is zero restraint in the concrete.

2.7 Degree of Restraint and Restrained Stress

If concrete is allowed to expand and contract freely, cracking is not likely to occur due to the fact that there is no external form of restraint on the concrete to induce stresses that would lead to cracking. In practice, however, all concrete is subject at least to some degree of restraint, whether from the subgrade or other structural elements on the macro scale. The leading cause of cracking as described by ACI in ACI 231R-10 is restrained thermal contraction that occurs when the concrete starts to cool [21].

The external sources of restraint in concrete pavements include friction with adjacent concrete pavement slabs, the pavement sub-base, the self-weight of the slab, and the length of pavement slab itself. Dowels that allow for the load transfer between adjacent slabs and tie-bars used to prevent slab movement can also be sources of restraint. The misalignment of dowels will increase the degree of restraint and can lead to cracking. Application of bond breaker is another important measure in minimizing restraint from adjacent slabs friction. As mentioned previously,

bond breaker should be applied to the dowels and the vertical faces of the existing slabs that will be in contact with the new concrete. If the bond breaker is not adequate, restraint stresses can be increased.

The predominant mechanism of restraint in pavements is the interfacial friction between the pavement slab and the sub-base. McCullough and Rasmussen indicated "sub-base type has a greater influence on the restraint level in a concrete pavement than any other factor." Furthermore, the sub-base type could have a strong thermal effect on the concrete, for example black colored sub base could have a much higher initial temperature than grey cement treated base. For example, if there were to be an afternoon placement the darker colored base would be hotter [38]. Zhang and Li investigated the effect of sub-base type on the stresses that develop in pavement due to restraint. They observed that the highest tensile stresses result from the use of stiff bases, like cement stabilized base, and much lower stresses were associated with loose unbound bases. They concluded that the tensile stresses from the frictional resistance of stiff bases could be high enough to cause cracking. However, these high tensile stresses can be significantly reduced by the use of a bond breaker between the base and pavement. The two types of bond breaker investigated in this study were a 2 mm layer of sand and a polyethylene sheet. The polyethylene sheeting was found to be most effective in reducing restraint, which is consistent with the experience of Caltrans [39]. McCullough and Rasmussen recommend the use of asphalt concrete as a bond-breaker [38].

The weight of the slab itself can also provide a degree of restraint because the magnitude of frictional resistance is directly dependent on slab weight. Wesevich et al determined that the slab weight had a direct effect on the frictional resistance to movement for loose unbound sub-bases and only a slight effect on stabilized sub bases. Additionally, it was noted that the slab

length determines the stress magnitude: as the length increases, so does the stress [40]. The rate at which the stress increases with slab length depends on the base type [39]. The stresses due to slab length can be eliminated by timely saw-cutting of transverse contraction joints of appropriate spacing as discussed previously.

2.7.1 Elastic Modulus

At about the same time that the microstructure starts to build due to the formation of hydration products, the early age concrete starts to become stiff and gain strength. The young concrete continues to gain strength over time and develops elastic modulus with time as it hardens. The development of elastic modulus can vary widely between ordinary concrete and high performance concretes, and is dependent on the admixtures. The elastic modulus of HPC develops much faster than ordinary Portland Cement concretes; it has been observed that the elastic modulus on the second day is approximately 80% or more than that at 28 days for ordinary concrete [41]. Bergstrom and Byfors reported that at early age when the concrete is only a few hours old, the concrete is very inelastic and most deformations from stresses will be permanent. At an age of about 8-10 hours, it starts to form elastic and inelastic regions, and by 14 to 18 hours it shows characteristics similar to hardened concrete. Elastic modulus is a mechanical property that develops over time as the concrete hardens and it relates the stresses and strains. However, Hagiwara demonstrated that tensile modulus is 1.1 to 1.2 times greater than compressive elastic modulus [42]. Still, concrete elastic modulus is mainly affected by the type and quantity of admixtures used in the concrete mixture [25].

2.7.2 Stress Relaxation

Creep is defined as “time-dependent deformation under load” [25]. When a compressive load is applied, strains will gradually increase over time which is what happens in the case of

compressive creep. When concrete experiences tensile stresses, for example due to shrinkage under restrained conditions, concrete will deform as well and stresses will be reduced over time; however, this is often referred to as stress relaxation. Stress relaxation and creep are often used interchangeably with respect to concrete [43]. Although the mechanism of creep is not well understood, it is believed that concrete creep is caused by the response of CSH gel to the applied stress and redistribution of adsorbed water from CSH to the capillary pores [25]. Mindess states that creep is the deformation under load in excess of free shrinkage and a considerable amount of the total creep a specimen undergoes is irreversible [25]. Creep and relaxation occur in early age concrete due to the visco-elastic response of concrete. Creep is a paste property like shrinkage, and the aggregates serve at the mode of restraint on the paste, where these stresses develop and relax. Creep, is believed to be related to drying shrinkage as it is influenced by the same parameters as drying shrinkage[25], [20]. Like all concrete mechanical properties, creep depends on the degree of hydration [25], [20]. As mentioned previously, stress relaxation is high at the beginning of hydration and decreases sharply as hydration proceeds. The mechanisms driving the cracking are the stresses developed from the restraint, but there are components that all have influence on the concrete stress level, there are free shrinkage, the elastic modulus of the concrete and the restraint factor (K_r). The modulus, free shrinkage and the restraint factor are changing as the concrete ages, therefore the stress changes with time.

2.8 Measurements of Cracking Potential

The free shrinkage frame provides a means to measure autogenous strain under isothermal temperature conditions or simulated temperature profiles to simulate actual slab temperatures with no restraint. The cracking frame, on the other hand, provides restraint at the start of the experiment. The frame is made of metal and when the concrete shrinks, the frame

does distort some, and it needs to. The distortion of the frame is measured by strain gauges mounted to the parallel Invar bars of known diameter. This distortion is representing the tensile stress the concrete is under in the rigid cracking frame. Important to note is that the level of restraint reduces as the concrete shrinks and puts the frame into compression. The variable designated as the restraint factor (K_r), which is used to quantify the level of restraint [22]. As a result of shrinkage strain developing in the frame due to the concrete contracting and compressing the parallel steel bars and shortening them, the level of restraint is reduced from 100% to about 80% by the end of the experiment. The degree of restraint can be calculated based on the strain measured from the strain gauges mounted on the Invar bars using Equation 4.

$$K_r = \frac{100}{1 + (\frac{E_c A_c}{E_s A_s})} \quad \text{Equation 4}$$

where,

K_r = the degree of restraint in (%)

E_c = the concrete elastic modulus (ksi)

A_c = concretes cross sectional area (in^2)

E_s = Invar restraining bar modulus of elasticity (ksi)

A_s = Invar restraining bars cross sectional area (in^2)

The temperatures of both sides of the Invar bars need to be recorded during the experimental testing so that thermal strain from temperature changes in the steel that may have caused some thermal movement, can be accounted for. The difference can be subtracted from the measured strain to calculate the actual strain induced by the concrete. Equation 5 can be used to account for this temperature difference.

$$\varepsilon_{Tadj} = \Delta T_{ib} * \alpha_{ib} * K_r$$ Equation 5

where,

ε_{Tadj} = temperature induced strain of the Invar bar

ΔT_{ib} = temperature change in the Invar bar

α_{ib} = coefficient of thermal expansion of the Invar bar

K_r = the degree of restraint in the Invar bar

2.8.1 The Coefficient of Thermal Expansion

This is a developing characteristic that changes substantially during the hydration phase. A constant value of CTE for hardened concrete should not be assumed since there is no general agreement on the time evolution of the concrete CTE [44]. Recent research point to the value of the CTE being very high in the first few hours due to the unbound water in the mixture that has a CTE (20 x 10^{-6} in/in/°F). The value of CTE levels off quickly and remains relatively constant at a value of about 10 x 10^{-6} in/in/°F. There are many factors affecting the development of the CTE of concrete and they include: the amount, type and fineness of cement, the type of aggregate used and the moisture content, the water to cement ratio, and the temperature fluctuations [45]

The thermal strain developed in any material is tends to have a change in strain proportional to the change in temperature and the coefficient of thermal expansion, and Equation 6 represents this change in strain.

$$\Delta\varepsilon_{Thermal} = \Delta T * \alpha(t)$$ Equation 6

where,

$\Delta\varepsilon_{Thermal}$ = the change in concrete strain due to temperature change (in/in)

ΔT = change in temperature (°F or °C)

α (t) = coefficient of thermal expansion of the concrete at a given time t (in/in/°F)

There is a definite need to determine the effects of calcium chloride accelerator on HPC, because this niche has not been explored. The objective of this research is to measure the shrinkage strain and the tensile stresses that develop in these HPC mixtures to evaluate if an accidental increase in accelerator dosage increases cracking potential. As mentioned, ac cracking frame was constructed to conduct the stress development in HPCs at early ages within the first 3 days following placement. Accelerator dosages were varied to observe differences in stress associated with these varying accelerator doses.

Concrete behavior in the cracking frame was described by Breitenbucher the original inventor; in a presentation, he states that stage 1 is placement, and the temperature is relatively constant [46]. Also there are no developed stresses due to the fact that the concrete has no stiffness because it has not set. Stage 2 begins with the hydration, setting begins to start but stresses have still not developed yet. In stage 3, final set begins and the mechanical properties start to develop (stresses originate from the temperature rise and the development of the modulus) stage 4 the temperature begins to reduce, compressive stresses are reduced at a rapid pace as a result of relaxation and increasing modulus all occurring simultaneously with the lowering temperature. In stage 5, the heat from hydration subsides and tensile stresses begin as the relaxation decreases and the modulus increases [14]. From the figure, points of interest include: when the concrete temperature rises and peaks, when the concrete has hardened but is in a stress free state, and when the concrete cracks. Also important to note, is that the earlier that concrete goes into tension, the higher the risk of cracking. These points of interest can be identified from figure 1. The plot in figure 1 is a generic representation of a typical temperature curve and a stress development curve with time. The plot is simply for illustration purposes and was not generated from research collected data.

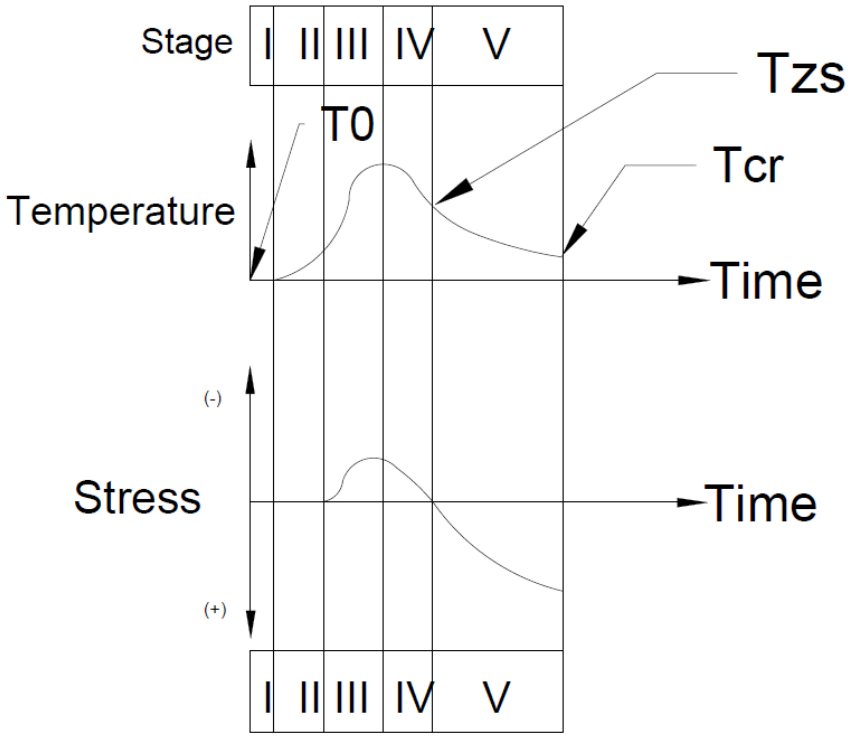

Figure 1 Example plot of temperature and stress behavior versus time for concrete in the cracking frame.

To become more familiar with the variables and what they mean:

- T_0 = Fresh concrete temperature (°F on °C)
- t_{pc} = concrete age when the peak compressive stress level is reached.
- $T_{z,2}$ = temperature at the seconds zero stress point, when the compressive strength are reduced to zero, referred to as the zero stress point
- Tc = temperature at cracking
- tc = concrete age at cracking

The concrete stress determined at cracking in the cracking frame may be more indicative of the pavement slabs resistance to cracking than tensile split cylinders. Mindess states that splitting tensile strength overestimates the direct tensile strength [25]. The reason is because a

more rapid loading is applied to the split cylinders than is developed due to thermal stress development. In the cracking frame the loads are applied slowly, and there is potential for stress relaxation, that is not possible in tensile splitting of concrete cylinders. In a presentation by Dr. Springenschmid at the TUM, it was pointed out that the maximum temperature that develops is not a good indicator of cracking risk and that the development of stresses and strength should rather be considered. It was concluded that the lower the cracking temperature, the lower the cracking tendency. The degree of restraint varies as the concrete hardens, and it is a function of the modulus of elasticity development for the mixture being tested. As the w/c ratio reduces, the tendency for cracking increases. Limestone aggregates mined in Florida tend to have a low coefficient of thermal expansion (CTE), have a lower cracking risk than other aggregates with higher CTE. As the placement temperature was reduced the cracking tendency is also reduced. Retarders did not have a significant effect on cracking tendency. Air entrainer could improve the cracking tendency. Ground granulated blast furnace slag can have a variable effect on concrete and it does not always reduce the cracking tendency. Fly ash has been found to generally reduce a mixtures tendency to crack because the stress development is slower in mixtures containing fly ash. Silica fume has been known to increase cracking potential, probably because it leads to smaller pore sizes and those lead to higher autogenous shrinking, when pore water migrates to capillary pores [36].

CHAPTER 3: METHODOLOGY

The experimental techniques and methodology used in studying the role of accelerator dosages on the cracking potential of pavement concrete mixtures will be presented in this chapter. Towards addressing this objective several experiments were conducted; namely, as-received materials characterization, mechanical properties development of different concrete mixtures, and cracking potential assessment using free shrinkage and cracking frames. The following sections will detail the experimental techniques used in this study.

3.1 Characterization of As-Received Materials

3.1.1 As-Received Cement

3.1.1.1 As-Received Cement Chemical and Mineralogical Analyses

The cement used in this study (SW) is Type I/II Portland cement. The elemental oxide analysis of the as-received cement was measured using X-ray florescence spectroscopy in accordance with ASTM C114-11b [47] The test was conducted by a certified commercial laboratory. ASTM C-150-09 [48] was used to quantify the potential phases content of the as-received cement; namely, tricalcium silicate (C_3S), dicalcium silicate (C_2S), tricalcium aluminate (C_3A), and tetracalcium aluminoferrite (C_4AF).

In addition to bulk elemental oxide analysis, direct quantification of crystalline phase content of Portland cement is of great significance. Different cement phases have different contributions to concrete properties. Stutzman [49] suggested that for cements, direct phase quantification improves the knowledge of their influences on cement hydration characteristics, concrete strength development and durability of structures. In this study, X-Ray Diffraction

(XRD) was used as the direct method of identification and quantification of the crystalline compounds in Portland cement [50]–[52].

Mineralogical analysis of crystalline phases was conducted using quantitative x-ray diffraction. The equipment used was X'Pert PW3040 and the scans were collected using Cu- K_α radiation. The samples were scanned using a step size of 0.02 degrees per step and counting time of 4 seconds per step. The tension and current were set at 45 kV and 40 mA. Divergence slit was fixed at 1°, receiving slit had a height of 0.2 mm, and anti-scatter slit was fixed at 1°. Cement phase quantification was performed using the Rietveld refinement. Rietveld refinement is based on fitting the whole collected pattern, which allows overlapped peaks to be resolved. A simulated pattern based on theoretical crystal structures input by the user is iteratively compared to the collected x-ray pattern and refined based on a number of parameters, which describe the crystal structure of the phases and their amount in the sample, and equipment characteristics.

3.1.1.2 As-Received Cement Physical Properties

Cement physical characteristics studied here were Blaine fineness, particle size distribution and specific gravity. It has been well established that cement fineness affects its hydration kinetics especially during early stages of hydration [17]. It is an indirect measure of the total surface area of each cement sample An air permeability apparatus complying with ASTM C204-11 "Standard Test Method for Fineness of Hydraulic Cement by Air Permeability Apparatus" [53] was used here. The air-permeability apparatus was calibrated in accordance with ASTM C204 section 4.

Particle size distribution analysis, however, offers more insight and accuracy on the distribution of fines fractions [19, 20]. Cement particle size influences the hydration rate and strength; it is also a valuable indicator for predicting cement quality and performance [54], [55].

While Blaine fineness is widely used in the cement industry for quality control, and is reported on mill certificates, it has its shortcomings. While several cements can share the same Blaine fineness, they can have very different fines distribution. In contrast, particle size distribution (PSD) measurements provide more accurate insight on the grading of the cements[56]. An LA-950 laser scattering particle size analyzer manufactured by HORIBA Instruments was used to analyze the particle size distribution of the cements. The instrument has the capacity to measure wet and dry samples in the range of 10 nm to 3 mm. Sample preparation was conducted per manufacturer procedures. An adequate amount of dry cement was homogenized by mechanical agitation through the flow cell of the instrument at the start of measurement [54]. The characterization of the particles of the as-received cements was conducted using the principle of laser diffraction. That is, a particle scatters light at an angle determined by its particle size and the angle of diffraction increases with a decrease in the particle size.

For concrete mixture preparation, the specific gravity of Portland cement is a required property. The specific gravity of the as-received cement was determined in accordance with ASTM-C 188-09 [3].

3.1.2 Physical Properties of Aggregates

The physical properties assessed on fine and coarse aggregates used in this study were bulk specific gravity (BSG), absorption capacity (AC) in addition to grading. The aggregates were washed, sieved, dried and separated into containers so that they could be compiled to the same grading for concrete mixing. Both the coarse and fine aggregates were separated in the same manner. Oolite, a limestone aggregate, graded to #57 stone blend was used as the coarse aggregate and silica graded sand was used as the fine aggregate. The coarse aggregates were tested in accordance with ASTM C127-07 [57] to determine the specific gravity and the

absorption capacity. The (AC) and (BSG) properties of the silica sand fine aggregate were conducted in accordance with ASTM C128-07 [58].

3.2 Mortar Tests

3.2.1 Apparent Activation Energy

The objective of this study is to study the effect of accelerator dosage on properties and cracking potential of pavement concrete mixtures. Towards satisfying this objective, mortar cubes, for different mixtures incorporating variable accelerator dosage, were prepared for strength measurements and apparent activation energy determination. The mortar proportions were identical to that of the concrete mixes, with the exception that, the coarse aggregate was replaced with fine aggregate as per instruction for mortar preparations in ASTM C 1074-11 [59], Annex A1.1.2 of the specification indicates that the proportion of mortar mixes has to be such that the mixtures have a fine aggregate-cementitious ratio (by mass) that is the same as the coarse aggregate-to-cement ratio of the concrete mixture under investigation. The paste shall have the same water-cementitious materials ratio and the same amounts of admixtures that are in the concrete mixture. This ratio of coarse aggregate-cement was determined to be 1.86 for the concrete mixtures used in this research. Therefore, a fine aggregate-to-cement ratio of 1.86 was used to proportion the aggregate used in the mortar cubes. Mortar cubes were prepared for 5 different mixture proportions. For each mixture proportions, 9 mortar cubes were prepared at a time, summing up to a total of 27 cubes of each mixture to assess the mortar strength with age at three different temperatures of 23°C, 38°C, and 53°C. The testing ages were at 2, 3, or 4 hours, 6 hours, 12 hours, 24 hours, 48 hours, 72 hours, 7 days and 28 days. The initial testing age was either: 2 hours, 3 hours or 4 hours depending on the setting time, dosage of accelerator used in

the mortar and the temperature. In Table 1 the mix design for a 9 cube batch is presented for the 5 different mortar mixtures.

Table 1 Table of mix proportions used in mortar cubes for all 5 mixes

SW MORTAR	C	CNA	CHA	CA	SMO
W/C Ratio	0.38	0.38	0.38	0.38	0.41
Materials in the Mix	(g)	(g)	(g)	(g)	(g)
Cement	926.9	926.9	926.9	926.9	926.9
Ottawa Sand (SSD)	1730.2	1730.2	1730.2	1730.2	1730.2
AEA	0	0.2	0.2	0.2	0.2
$CaCl_2$ Accelerator	0	0	17.3	34.6	59.9
Water from Accelerator	0	0	10.5	21.1	36.5
Water Reducer/Retarder	0	3.5	3.5	3.5	3.5
Mix Water	361.1	361.1	350.5	339.9	339.9

3.2.2 Setting Time

The time of set experiments described in ASTM C403-08 [60] was utilized and followed to determine the setting time for concrete mixes used in this research. Basically, the setting time experiment determines the resistance of mortar to penetration by standard needle sizes over time at regular time intervals. The testing begins a short time after mixing and continues until the mortar resists penetration by a needle of known area to a penetration resistance of 4000 psi. The mortar which is tested can be obtained by sieving a representative portion of fresh concrete through a #4 sieve or obtained directly from prepared mortar. Immediately after each test, the mortar needs to be returned to a temperature controlled environment depending on the temperature that setting is being determined, and the test is continued until final set is reached.

The setting time of concrete is defined as the length of time until the concrete is no longer plastic and can sustain some specified load. In this research, the setting time was an important parameter to determine for multiple reasons. Setting time was used as an indicator to specify the initial age for mechanical properties testing; additionally, it was used to identify the timing of initiating free shrinkage measurements as described in section 3.3.4.

Fresh concrete was wet sieved through a 4.75 mm opening sieve (#4) and then placed into the appropriate container for testing. Determination of the setting time for mortar was conducted at three temperatures: 23°C, 38°C, and 53°C for apparent activation energy determination. The apparent activation energy is a necessary property to generate the maturity curves for the different concrete mixtures.

3.3 Concrete Tests

Several concrete mixtures were prepared according to the mix design in Table 2. The proportions in the table are for a yield of 1 cubic yard, typically a 1 cubic foot batch was made in the lab.

Table 2 Mix design followed for cylinders cracking frame & free shrinkage frame

Mixture Proportions	C	CNA	CHA	CA	SMO
	(lbs)	(lbs)	(lbs)	(lbs)	(lbs)
Cement	900	900	900	900	900
Oolite (SSD)	1680	1680	1680	1680	1680
Silica Sand (SSD)	831	831	831	831	831
AEA	0	0.2	0.2	0.2	0.2
Accelerator	0	0	16.8	33.6	67.2
Retarder/WR	0	3.37	3.37	3.37	3.37
Mix Water	346	346	335.4	325	325
W/C	0.38	0.38	0.38	0.38	0.41

3.3.1 Fresh Concrete Properties

In order to assess the effect of accelerator dosage on concrete fresh properties, the following tests were conducted: temperature, slump, and unit weight. The tests were conducted according to the procedures outlined in ASTM C 1064-12 [61], C143-10 [62], and C138-12 [63]respectively. Please include references. The pressure method was used to measure the fresh concrete air content according to ASTM C231-04 [64].

3.3.2 Mechanical Properties Development of Concrete Mixtures

For each mixture design, a set of 31, 4 x 8 in, concrete cylinders were prepared to assess mechanical properties development of concrete mixtures with variable accelerator dosage. Compressive strength, tensile splitting strength, elastic modulus and Poisson ratio at 6 different ages were measured using a hydraulically driven (MTS) machine Model 810. The testing ages for cylinders were: 3 or 4 hours (depending on setting time), 6 hours, 12 hours, 24 hours, 3 days, 7 days, and 28 days after mixing. The cylinders were de-molded and tested just after reaching final set, as determined from ASTM C403-08 [60]. All of the mentioned mechanical properties were determined for concrete cylinders prepared and stored at 23°C. For each testing age, 2 cylinders were tested for compressive strength in accordance with ASTM C39-12 [65], 2 cylinders tested for tensile splitting strength ASTM C496-11 [66]. Thermocouples were inserted into two of the cylinders to monitor concrete's temperature throughout the test for development of the appropriate maturity curves. In the concrete mixtures containing accelerator, the compressive strength was measured as early as 3 hours after mixing. For compressive testing and elastic modulus testing the loading rate was 370 pounds/second, and 200 pounds/second for tensile splitting.

Tensile splitting tests were conducted on concrete cylinders as early as 3 hours at each age for the five different mixtures tested in this study. The testing was performed in accordance with ASTM C496-11 [66]. Two 4 x 8 inch cylinders were tested at each age so that the average tensile strength could be reported. The loading rate that the cylinders were subject to during testing was 0.20 Kips/sec until failure.

Two cylinders at each age were tested for compressive strength measurements following procedures in ASTM C 39-12 [65]. The cylinders were tested in compliance with the procedures outlined in the ASTM. The load rate for the cylinders was 0.37 Kips/sec, until failure. The tops of the cylinders were carefully finished to ensure good testing surfaces were achieved. Testing caps fitted with neoprene pads were utilized as per the specifications of the ASTM C1231 [67].

A Humboldt compressometer/extensometer was used to determine the elastic modulus of concrete throughout the test from ages from 6 hours to 28 days in accordance with procedures specified in ASTM C469-02 [66]. The static elastic modulus test was conducted in compression using a cylinder fitted with the compressometer device. Three tests were performed per testing age. The first test was to seat the gauges, and the following tests were used to determine the elastic modulus. Determined from the compressive strength tests on the concrete cylinders, forty percent of the ultimate concrete strength was used as the maximum load applied to the cylinder in the compressometer/extensometer device. The data was recorded using a p-daq software program and a data-logger module, model OMB-DAQ-56, connected to a laptop which displayed and recorded the data in excel in real time. There are 8 contact points that screw driven pins make with the cylinder when it is in the device. These pins and these are tightened to not permit the cylinder to move during the loading for the duration of the test. The cylinder is loaded and

unloaded at a rate of 370 pounds per second (0.37 kips/sec) up to the 40 % of the compressive ultimate failure load.

3.3.3 Cracking Potential Tests

The cracking potential of concrete mixtures was assessed using two different measurements: autogenous shrinkage using a free shrinkage frame and restrained stress development using a rigid cracking frame. Both frames were able to be temperature controlled using simulated field temperatures by circulating tempered fluid through copper pipes embedded in the forms and fluid jackets in the steel crossheads. The copper pipes in the forms and fluid jacket in the crossheads were connected through insulated flexible hoses with quick connect fittings. The free shrinkage frame allowed the concrete to expand or contract freely. Electronic measuring devices were used to measure these displacements [36]. The rigid cracking frame is a rigidly constructed frame that provides restraint on the concrete and as the concrete expands or contracts, strain gauges mounted on the frame measure the forces that the concrete puts on the frame [68]. Through a calibration factor determined by loading and unloading with hydraulic rams, a calibration curve was generated to relate deformation to a force and stress when the cross section of the concrete specimen is factored in.

Simulated field temperatures were generated using Concrete Works software for all the mixtures tested in the cracking frame and free shrinkage frame [69]. The software has several input parameters that are used to simulate the temperature of concrete elements in field conditions for different geographical locations as well as the concrete mixtures potential for heat generation. These temperature profiles were generated using the environmental conditions, geometric properties, construction practices, batch proportions, and hydration parameters representative of each mixture and their respective site conditions. Some input parameters

include daily maximum and minimum air temperatures at the site location, cloud cover, humidity, the cement properties and fineness, the type of subgrade/ sub-base used, the curing method and the materials used to cure can also be specified.

When first using the software, several inputs need to be entered. The first step is to establish the scope of the concrete work and to identify a geometry for the element, and then to determine a geographical site location for the work. If pavement is selected as the scope of the work, the next step is to specify the pavement thickness or depth and sub-base/ subgrade type and thickness. Once that is finished, the concrete mixture proportions need to be input, including cement, water and aggregate ratios plus all liquid and mineral admixture quantities, if any are to be used. Additionally, there are inputs for heat of hydration based apparent activation energy from isothermal calorimetry, as well as the hydration parameters α, β and τ as determined from semi-adiabatic calorimetry.

The construction inputs pertaining to site conditions are the next inputs, allowing for fresh concrete temperature to be input as well as placement temperature. Details about the curing method, number of coats of curing compound or sheeting material/blanket and the color of the blanket are input next. The time between placement and curing application can be indicated as well. The daily environmental changes can be input next, from the daily maximum and minimum temperatures to the average wind speed, the average percent cloud cover, the relative humidity, and the yearly temperature for that region.

When all the inputs have been entered, a summary page indicates to the user if any parameters are questionable. If all the inputs are correct, a predicted concrete temperature can be generated for a period up to one week. The outputs that are generated from the simulation include, the maximum and minimum temperature in the concrete member, the maximum

temperature difference and an ambient temperature. Additionally, Concrete Works can output the temperature at every depth of the slab, not just maximum and minimum. To summarize the inputs used in Concrete Works to generate the simulated temperatures, see the following list:

- Geographic location
- Time of placement
- Slab thickness
- Mix proportion
- Environmental conditions
- Placement temperature
- Curing method
- Curing time
- Hydration parameters
- Aggregate type
- Cement type

3.3.4 Free Shrinkage Frame

To measure the strain developed in high performance concrete mixtures a free shrinkage frame was constructed and utilized for this research. The frame is a rigid formwork that is temperature controlled, and features movable form walls that can be backed away from the concrete at the time of setting. The concrete in the free shrinkage frame experiences thermal strain and autogenous strain; it is not subject to drying shrinkage since specimens are completely sealed up using water proof tape and silicone to prevent any loss of moisture from the concrete in the frame. A schematic of the frame can be seen in Figure 2. Additional schematics and instructions on how to construct a free shrinkage frame can be found in the Appendix A.1.

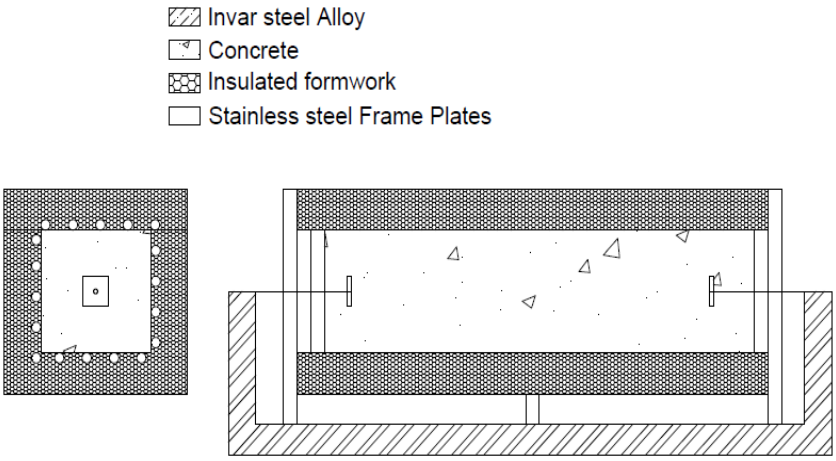

Figure 2 Cross sectional drawing of free shrinkage frame and elevation view of frame

The frame has a copper plate lined formwork and temperature controlled cooling lines to control the temperature inside an insulated box. The ends of the box can be moved away from a fresh concrete specimen at setting. The frame allows measurements of the concrete free strain from deformations and volume changes, after the concrete is placed [30]. The free shrinkage frame sits on an Invar steel chassis to increase the accuracy of recorded deformations.

Figure 3 Free shrinkage frame empty

The measurements recorded before setting are not important because the concrete is still hardening. Therefore the data is analyzed from when the concrete reaches final set, onward. Free autogenous deformations are measured from the ends of the concrete prism, by two linear conductive potentiometers (LCPs), which are fixed at each end of the frame on two Invar rods. The fixed LCPs are connected to a thin 1/8th inch diameter Invar rod that is attached to a thin metal plate that is embedded in the end of the concrete. This allows for deformations to be transferred to the LCP devices. The aluminum squares are only situated an inch and a half into the concrete ends to get good confinement all around them. The deformations from the two opposite ends of the frame are summed together to obtain a total deformation. This practice of measuring from both sides is done to capture the entire shrinkage that takes place in case any differential deformations occur. Since the two LCPs were calibrated individually to a known displacement, they both have different calibration factors. Each LCP device comes with small threads so that the thin Invar rod can be threaded to the LCP, for a firm connection. The thin Invar rod passes through the stainless steel plates of the free shrinkage frame and into the concrete prism approximately 1-3/4 inches. The entire concrete specimen is 23.5 inches long or approximately 600 mm long. The distance between these two plates is referred to as the gauge length. The gauge length between plates is approximately 500 mm or 19.8 inches.

Strain in the concrete is calculated by dividing the change in displacement by the original length, or in this case the gauge length. Concrete prism dimensions for the free shrinkage frame are 6 inches x 6 inches x 23.5 inches. The frame used in this research was constructed by the author and is depicted in Figure 4.

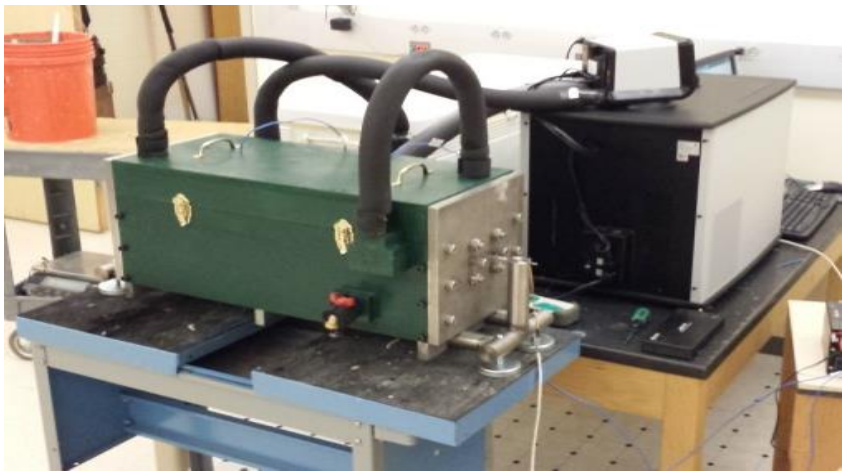

Figure 4 Free shrinkage frame set up

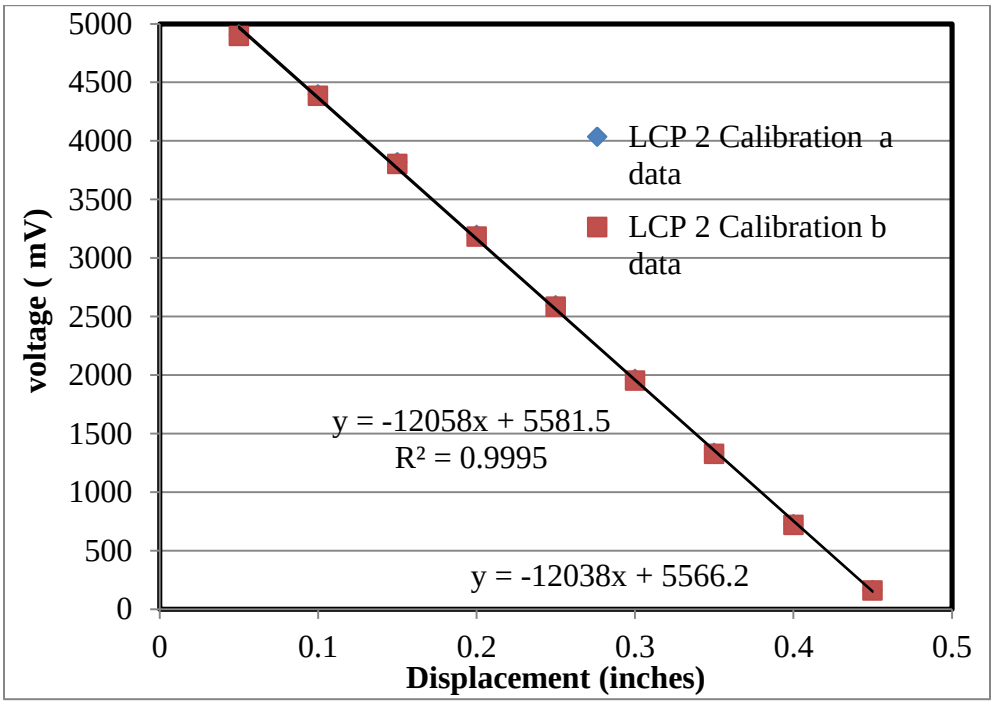

Figure 5 Calibration curve for LCP device, measured in steps of 0.05 inches

Before concrete is mixed, a great deal of preparation must take place to get the frame ready. First the polished copper formwork must be free of any debris or damage. Plastic sheeting must be placed as a form liner. Any gaps or seams must be sealed with silicone or waterproof

tape to create a water tight liner that prevents any loss of moisture during the experiment. Minimum folds and flaps are made in the plastic and the plastic sheet is folded in a manner that reduces any unnecessary friction with the concrete. A combination of Nashua air conditioning aluminum tape, GE type II silicone caulking and Lucas Oil brand bearing grease were used to prevent moisture loss from the frame and in locations where holes need to be made for strain measuring rods and thermocouples. The aluminum tape is used to tape down plastic folded flaps, and to tape the cover plastic sheet after concrete has been placed. The bearing grease is used to lubricate the ports that the 1/8th inch diameter Invar rods pass through. Additionally, a small length of plastic tubing is packed with grease and then slid onto the Invar rod to provide a bond breaker between the concrete and rod. The thin rods are threaded onto small aluminum plates that are embedded in the concrete prism to give the LCP an anchor point to measure deformation from. The aluminum plates are located 1-3/4 inches in from the stainless steel plate giving the specimen an effective length of approximately 20 inches. Efforts were made to prevent any friction or restraint on the concrete in the free shrinkage frame. In between the plastic sheeting, lubricant was used to reduce friction between the concrete, plastic and the copper form walls. When a sample was prepared, careful placement of concrete around the thin Invar rods and aluminum plates was critical so the thin rods did not get bent during the concrete placement. Small bends in the thin Invar rods can be a source of restraint for the small displacements being measured, and can affect the results of the test. If the test is prepared correctly, the LCPs allow for the deformations to be measured without affecting or restraining the sample inside the insulated formwork.

Retractable formwork end plates inside the frame are required to be in place during placement and before setting to form the concrete prism's ends. The form end plates are reverse-

threaded so that after the concrete sets, they can be backed away from the concrete surface evenly, with just the turn of a few screws. Just after the plates are moved, allowing the concrete to expand freely, the data analysis begins. A CR1000 data logger from Campbell Scientific was used for data collection. A stand-alone battery power supply is used for the data logger to limit fluctuations in supplied current to the LCP devices. A desktop computer was used to interface between devices and was used to control a water bath connected to the free shrinkage frame formwork. Copper pipes were embedded in the formwork to allow tempered water to flow through and control the temperature of the concrete. There was also flexible Blue-push lock insulated tubing connecting the frame and circulator, with quick connecting hose fittings. The concrete temperature was monitored using thin type T thermocouples embedded in the center of the concrete prism.

Figure 6 Type T stainless steel thermocouples used to determine the temperature of the concrete in the free shrinkage frame

Through the use of the VWR 28 Liter model number 89203-010 circulating bath, the concrete temperature was controlled within the ± 1°C for the duration of the experiment with some tests deviating to within 3°C. The computer interface responds to the concrete temperature

by rapidly and constantly adjusting the bath temperature, by heating or cooling when necessary to keep the concrete at the target temperature. As the temperature rises due to heat of hydration reactions, the bath responds with cooler water circulating in the lines to keep the temperature of the system at the desired target temperature. As the heat generating reactions slow, the bath responds with increasingly warmer water to maintain the target temperature. The system can run in an isothermal setting, maintaining a specified temperature or it can be operated under a varying temperature control using a pre-programmed temperature profile. Isothermal tests were run to provide autogenous shrinkage measurements that are not altered by thermal stimulation, and the heat generated during heat of hydration is curbed by the bath. The free shrinkage tests performed using simulated realistic field temperatures are to determine deformation measurements that are generated as the temperature changes. For example, cooling would induce thermal shrinkage and heating would lead to expansion.

3.3.5 Cracking Frame

A scaled version of the rigid cracking frame developed by the Technical University of Munich, was constructed and used to measure uniaxial stress under restrained conditions on concrete specimens. The dimensions of the concrete in the frame are 4 inches x 4 inches x 40 inches with dovetail ends that are designed for restrain development in the frame. Like the free shrinkage frame, the cracking frame also features active temperature controlled formwork with polished copper formwork and copper tubing throughout the frame. The cross heads are constructed of half inch thick steel plates are connected through solid parallel 2.67 inch diameter Invar steel bars. The frame is constructed with large ¾ inch diameter grade 8 high strength steel bolts for non-slip bolted connections. The crosshead formwork feature teeth that provide a hold-fast connection between the concrete and the frame. When the concrete starts to shrink after it

has hardened, it pulls on the teeth and the frame start to go into a compressive state. Specifically the parallel Invar bars go into compression and their cross section gets deformed, deforming the train gauges that are mounted on the steel Invar bars. The Invar steel alloy contains 36% chromium and has a very low coefficient of thermal expansion (CTE), which is 1.2 m/m °K, which is only second to diamond on the scale the scale of thermal expansion of materials. This low CTE is critical for the small changes in strain that are measured during the experiments and to ensure that temperature fluctuations in the air temperature in the laboratory and the temperature of the frame do not influence the strain readings that are being collected during the test.

The steel cross-heads are fabricated from ½ inch cold rolled steel plates. These plates were cut according to schematics and were then cut and welded for construction. The conductive steel cross head are capable of conducting temperature quite well; therefore, water chambers were designed into the crossheads to control temperature of the ends of the concrete element. Quick connect ½ inch inner diameter pipes connected to the circulating bath flow temperature controlled water into and out of the water chambers in the cross heads to control temperature in the frame.

Upon construction, the crossheads and chambers were cleaned and leak tested after all the fabrication, cutting and welding. The metal parts were cleaned with automotive Brake-kleen® parts cleaner inside and out. They were then coated on the inside with liquid gas tank liner twice to protect the steel from coming in contact with the water and ethylene glycol circulating fluid. The crossheads were also painted on the exterior with Rustoleum® metal paint to protect the exterior surface.

The strain is measured from both of the parallel Invar bars on the frame in the event that the strain was non symmetrical. The strain gauges used on each Invar bar are four 90 degree rosette gauges purchased from Vishay micro-measurements manufacturing; model number CEA-06-250UT-350. Each rosette consists of a pair of 350 ohm strain gauges oriented 90 degrees from each other so to measure the very mall axial strains. The gauges are wired in a four wire full bridge circuit; a schematic of the circuit is displayed in Figure 7. The dovetails on the cross heads are cambered in at the bottom slightly to allow for easier removal of concrete once the test is over.

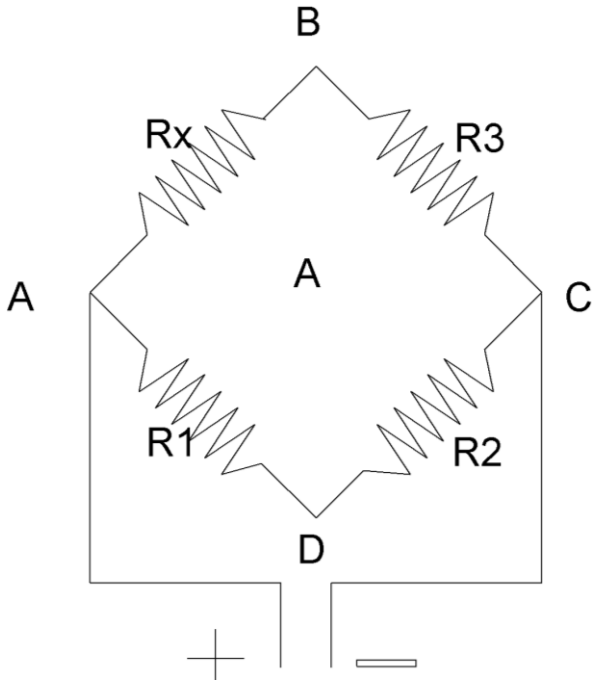

Figure 7 Example schematic of Wheatstone bridge circuit used to wire strain gauges on Invar bars

The rigid cracking frame was designed to provide 100% restraint on fresh concrete placed in the frame however, the amount of restraint does decrease as the concrete hardens. The degree of restraint is dependent on the ratio of stiffness of the concrete to the stiffness of the Invar steel bars, see Equation 3. The restraint comes from the fact that as the concrete shrinks it

is resisted by the steel going into compression. The steel deforms some because of its modulus of elasticity, meaning that the concrete moves the same amount as the steel. The amount of restraint is dependent on the stiffness ratio see Equation 4.

Temperature rise in the Invar bar may have an effect on the strain measurements that are recorded directly from the bars; therefore, thermocouples were installed on the bars to determine the temperature.

$$\varepsilon_{Tin} = \Delta T_{ib} * \alpha_{ib} * K_r \quad \text{Equation 7}$$

where,

ε_{Tin} = temperature induced strain of the bar

ΔT_{ib} = the temperature change in the bar at the strain gauge (°C)

α_{ib} = coefficient of thermal expansion of the bar (1.2 x 10^{-6} K^{-1}) or (1.2ppm/°C)

K_r = the degree of restraint

The force in the Invar bars is measured by calibrating the strain measured in the Invar bars with increasing known loads. A calibration sequence was followed that consists of loading the frame by placing a threaded steel bar through holes in the frame in the crossheads. The threaded bars were then loaded using a hydraulic ram. A load cell was placed between the ram and crosshead to measure the force on the frame. The force in the bar was plotted against the strain in the Invar steel bars, see Figure 8. A best fit line was then drawn through this plot to verify the accuracy of the calibration. When the concrete is in the cracking frame and shrinking, the Invar contracts and the voltage difference from the strain gauges is used to calculate the stress.

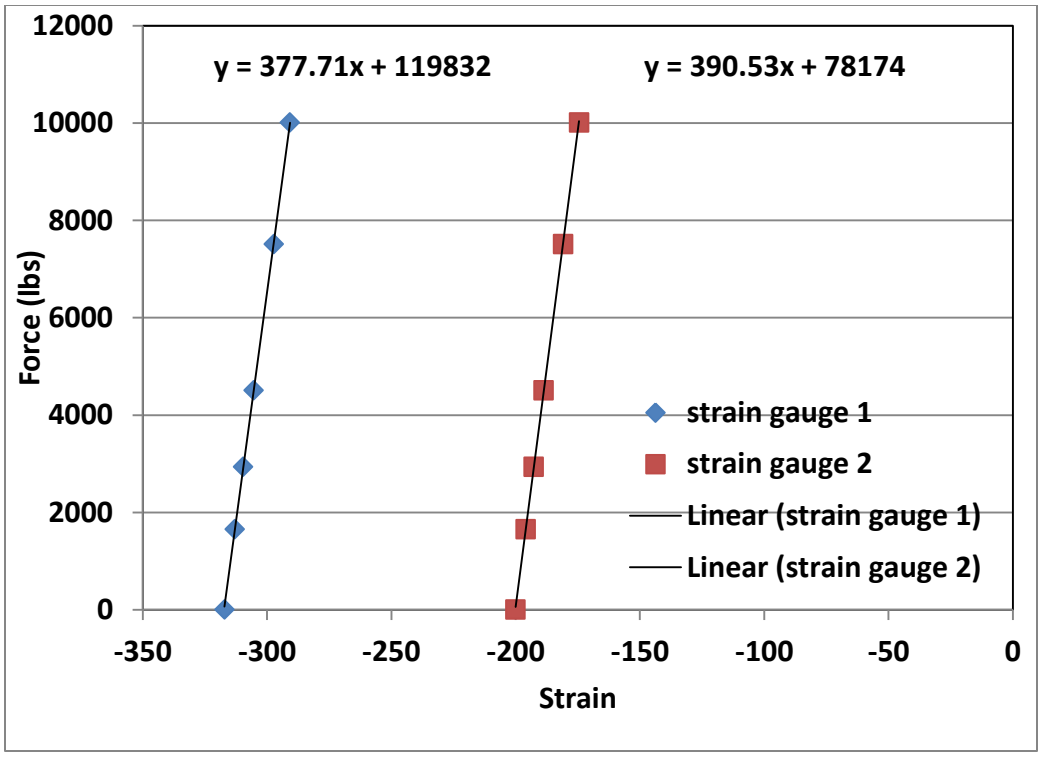

Figure 8 Calibration curve for the Invar bars used on the rigid cracking frame

The Invar bars are tensioned through the use of high strength nuts threaded onto short length threaded rods that thread into the Invar and through the back of the steel crossheads. The Invar bars are tensioned so that at no time during the expansion or contraction of the frame does the bolt connecting the frame to the Invar bar switch sides of the hole it bears against. Additional nuts both standard and reverse thread are in place on the frame to prevent loosening. The frame should be recalibrated or every twenty tests so that the readings collected areas accurate as possible.

CHAPTER 4: RESULTS AND DISCUSSION

In this chapter, the findings of the experiments will be presented and discussed. The characterization of the as-received materials will be first presented followed by the setting and fresh concrete properties. Mechanical properties of hardened concrete and maturity curves of concrete mixtures and mortar will be discussed next and finally the results on the effect of chloride-based accelerator dosage on the cracking potential and autogenous shrinkage of concrete will be discussed.

4.1 Characterization of As-Received Materials

4.1.1 As-Received Cement

4.1.1.1 Oxide Chemical Composition Using X-Ray Fluorescence

The oxide chemical analysis of the as received SW cement is presented in Table 2. The potential phase content of the cement was calculated using Bogue equations with and without limestone corrections. The cement can be classified as Type II cement according to ASTM C150 [48]. It is noted that heat index is above 90 which then would indicate that fineness maximum limits will be implemented if the cement is to be classified as Type II (MH). However, with limestone corrections, the heat index drops to below 90 and the cement could also be classified as Type II (MH).

4.1.1.2 Mineralogical Analysis Using XRD and Rietveld Analysis

It is well established that the phase content of Portland cement is very useful in predicting and modeling concrete performance [28]. Direct determination of cement phases using x-ray diffraction and Rietveld analysis yields more accurate results than indirect methods of phase

quantification [70]. The mineralogical composition of the cement is presented in Table 4, where it is noted that there are differences in phase quantification between the phase content determined by XRD versus Bogue formulae. This is expected as the Bogue formulae gives potential phase content and relies on several assumptions while Rietveld refinement of XRD data calculates the phase content from fitting a diffraction pattern to the measured diffraction [50]. Mineralogical analysis indicates that the sulfates present in the cement are predominately calcium sulfates (gypsum, anhydrite or hemihydrate). There are no double alkali sulfate compounds, which could indicate that the alkalis present in the cement are probably present as impurity oxides.

Table 3 Oxide chemical analysis for as-received cements*

Analyte	SW cement (wt. %)
SiO_2	20.4
Al_2O_3	5.2
Fe_2O_3	3.2
CaO	63.1
MgO	0.8
SO_3	3.6
Na_2O	0.1
K_2O	0.38
TiO_2	0.28
P_2O_5	0.12
Mn_2O_3	0.03
SrO	0.08
Cr_2O_3	0.01
ZnO	<0.01
L.O.I(950°C)	2.8
Total	100.1
Na_2O_{eq}	0.35
Free CaO	2.23
SO_3/Al_2O_3	0.69

***** Tests conducted by a certified commercial laboratory

Table 4 Bogue calculated potential compound content for as-received cements

	Without Limestone Correction	With Limestone Correction
Phase	SW	SW
C_3S	52	50
C_2S	19	19
C_3A	8	8
C_4AF	10	9
C_4AF+2C_3A	26	26
$C_3S+4.75C_3A$	92	89

Table 5 Mineralogical composition of as-received cement using x-ray diffraction

Cement Phase	SW
C_3S (%)	52.0
C_2S (%)	20.7
C_3A (%)	10.2
C_4AF (%)	5.7
Gypsum	4.4
Hemihydrate	1.6
Anhydrite	0.2
Calcite	2.1
Lime	0.1
Portlandite	2.0
Quartz	0.9
Periclase	0.0
Arcanite	0.0
Syngenite	0.0

4.1.1.3 Physical Properties of As-Received Cement

Blaine fineness and specific gravity of SW cement are presented in Table 5. The Blaine fineness reported here is above the limit specified for Type II (MH). The specific gravity reported here for SW is typical for what is reported for Portland cement.

Table 6 Blaine fineness and specific gravity of cement

Physical Properties	SW
ASTM C204-Blaine Fineness (m^2/kg)	442
Density (Mg/m^3)	3.14

4.1.2 Aggregate Properties

Aggregates used in the experiments were oolite for the coarse and silica sand for the fines. A #57 coarse aggregate grading of oolite limestone was used in concrete preparation. The aggregate properties necessary for concrete mixtures proportioning were measured experimentally. Figure 9 and Figure 10 show the grading curves for the fine and coarse aggregates.

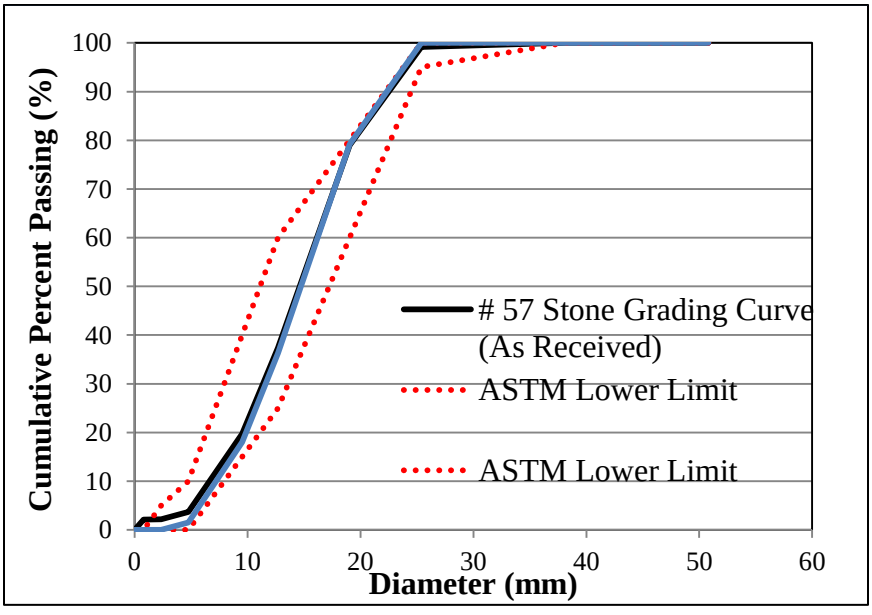

Figure 9 Plot of grading curve for the coarse aggregate Oolite

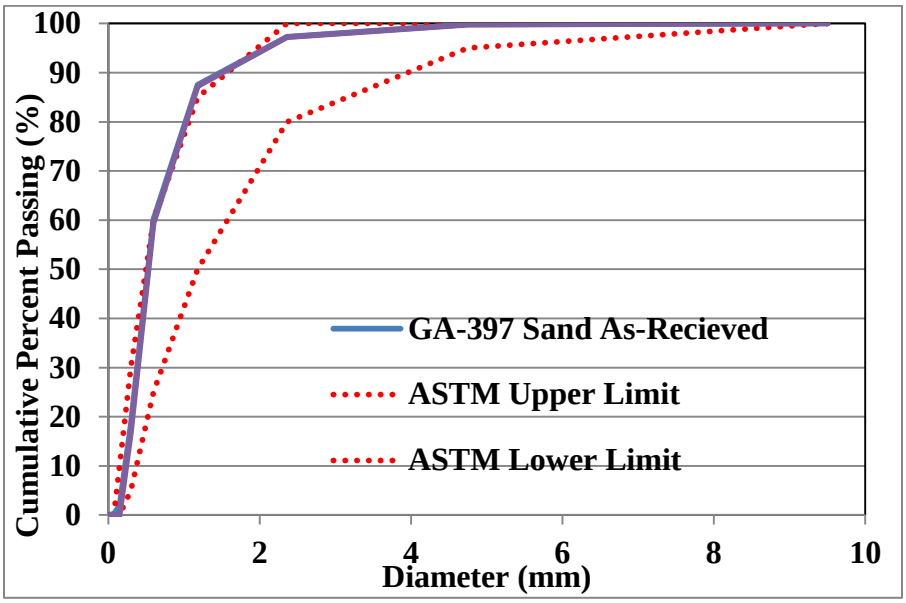

Figure 10 Plot of grading curve for the silica sand fine aggregate comparing as received and graded for experiments against the ASTM limits

Table 7 Specific gravity for coarse aggregates

Property	Oolite	Silica sand
BSG_{OD}	2.36	2.65
BSG_{SSD}	2.43	2.66
% AC	3.1	0.34

4.2 Fresh Properties

4.2.1 Setting Time

The setting time needs to be determined for multiple experiments and purposes. First, it was necessary to know when to de-mold cylinders to be able to test the concrete as early as possible. Second, to know when to de-mold the mortar cubes, so they too could be tested as early as possible. Lastly, the setting time needed to be determined so the movable plates of the

free shrinkage frame could be moved at the moment that the concrete set, so that the deformations from autogenous shrinkage could be measured from this moment forward.

The results for the setting time experiments are presented in Table 7 and Table 8. As expected the higher temperature resulted in shorter setting times. The mixtures containing accelerator don't leave much time for placement, especially at the higher temperatures.

Table 8 Initial setting times for concrete and mortar prepared at 23°C, 38°C, and 53°C

Mixture	Initial Set (23°C) (minutes)	Initial Set (38°C) (minutes)	Initial Set (53°C) (minutes)
CA	145	65	53
CHA	175	85	65
C N A	245	135	105
C	170	85	65

Table 9 Final Setting times for concrete and mortar prepared at 23°C, 38°C, and 53°C

Mixture	Final Set (23°C) (minutes)	Final Set (38°C) (minutes)	Final Set (53°C) (minutes)
CA	180	95	75
CHA	205	120	95
C N A	320	180	160
C	240	135	100

The times of set reveal that the CNA mixture was the slowest mixture to set at all temperatures followed by C and then the mixtures with accelerator in the order of increasing dosage. There is an increase rate of setting as the temperature increases, and that could be troublesome for actual pavements that get too hot.

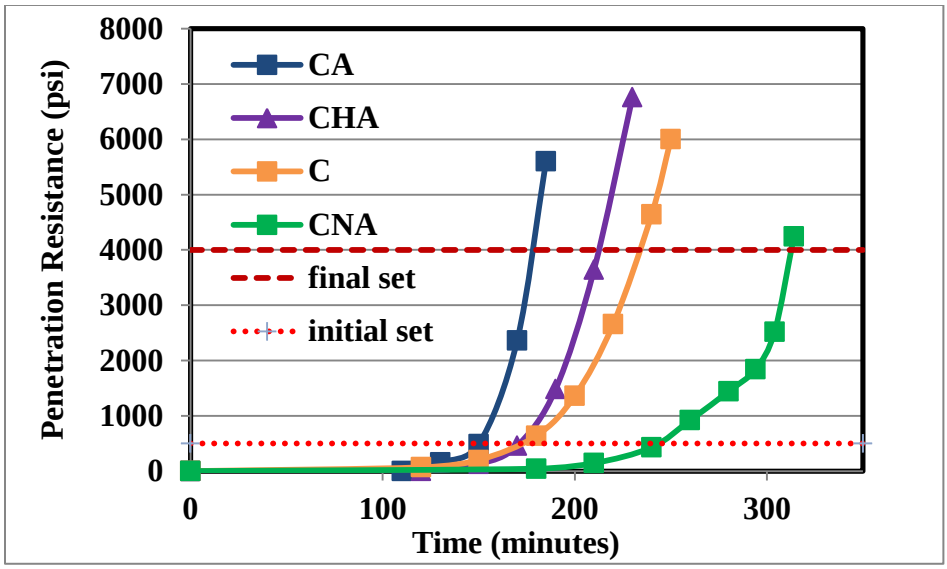

Figure 11 Setting time at 23°C

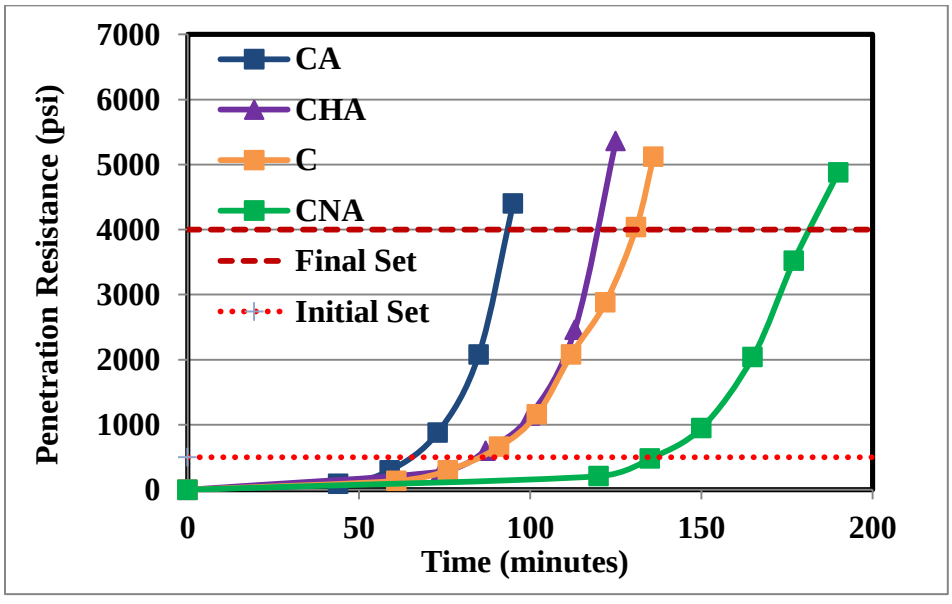

Figure 12 Setting time at 38°C

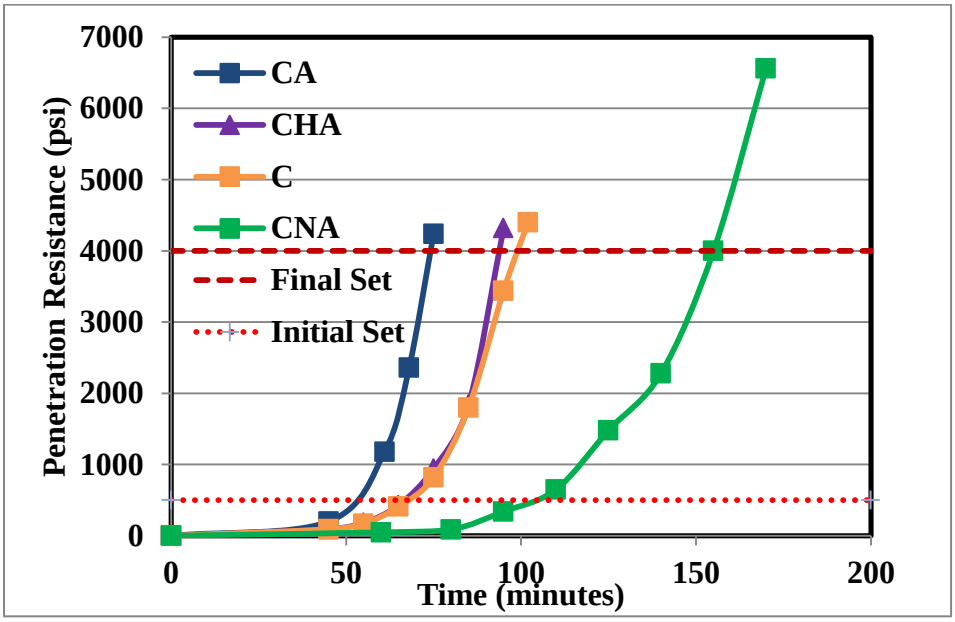

Figure 13 Setting time at 53°C

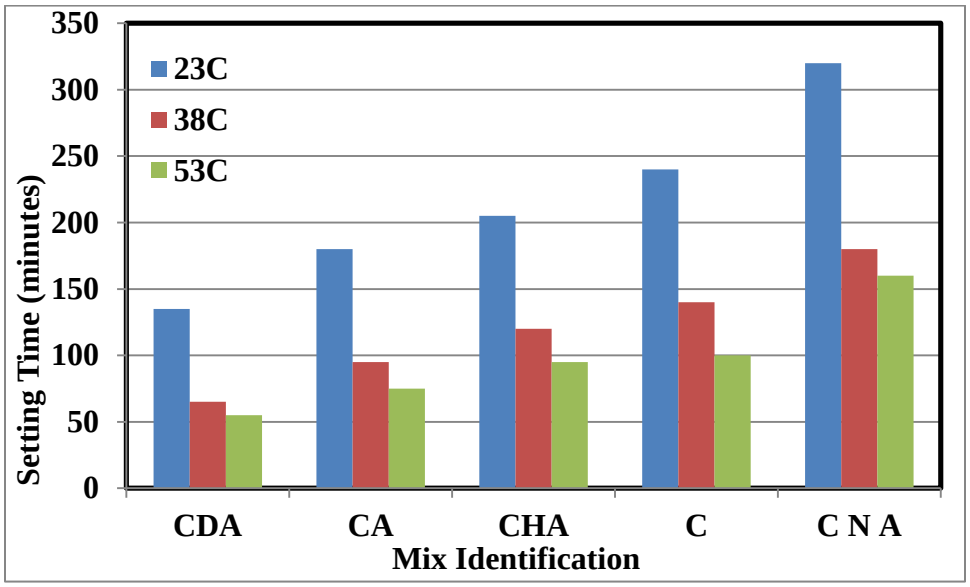

Figure 14 Final setting time trend at 3 different temperatures for all mixtures

4.2.2 Plastic Concrete Properties

In assessing the effect of the chloride-based accelerator on the mechanical properties development and cracking potential of concrete, several concrete mixtures were prepared. The fresh concrete properties that were determined for each mixture are presented in Table 9 where it can be seen that the air content was highest in the CNA. The control mixture, C, had no air-entrainer and therefore the air reported here is entrapped air due to agitation action in the concrete mixer. All other mixes containing the same air-entraining dosage had similar air content with modest decrease on addition of accelerator. Increasing the accelerator dosage appears to reduce the reported air content.

Table 10 Fresh concrete properties determined for SW concrete prepared at 23°C

Mixture	Slump (inches)	Air Content (% Air)	Unit Weight (lb/ft^3)
C	6.75	1.8	140.4
CNA	4.5	4.0	136.7
CHA	8	3.3	140.5
CA	8	3.2	138.9

4.3 Concrete Mechanical Properties Development

Concrete cylinders were prepared and tested to determine the mechanical properties development with age for different mixtures. The concrete mixtures were designed in order to establish the effect of chemical admixtures on concrete properties. Mechanical properties studied were: compressive strength, tensile splitting strength, elastic modulus and Poisson ratio. Wet curing at ambient temperature of 23°C was implemented after the concrete had reached final set

as determined following procedures described in ASTM C 403 [60]. For mixtures containing $CaCl_2$ accelerator, the mechanical properties developed very rapidly at early age, and then the development started to slow. In mixtures without accelerator the strength gain was steady and the mechanical properties continued to develop into later ages, surpassing the performance of the mixtures containing accelerator. Carino and Lew observed this phenomenon when studying the strength maturity relationship [71].

4.3.1 Tensile Splitting Strength

The tensile splitting strength was determined from the concrete cylinders prepared at 23°C. The splitting performance measured from the time of setting to 28 days old is presented in Figure 15. From the presented data in Figure 15, it can be observed that during the first 6 hours the concrete cylinders that contained accelerator had increasing tensile strength with increasing dosage. In other words, the highest tensile strength was attained by CA concrete cylinders, followed by CHA, then by C. However, as the concrete continued to age, development of tensile strength slowed in the mixtures containing accelerator quite rapidly in the same order. CA was passed by the other concretes by the time it was only 12 hours old. The development of tensile splitting strength in the C and CNA mixtures surpassed all the $CaCl_2$ containing mixtures by day 3. These trends imply that the concrete with $CaCl_2$ will quickly develop higher tensile strength than mixtures without, but the tensile strength gain will quickly slow and these mixtures will not develop as high a tensile capacity at later ages. It is critical for the concrete to develop a high tensile strength early on, to resist early age cracking.

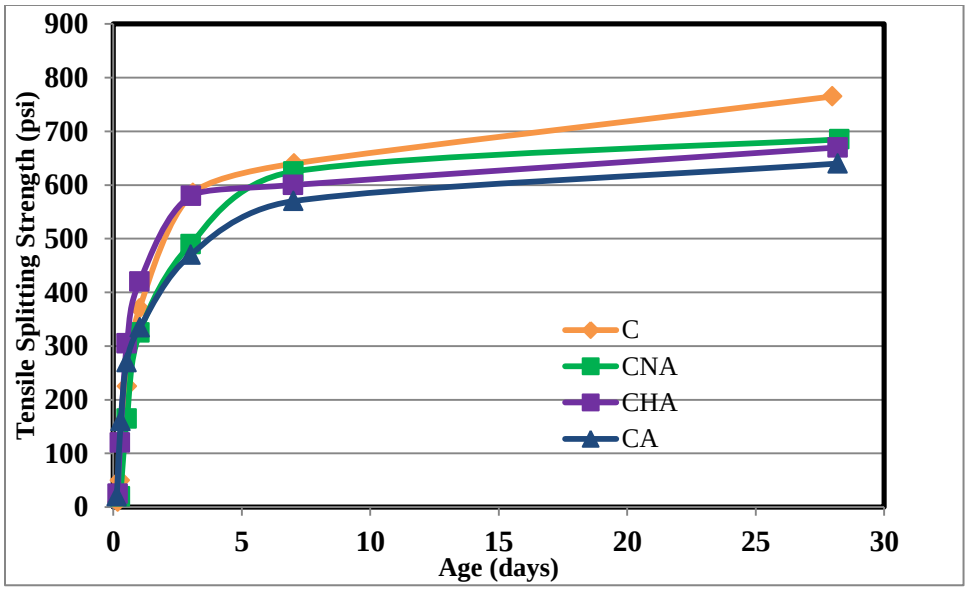

Figure 15 Tensile splitting strength for concrete mixtures cured at 23°C

4.3.2 Compressive Strength

The results for the compressive strength testing of concrete cylinders, mixed, cured and tested at 23°C are presented in Figure 16. Mixture CA which had a short setting time, was tested at 3 hours. For CHA and C mixtures, testing commenced at 4 hours, for the CNA mixture the testing was not possible prior to 6 hours due to the water reducer/retarder action on the setting behavior.

From the results depicted in Figure 15 and Figure 16 it can be observed that incorporation of an accelerator increased the rate of both tensile and compressive strength gain at early age. The effect appears to be dependent on the accelerator dosage. CNA mixture, which had retarder/water reducer, had the lowest compressive strength through the 7 day testing. At later age, concrete compressive strength was consistently lower among the mixtures with increasing dosage of accelerator, and highest in the control mix that contained no chemical admixtures.

From these observations, it is apparent, when compared to the control mixture that the inclusion of admixtures reduces later age performance.

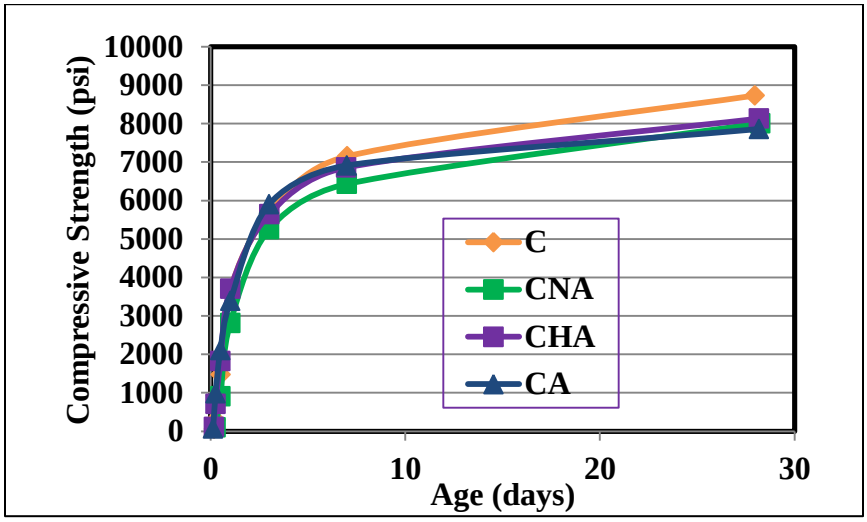

Figure 16 Compressive strength gain for concrete mixtures cured at 23°C

Comparison of the C and CNA mixtures shows that the addition of the water reducer/retarder admixtures has a negative effect on strength gain at early age and the rate of strength development is not fast enough to be used for pavement replacements.

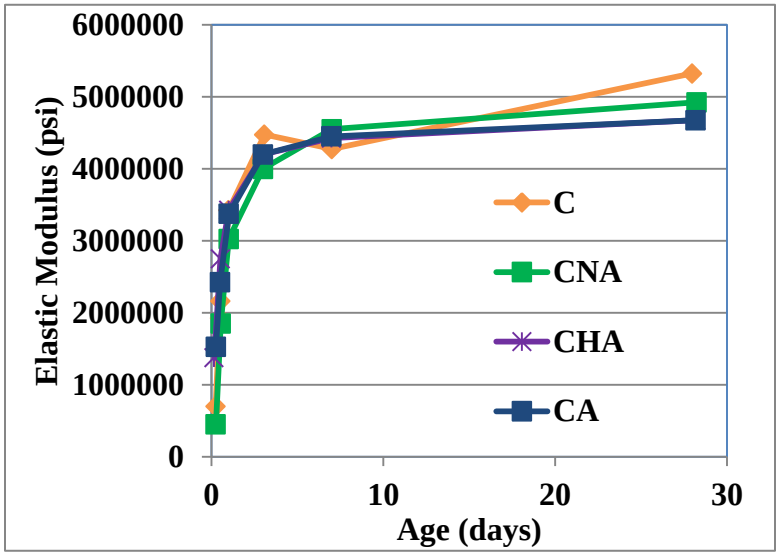

Figure 17 Comparison of elastic modulus measurements from cylinder cured at 23°C

From the analysis of the results, the inclusion of accelerator did promote faster development of the elastic modulus in the concrete mixtures as seen in Figure 17, similar to the trends observed for compressive strength development. Towards the later ages, CNA had the highest elastic modulus, but was surpassed by the control mix in the final round of testing. The control mix was somewhat slow to develop a high value of elastic modulus, but by 7 days, the modulus was comparable to CNA, CHA, and CA mixtures. It seems that low to medium dosage of accelerator will promote reasonable modulus values, but too much accelerator can destroy the potential for elastic development, even in the first 12 hours. Also noteworthy is how the CA and CHA are almost identical in performance in Elastic modulus development too.

Looking at the modulus development curve for the isothermally prepared concrete in Figure 17, there are some trends to note. All of the mixtures had relatively the same modulus development from 12 hours on. The Poisson ratio was developed quickly in the cylinders and by 24 hours all the mixtures had relatively the same ratio, although there was some additional development into 28 days.

4.4 Apparent Activation Energy

The temperature sensitivity of concrete mixtures, or apparent activation energy, is an important property that is used to predict concrete strength development in the field. It can be used to generate maturity curves and therefore identify the time of form removal or opening the construction site to traffic. In this section, the apparent activation energy data will be presented.

4.4.1 Apparent Activation Energy Data Plots

The results of the mortar cubes are presented in Figure 18 through Figure 21. The compressive strength was determined for cubes cured at three different isothermal temperatures of 23°C, 38°C, and 53°C in order to determine the apparent activation energy and equivalent age.

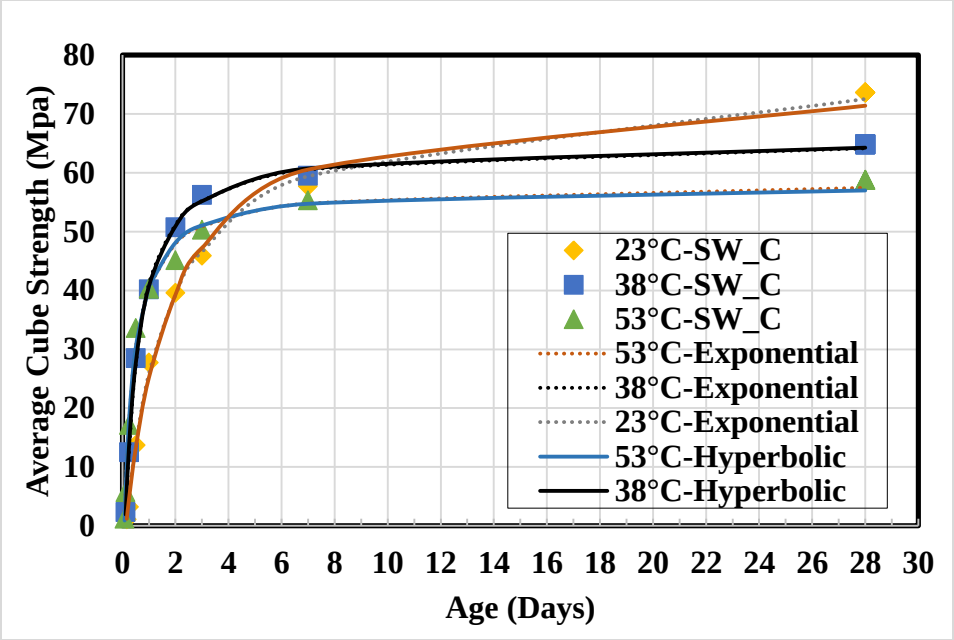

Figure 18 Plot of strength gain for C mortar cubes at 23°C, 38°C, and 53°C. Compared against strength prediction using hyperbolic and exponential maturity methods

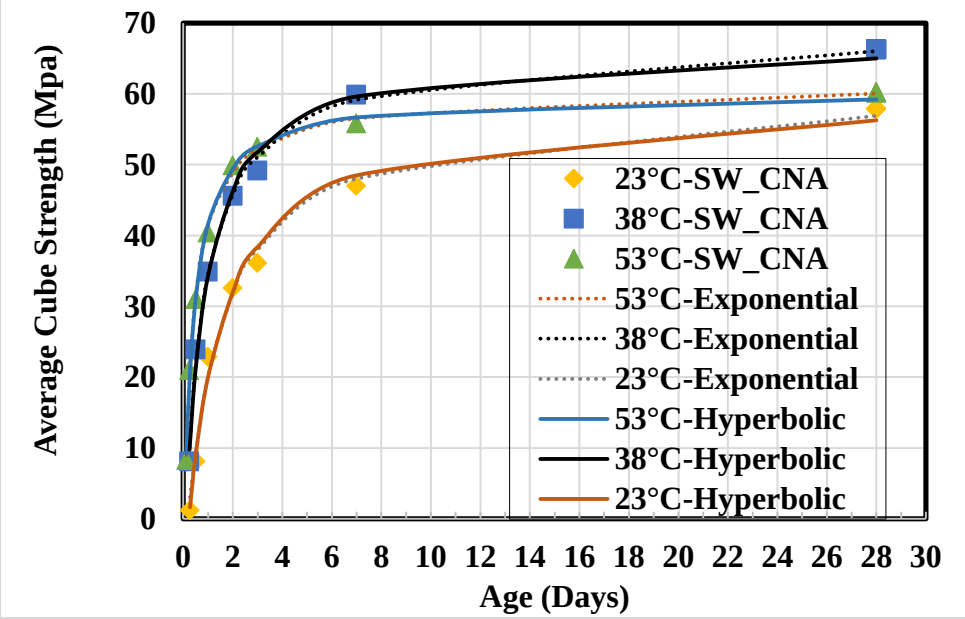

Figure 19 Plot of strength gain for CNA mortar cubes at 23°C, 38°C, and 53°C. Compared against strength prediction using hyperbolic and exponential maturity methods

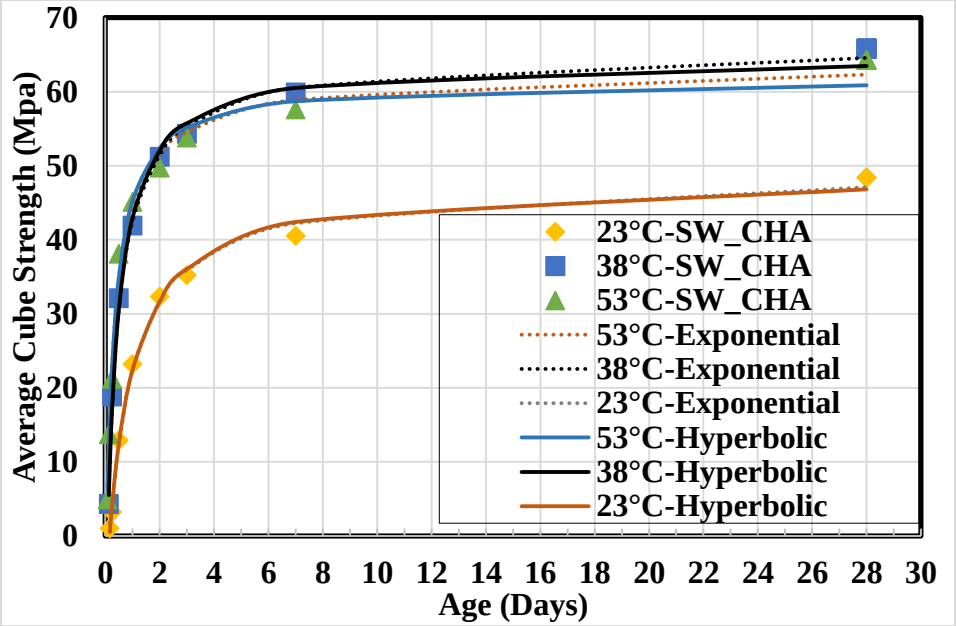

Figure 20 Plot of strength gain for CHA mortar cubes at 23°C, 38°C, and 53°C. Compared against strength prediction using hyperbolic and exponential maturity methods

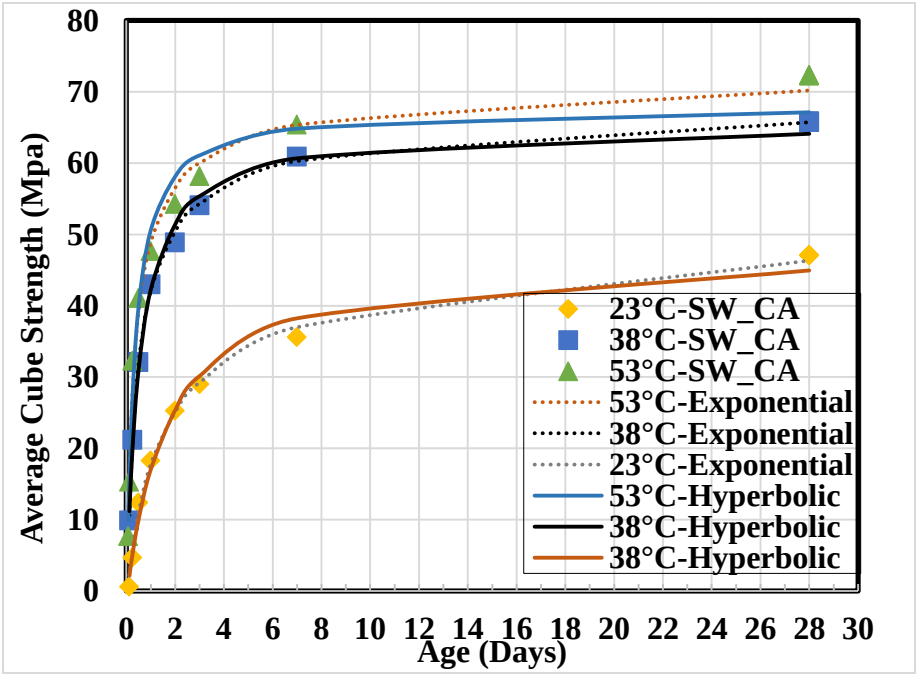

Figure 21 Plot of strength gain for CA mortar cubes at 23°C, 38°C, and 53°C. Compared against strength prediction using hyperbolic and exponential maturity methods

The compressive strength of the mortar cubes was an important element of the research because it provided information on the effect of temperature in combination with the accelerator. In the mixture CA cubes, the higher temperature coupled with the accelerator resulted in significantly higher early and late strengths for both the mortars at 38°C.

Both the hyperbolic and exponential methods were used to calculate the apparent activation energy and they were then compared to determine which method presented a better fit for the data. Recall that for each of the three temperatures, a k-value is generated, and plotted with a line of best fit. Comparing the R^2 values for each of the plots gives an indication as to which model is a better fit. A few things should be mentioned about the model fitting the data. First, the prediction must be performed on the same concrete mix in relatively the same time frame. The hyperbolic functions limitations are applicable only up to 28 days and it also assumes no strength gain until setting time [72].

For the comparison in the C mixture see Figure 18, the hyperbolic method fits the data better. It has been speculated that the hyperbolic function is best suited to determine the change in rate constants with curing temperature because unlike the exponential function, it is not susceptible to variation in temperature [73]. Bien-Aime concluded that the hyperbolic method is the favored method for determining the apparent activation energy to be used in the equivalent age computations at early ages [73].

4.4.1.1 Plotting the Data Using the Constant k

Strength predictions were compared to the actual measured strengths at the different test temperatures. The plots used to obtain the apparent activation energy can be found in the appendix. A plot of the natural log of the k-value versus the inverse absolute temperature in Kelvin was utilized for the slope of the line to enable a hyperbolic function to be used to

determine the value of Q. The Q value was used in determining the equivalent age for CA mortar cubes at 23°C, 38°C, and 53°C isothermal curing. From ASTM C1074-11, it is known that Q is equal to the apparent activation energy divided by the universal gas constant. There is an expected range for Q values that is used to compute the equivalent age, if the Q value is outside of the typical range, apparent activation energy and the equivalent age will not be very accurate.

Based on the best fit curve for the C mix, it is apparent that the hyperbolic method provides a better fit. Therefore the hyperbolic function was used for apparent activation energy determination for all mixtures.

4.4.1.2 What Fits the Data Better?

It appears that the hyperbolic method provides a better fit to the measured data. The exponential estimations are not so far off to warrant saying that the exponential method is not valid.

4.4.1.3 Comment on Strength vs Equivalent Age

What can be seen from the data is that the equivalent age predictions from both methods are reasonable and both methods seem to be valid in that they both fit the data at the different temperatures dosage of accelerators variations. There is a strong predictability from both functions in the early age, but the temperature seems to have a strong impact on the strength gain after 2 days in the warmer mixtures.

4.4.1.4 Comments on Apparent Activation Energy with Accelerator Dosage

The results of the apparent activation energy determinations can be seen in Table 10. The apparent activation energy was estimated to be highest in the CA mixture, which contained the standard dose of accelerator. The exponential estimates were all higher for all mixtures but surprisingly high for the control mix. There was little difference between the prediction of

apparent activation energy between the CNA mixture and the CA mixture, which does not agree with expectations.

Table 11 Apparent activation energy determined with methods in ASTM C1074

Method	C	CNA	CHA	CA
Units	(J/mol)	(J/mol)	(J/mol)	(J/mol)
Hyperbolic	40470	34050	28050	44240
Exponential	38220	36940	29110	47880

The apparent activation energy estimates were compared with heat of hydration (HOH) activation energies, and although these two activation energies are not equivalent there were some interesting similarities with the hyperbolic estimates of Ea. The HOH Ea for mix C was 42000 J/mol-K and the hyperbolic strength estimated value was 40470 J/mol-K. The strength Ea estimate for CNA was 34050 J/mol-K, while the HOH-based value was 35000 J/mol-K. Finally the CA mix strength Ea estimate was 44240 J/mol-K, and the HOH-based value was 52000 J/mol-K.

Using Equation 3 mentioned earlier, the average compressive strength was plotted as a function of the average value of the maturity index. The resulting curve is the strength maturity relationship which is used to estimate the strength of the same concrete mixtures cured at different temperatures.

As can be seen by the data in the previous plots the equivalent age at 23°C matches the data of the actual cylinder compressive strengths, indicating that the equivalent age approximations are very close to the actual age of the concrete. The low variation between curves provides confidence that the data collected is satisfactory to determine the apparent activation energy.

4.4.2 Maturity Curves for Determined Mechanical Properties

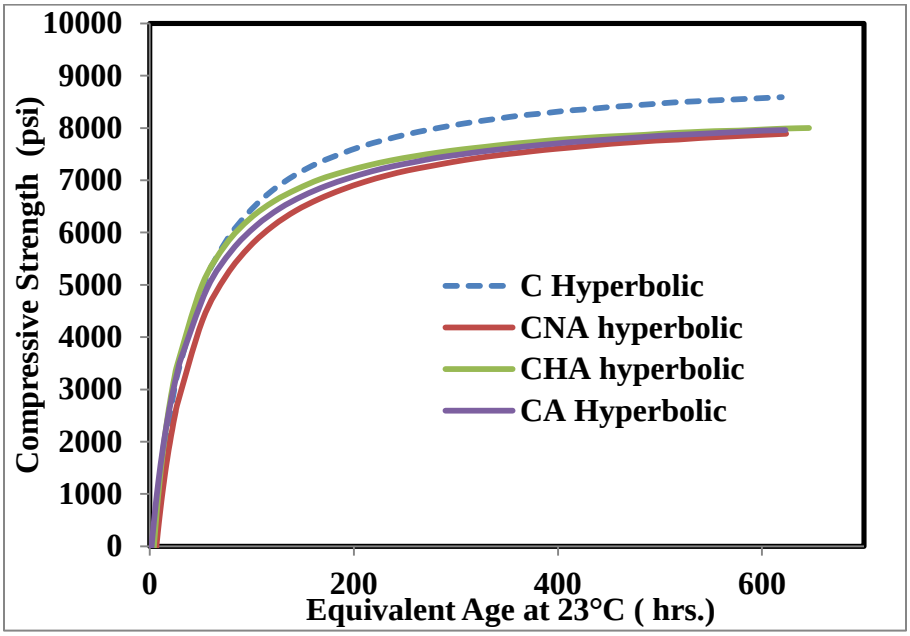

Figure 22 Compressive strength gain versus equivalent age strength curves for hyperbolic strength estimates

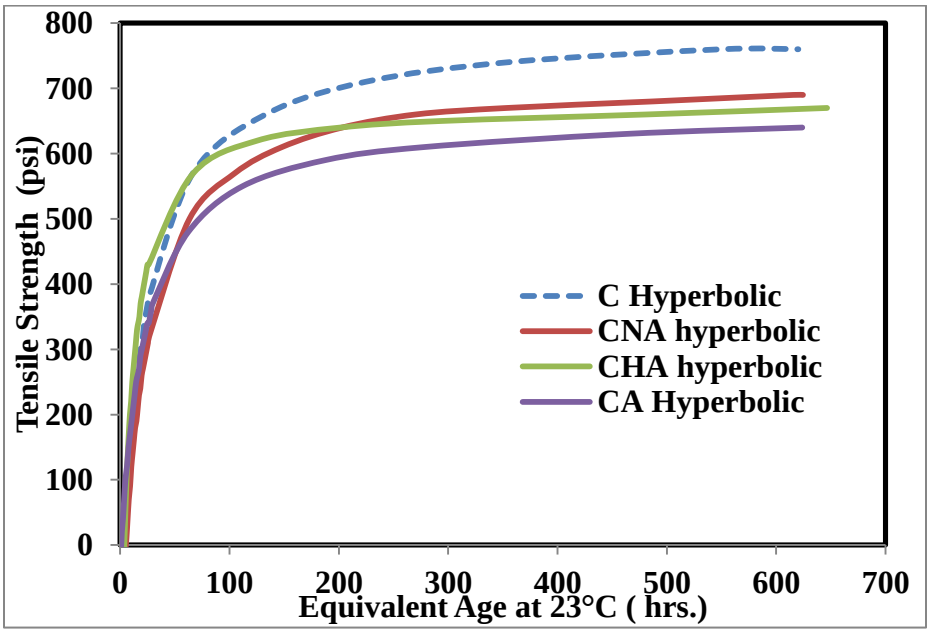

Figure 23 Tensile strength versus equivalent age strength curves for hyperbolic strength estimates

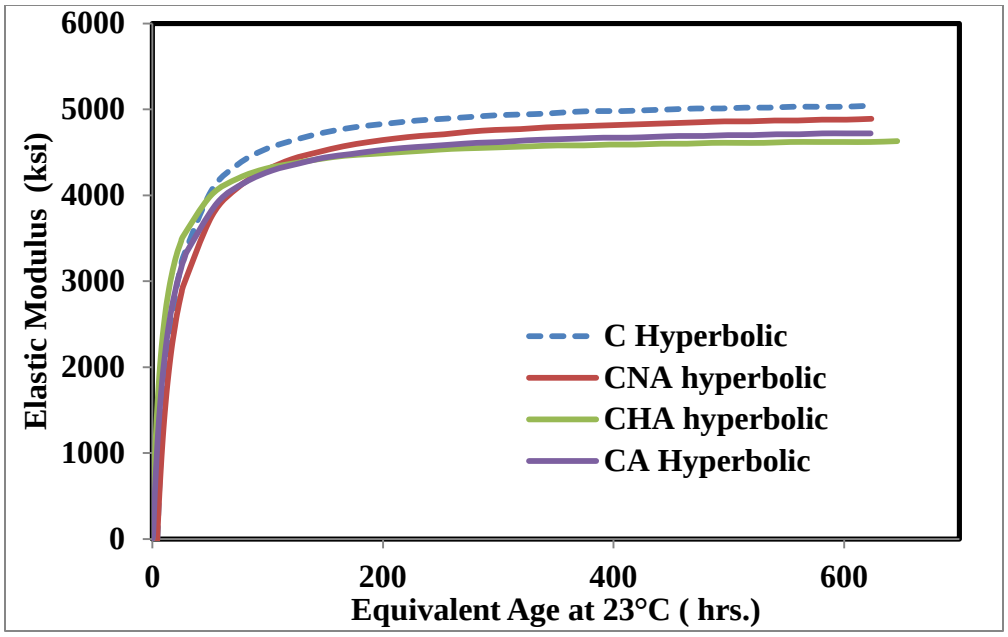

Figure 24 Elastic modulus versus equivalent age

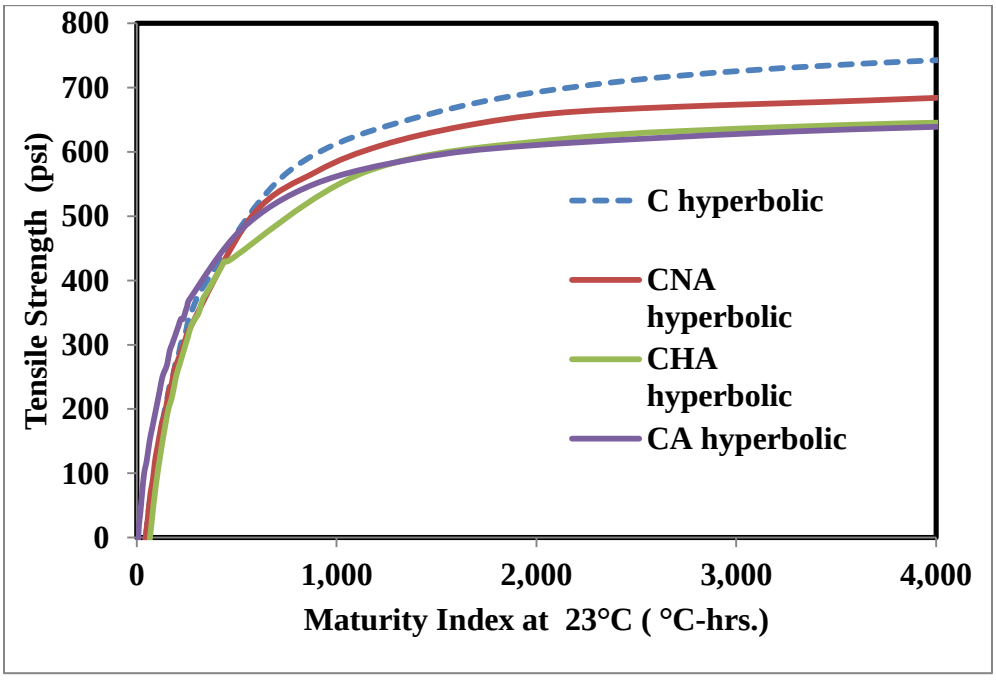

Figure 25 Tensile strength versus maturity index for concrete

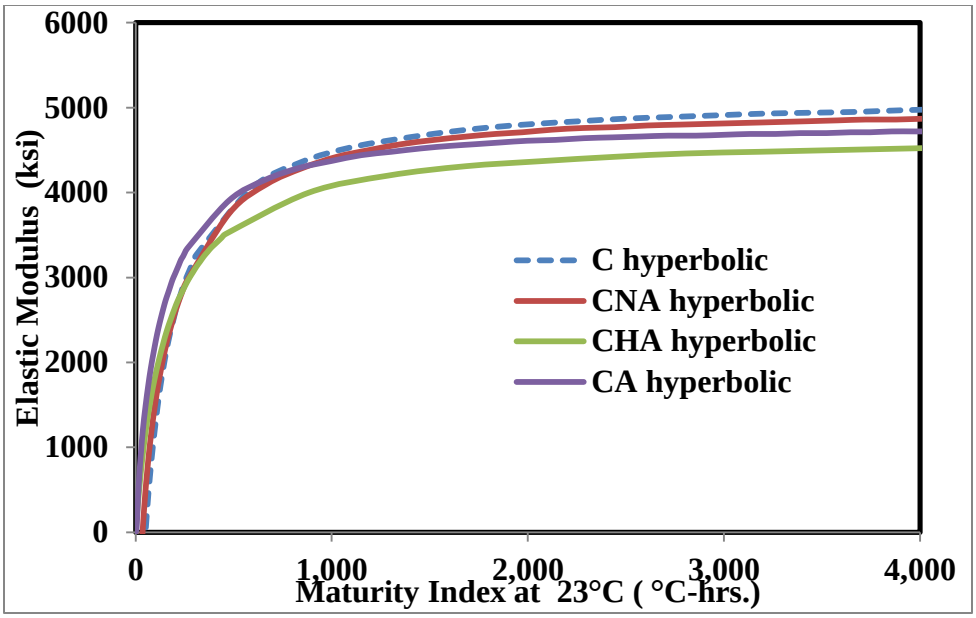

Figure 26 Elastic modulus versus maturity index

4.5 Assessment of Chloride-Based Accelerator on Concrete Cracking Potential

Towards satisfying the objective of this study, two main tests were used to assess the effects of an overdose of chloride-based accelerator on the potential of concrete pavement slabs to crack; namely, free or autogenous shrinkage frame trials and rigid cracking frame trials.

There was a simulated temperature profile generated for the cracking frame and free shrinkage frames through the use of concrete works software. The field data collected from a pavement slab containing a 1-1/2 dose of accelerator, named the SW SMO mixture, was used as a means to best fit the temperature profiles generated for the other concrete mixtures in concrete works. Therefore, simulated profiles were generated for each mix and the fit was compared to this field slab, to validate the temperature profile predictions made by concrete works. Once these temperature profiles were generated and validated, they were implemented in concrete testing in the cracking frame and free-shrinkage frame. The imposed temperatures were closely maintained through the use of the circulating bath and insulated form-work. Concrete mixtures

were prepared using the approved mix design and simulated field temperatures. The field slab temperature and mixture were also run in both the free shrinkage frame and the cracking frame to compare strains and stresses to the other concretes tested. It can be seen in Figure 27 through Figure 30 that the imposed temperature for certain mixes was closely followed during testing.

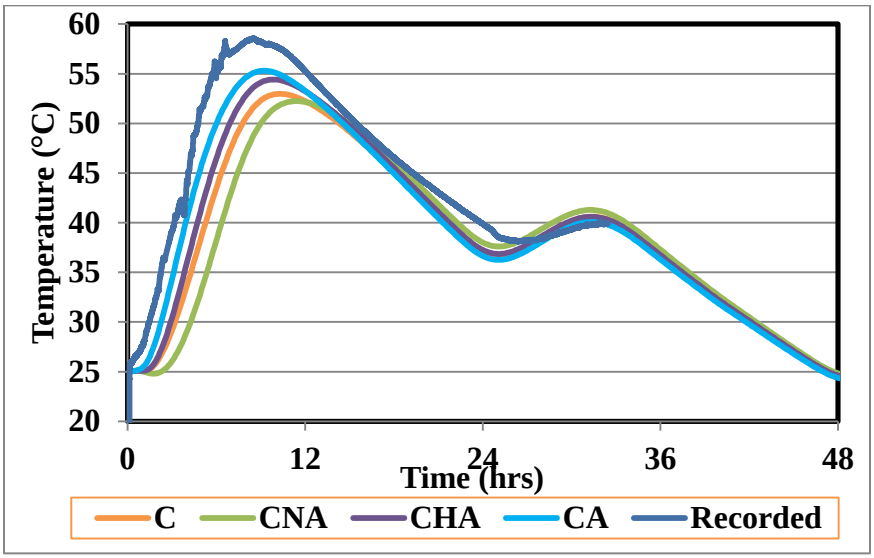

Figure 27 Plot of measured temperature from field slab SMO, named recorded, and the predicted temperature profiles generated by concrete works

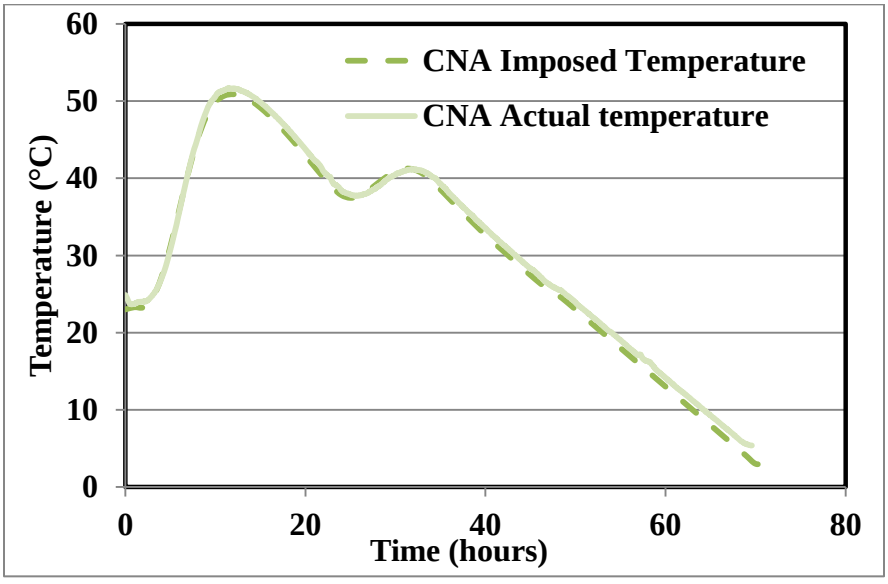

Figure 28 Plot of CNA imposed temperature and the actual recorded temperature in the cracking frame

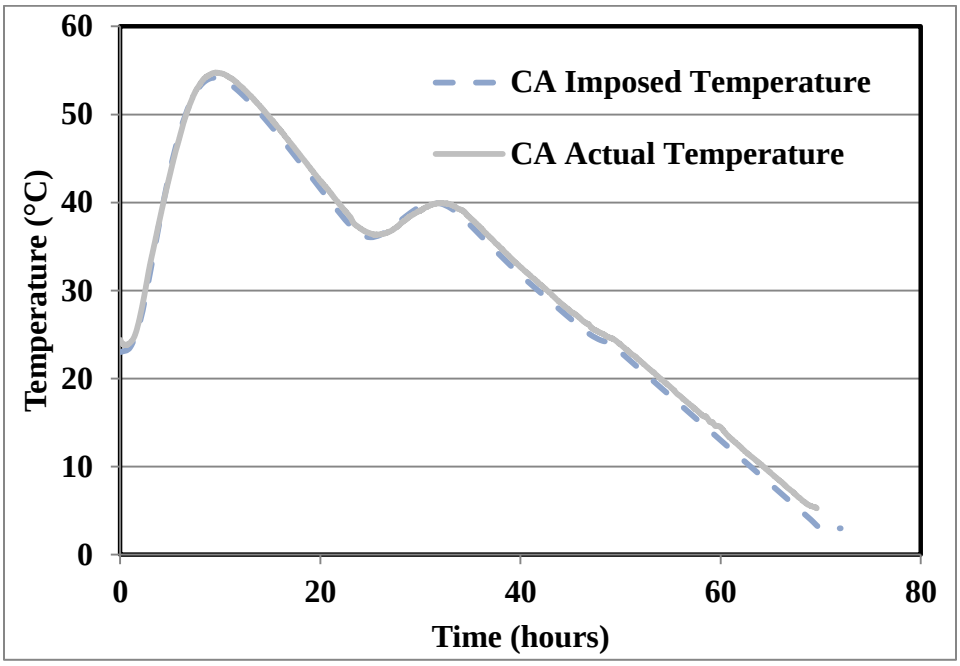

Figure 29 Plot of CA imposed temperature and the actual recorded temperature in the cracking frame

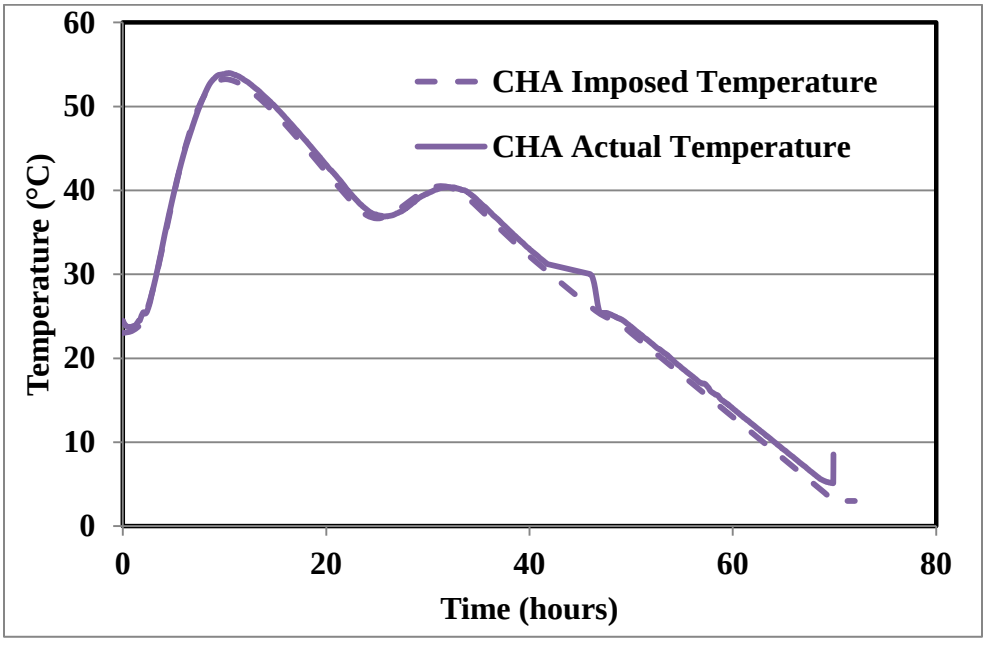

Figure 30 Plot of CHA imposed temperature and the actual recorded temperature in the cracking frame

4.6 Isothermal Free Shrinkage Testing

Restrained concrete testing was performed to measure stresses and try to explain their development in concrete mixtures with variable accelerator dosage. Tensile strength development and stress relaxation are a concretes defense against these early stresses. Unrestrained testing was also performed to determine the strain the concrete will experience from autogenous shrinkage. A short duration of time after placement and sealing of the free shrinkage frame, the movable stainless steel plates were immediately backed off of the concrete after the concrete reached final set. Recall that the setting was determined from the mortar penetrometer tests conducted following ASTM C 403[60]. The same procedure was implemented for all the free shrinkage experiments, and the plates were moved at the time of set in every experiment. The timely moving of the plates away from the concrete allowed the concrete to expand or shrink freely along the longitudinal axis of the concrete prism in the free shrinkage frame. The small Invar rods connecting the concrete to the LCP devices that measured the strain, extended into the concrete's ends through small lubricated ports in the plates and ends of the free shrinkage frame. The ports were fabricated to allow the rods to remain unaffected by the moving of these plates. The strain in the concrete was measured after final set because before then, while the concrete is in a plastic state, volume changes were occurring on plastic concrete. Additionally, the concrete had not hardened enough to measure shrinkage. From the setting time forward, the strain measurements were collected every minute until the end of the test. The strain measuring devices were calibrated before any testing took place, by making small measurements of displacement that corresponded to voltage differences in the LCP measuring devices.

As can be seen in Figure 31, the initial temperature of the concrete at placement and heat generation can be a hurdle that the cooling system needed to overcome. The hotter the placement

temperature, the longer and more aggressive the bath needed to work to lower the temperature to the target temperature. This chasing of the temperature can lead to oscillating temperature changes in the fresh concrete. The oscillating temperatures that occurred during the first few hours of the test should not be a concern because they were relatively stabilized by the time the concrete set and the plates were moved.

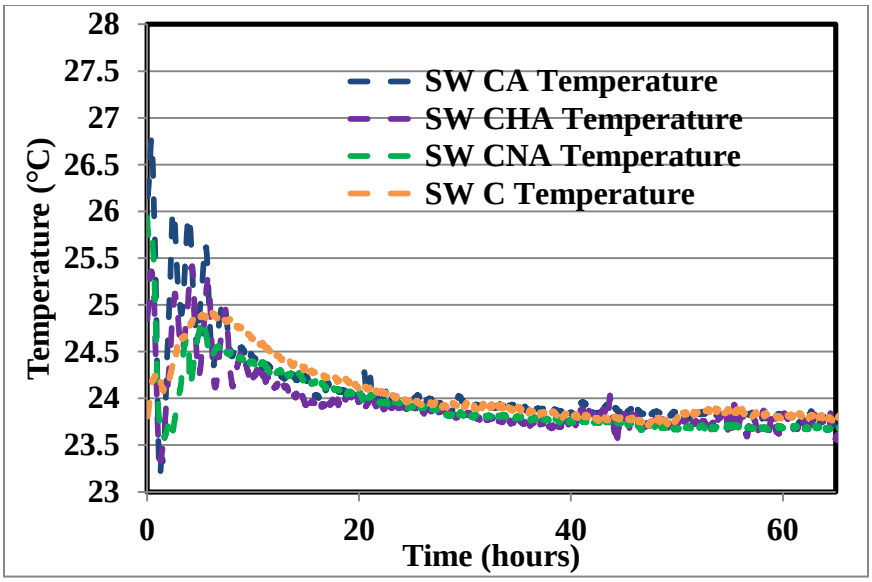

Figure 31 Temperature of concrete in free shrinkage frame (isothermal 23°C)

As seen in Figure 33, the concrete in the free shrinkage frame experienced considerable shrinkage in the first twenty hours of the experiment from self-desiccation or autogenous shrinkage. The hydration products occupy less volume than the unhydrated reactants and this is a source of volume change. This chemical shrinkage, along with a decrease in the internal relative humidity from water consumption during the hydration reaction is the driving force for the shrinkage. Consumption of pore solution reduces pore volume, which places compressive stresses on the pore walls as the capillary action causes the pore walls to contract as a result. As the hydration continues, the reduction of the smaller pores volume induces more contraction than

larger pores do from this phenomenon. It has been observed that the utilization of $CaCl_2$ accelerator can lead to formation of more small pores than would normally form in concrete without accelerator [74]. With increasing dosages, there could be a shift toward more small pores which would enhance the effects of autogenous shrinkage. Additionally, a faster reaction would also mean that the autogenous shrinkage would occur faster, as was seen in Figure 32. Suryavanshi, Scantlebuy, and Lyon found that the addition of $CaCl_2$ caused a decrease in pore volumes when addition rates for mortars contained 1.75% $CaCl_2$. The addition of $CaCl_2$ increased the pore volume for finer pores but decreased the number of coarse pores, which was attributed to a change in morphology of C-S-H gel from a fibrous to a dense morphology [34]. The heat generation keeps the concrete warmer than the target temperature of 23°C until all the heat from generation subsides, about 40 hours at which point the temperatures stabilize out and the concrete temperatures remain relatively constant. At about the 10 hour mark in any of the tests, the concrete temperature in all mixtures is within 1°C from the stabilized temperature of 23.7°C. This small deviation in temperature caused only very small changes in the length change measured.

Recall from the literature review, that California does not allow the use of chloride containing accelerators. It has been concluded that the use of chloride-containing accelerators doubles the amount of shrinkage experienced by concrete compared to shrinkage with no accelerator [11]. As expected, higher shrinkage was observed in the mixtures containing increasing dosages of accelerator. Mixtures CA and CHA, both shrunk much more than the control mixture C and to almost equal magnitudes of one another and both at nearly the same rate. Mixture C and CNA experienced the least shrinkage of all the isothermal testing, but CNA continued to shrink more than C and at a higher rate. Mixture C shrank at the slowest rate,

probably due the fact that there were no admixtures present. Retarders are known to accelerate hydration after the concrete does finally set.

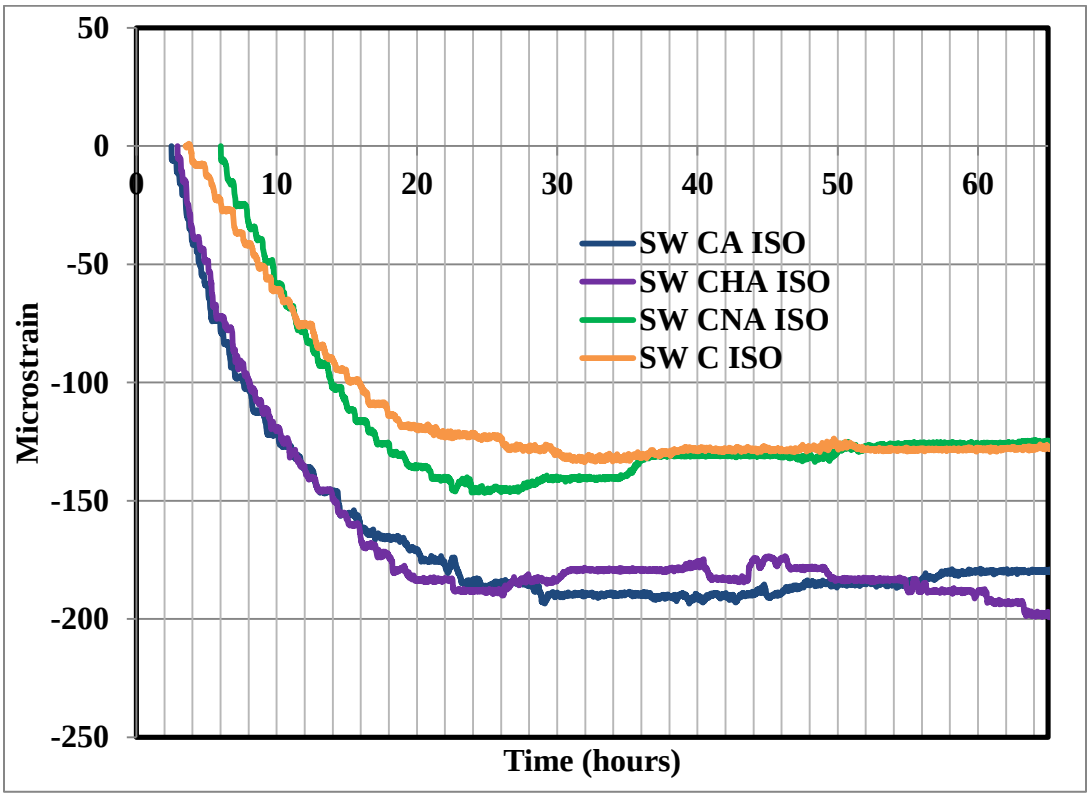

Figure 32 Effect of accelerator dosage on free shrinkage of concrete (Isothermal 23°C)

The increased dosage of accelerator causes more autogenous shrinkage because the cement hydration is accelerated and water demand from the pores increases. At this faster rate of hydration more stress is put on pore walls earlier and the since the modulus of elasticity was low and was still developing at this early age, a higher rate of shrinkage took place.

4.7 Varying Realistic Temperature Free Shrinkage Tests

Due to the changing temperature profile, the autogenous shrinkage was harder to decipher from thermal strain effects and from shrinkage strains. There were subtleties that were observed however, when the data was plotted as seen in Figure 33.

The slopes of the strains tell a lot about the amount of deformation that took place during the testing. The strains were plotted in such a manner, so that after moving the plates marked a single starting time that all the tests were plotted. First analyzed was the deformation during the first 20 hours of the experiment after mixing. It was important to see which mix exhibited greater stress relaxation during the first 20 hours after setting and which mixtures used up all the shrinkage in the beginning of the testing. Faster contraction rates can be identified from a steeper slope, the increased shrinkage from the use of the admixtures corresponds with the higher rate of hydration. Mixture SMO, which contains an accelerator dosage above manufacturer specified dosage, would be expected to have the largest shrinkage strain in the realistic simulated temperature testing. In fact there was more shrinkage in the SMO concrete compared to the other concretes tested in the free shrinkage frame with varying temperatures. The SMO mix also experienced a higher degree of shrinkage in the 10-20 hour age, and the slope for the SMO mixture was steeper than the other mixes in this time frame. CHA were similar during this interval.

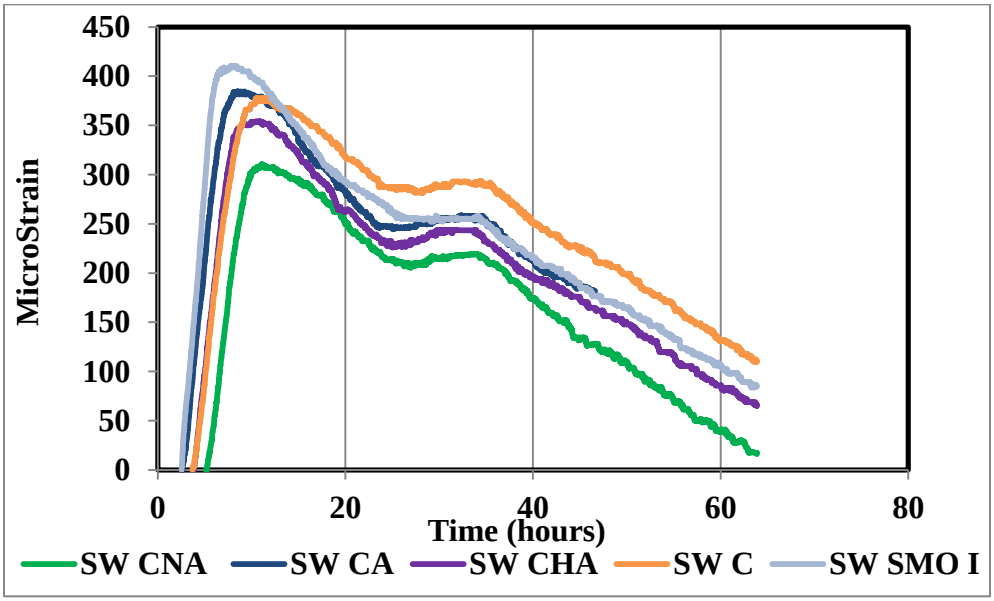

Figure 33 Free shrinkage experiment results with varying temperature starting at 23°C

The dosage of the accelerator used coupled with heat generation, and the temperature of the bath had strong influence on the maximum shrinkage, but there might be more to it that thermal strain alone. Mixture SMO expanded nearly 25% more than the CNA, and the expansion was much more rapid than any of the other mixtures. The SMO mixture also experienced a steep slope with respect to the cooling after peak temperature was reached, almost the same as the CA mixture, between 10 and 20 hours. The early expansion could also be partly explained by a shift in hydration product formation and more specifically an increase in calcium hydroxide production. There is also the possibility of higher ettringite formation due to the higher temperature induced by the use of the accelerator [1]. Mostly the change in volume is due to temperature induced strains. These thermal strains are validated through the analysis of the rigid cracking frame results, where temperature rise leads to expansion and compressive stresses, and temperature reductions induce contraction and tensile stresses. Early temperature rises will have larger effects on the volume of the concrete due to the developing coefficient of thermal expansion (CTE), as the concrete hardens, this CTE lowers, but deformations from temperature will be greater following the time of setting as seen after 20 hour in Figure 34. Though higher temperatures cause higher expansion, they also promote faster reactions and can lead to larger chemically induce autogenous deformations than those in the isothermal experiments. The plot for the portion of the test occurring after 20 hours can be found in Figure 34.

The temperature of the concrete was purposely decreased to simulate overnight temperature changes, implemented by the circulating bath. It is at these times that all the concrete test temperatures were within 1°C of each other, with the exception of mixture CNA which was warmer at this point because it experienced a slightly delayed hydration because of the use of a retarder. All the strains were compared from this point, since the temperature

differences between mixtures could be basically ruled out as a variable. There are differences among the trends in the different mixtures that are interesting for this latter part of the test.

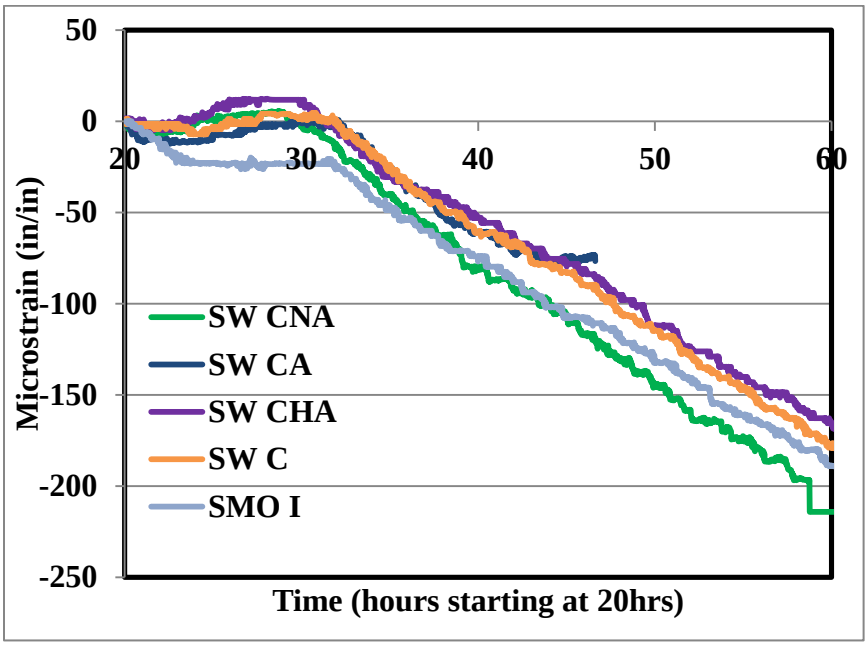

Figure 34 Plot of 23°C free shrinkage mixes after 20 hours from initial mixing

Mixture CA had a computer issue after 46 hours due to a power failure and the data after this point is inconclusive for this mix, but before that, there were some valuable trends observed. First the strain in CA was lowest at 20 hours but it did not contract as much as the SMO concrete had. During the second temperature rise, the concrete did expand but then as the temperature reduced again at around 30 hours, CA started to contract rapidly again from autogenous shrinkage, but then at 40 hours, the contraction slowed. This late reduced contraction could indicate that either most of the autogenous shrinkage was used up by this point or that higher relaxation was occurring during this period. It is apparent that the mixtures with accelerator

experienced the bulk of the autogenous shrinkage early on, and conversely, the ones with lower dosage or no dose had the opposite effect and experienced more autogenous shrinkage later.

From 35 hours on, the temperature of the concrete was slowly reduced to simulate the sun going down and as a result the temperature of the concrete would cool. At 48 hours into the testing the cooling system induced the concrete to cool at 1°C per hour until the temperature reached 3°C.. The drop in temperature at the end of the test would cause a high degree of thermal strain on the concrete, and some mixes contracted more than others. The SMO mix contracted the most after 20 hours from the time of moving the plates, and when the other concretes expanded due to an increase in temperature, the SMO was still shrinking and resisted this expansion. The CNA mixture contracted the most compared to the other mixtures with the same water to cement ratios of 0.384 under this same thermal regiment. There was more activity in the CNA contraction than in the other mixtures, in terms of small shrinkage and relaxation turnovers. It is believed that the concrete would shrink and then relax and shrink and relax some more as the temperature was dropping, indicating that the CNA mixture had more late age shrinkage compared to the other mixtures.

The accelerated mixtures would shrink rapidly in the beginning and there were others that would shrink slowly and more steadily with time. The mixtures that exhibited high shrinkage in the beginning of the testing would then exhibit more relaxation with time. The relaxation appears to be much higher in the CA mixture and the contraction seemed much steadier as well, with fewer fluctuations into the later age. Mixtures C and CHA had about the same contraction rate as one another as the temperature reduced, and relaxation is apparent in both mixtures from the activity in the plotted data. Mixture C and CNA both had higher shrinkage after 20 hours during this latter part of the test.

From the tensile strength data determined from concrete cylinders cured a 23°C, and tensile strengths were highest at 48 hours in mixtures C and CHA. Additionally, both the compressive strength and the elastic modulus developed faster in mixtures C, CHA, and CA between ages of 1 and 3 days. The rapid development of these mechanical properties is a strong reason that there was more shrinkage taking place. There was more consumption of pore water and more rapid changes in microstructure at this age, which led to the higher shrinkage observed in the free shrinkage experiments.

4.7.1 What Changed During the Test?

During the experiment there are many changing and developing mechanical properties. The setting times are different for the different mixtures, tested due to increased accelerator dosages. The temperatures that develop and the rates at which they develop all can affect the potential for cracking. The chemical admixture combinations affect the microstructure development differently and have short term and long term effects on the concretes potential for shrinking, stress relaxation and ultimately affect the cracking potential.

4.8 Rigid Cracking Frame

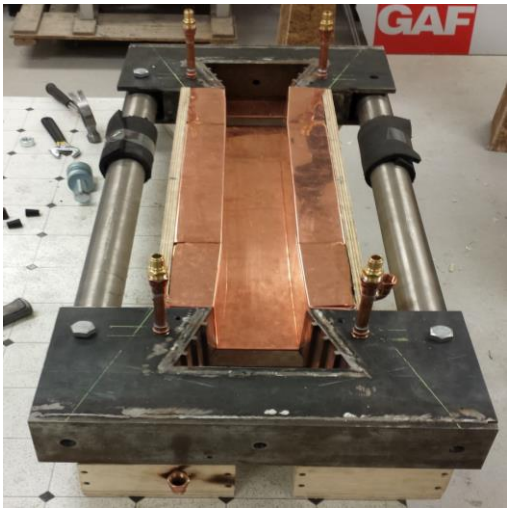

Figure 35 Cracking frame under construction

There were many interesting findings after the cracking frame experiments data was analyzed. The fresh concrete placement temperature, and concrete accelerator dosage were evaluated and compared for the mixtures used in this study based on the plotted results obtained from rigid cracking frame experiments which are presented in Figure 36. Since there are many different data values of interest, it is important to identify what will be compared and why it is of interest for comparison.

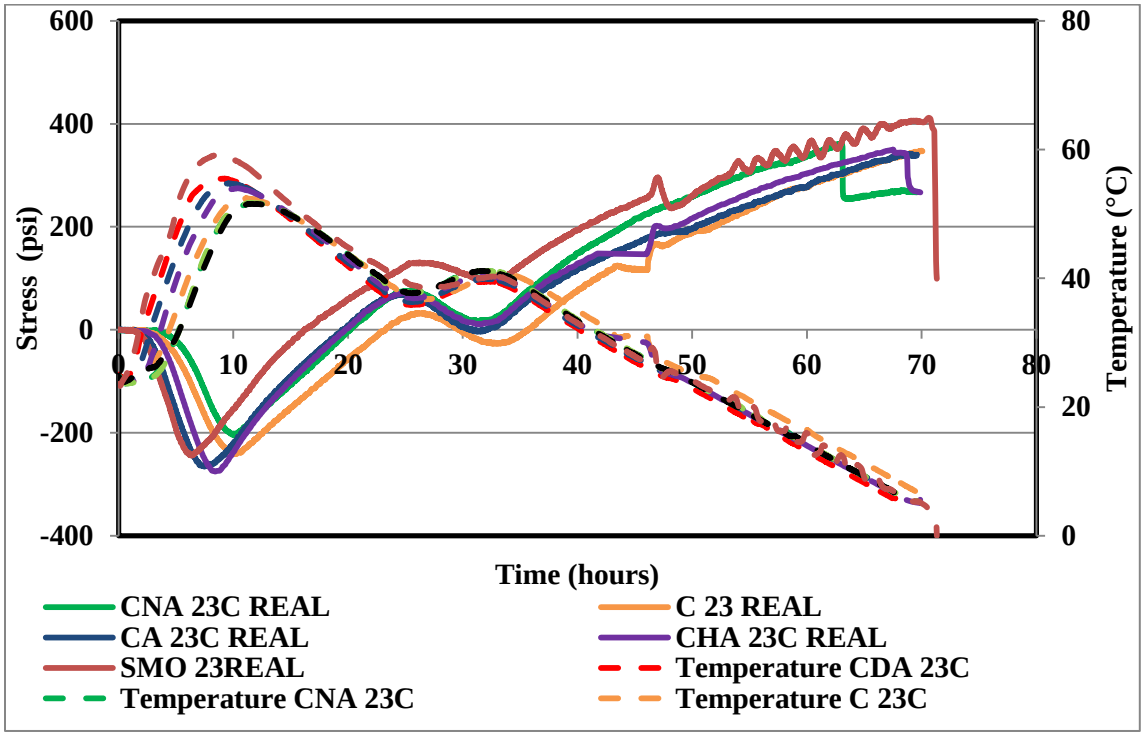

Figure 36 Comparison plot of CA, C, CNA and SMO at 23°C temperature profile stress vs time from the cracking frame experiments

Table 11 explains these points of interest with a brief description of each and why they are of interest. The first comparison made between tests was the fresh concrete placement temperature. Other temperatures that were of interest are: the temperature at the time when compressive and tensile stresses are highest and the temperature when the transition from compression to tension takes place, and lastly if and when cracking occurs. These temperatures

and the stresses at those times are important because they are the comparable data points to evaluate which mixtures are at higher risk. All the points of interest are compared in Table 12.

As the mechanical properties of concrete develop there are stresses that develop at the same time that stem from chemical reactions, development of the microstructure, autogenous shrinking, and drying shrinkage. To some degree the concrete has the ability to relax a portion of these stresses, and these relaxations can be higher at early ages. The dosage amount of accelerator has an effect on this relaxation, and the microstructure that forms is a product of this relationship. For instance, looking at the cracking frame results, it is apparent that the SMO mixture experienced the highest temperature in the frame but it did not expand as much as other mixtures had. Early age stress relaxation is highest at early ages, and since the loads were applied quickly with the SMO mixture because it hardened the fastest, it is possible that more stress relaxation occurred with this mixture. Mixture CA and CHA also had high temperatures, but, less accelerator and as a result, each mixture expanded more than the warmer, higher dosed SMO. The expansion is most likely due to the fact that there is more unconsumed water with a high CTE in the mixtures with less accelerator during the peak temperature period.

Table 12 Term definitions used to describe data collected from cracking frame

Term	Description
T_{Ci} =	Fresh concrete temperature at placement (°c)
$\sigma_{maxCompression}$ =	Max compressive stress (psi)
$t\sigma_{maxCompression}$ =	Age when max compressive strength was reached (hours)
T_{max} =	Max in-place concrete temperature (°C)
t_{Tmax} =	Age when max temperature is reached (hours)

Table 12 (Continued)

T_{zs} =	Temperature when compressive stresses are reduced and tensile stresses first develop (°C)
t_{zs} =	Concrete age when zero stress temperature occurs (hours)
T_{48} =	Concrete temperature at start of cooling or 48 hours after mixing (°C)
σ_{48} =	Concrete stress at start of cooling which is 48 hours after mixing (hours)
$\sigma_{maxTension}$ =	Max average tensile stress at center (psi)
Tcr =	Concrete temperature at cracking or max tensile stress (°C). This temperature may have to be induced by the external cooling.
$t\sigma_{max\ Tension}$ =	Time at max tensile stress or age at cracking (hours)
ΔT_{cr} =	Temp difference required to produce cracking (tzs-tcr) (°C)

4.9 Effects of Fresh Concrete Temperature

The degree of restraint for the cracking frame began at 100% when the concrete was fresh and still in a plastic state. After hardening the restraint decreased from 100% to 77%, in all mixes tested. This calculation was performed using Equation 4, which is a degree of restraint equation used by Springenschmid for hundreds of cracking frame tests, this equation can be found in the background section, Chapter 2.

A number of differences can be seen between the mixtures containing the accelerator and the other liquid admixtures. First, the mixtures SMO, CNA, and CHA were the only 3 specimens that cracked during the testing period of 72 hours. The primary reason for the cracking was that the tension developed in the concrete exceeded the tensile capacity of the concrete. CNA was tested a second time to verify the result, and the second experiment also resulted in a crack. In

these four tests, the concrete in the frame went into a state of tension, due to the reduction in temperature after the heat of hydration reaction stopped generating heat. When the temperature of the frame started increasing at 25 hours into the test, simulating a temperature rise in a pavement slab, the concrete in these mixtures did not go back into a state of compression like it did in the other experiments. This transition back into a state of compressive stress is necessary to alleviate the tensile stresses developed at this early age, and allow the tensile strength to continue to increase raising the concretes tensile capacity. From the free shrinkage experiments that were subject to the same temperature profile it is evident that SMO, CNA, C, and CHA mixtures do not exhibit the same amount of stress relaxation at the 48 hour age, and therefore lead to a higher risk of cracking.

4.10 When Did Tension Develop in the Cracking Frame?

Under the thermal control of the frame, the concrete first expanded and went into a state of compression due to the restraint provided by the frame. This expansion was onset from heat generation from the heat of hydration reaction, coupled with a daytime placement time. Early creep development in mixes with accelerator could explain how much compression was measured in the strain gauges mounted on the Invar bars. As the temperature decreased in the frame to simulate the end of the heat generation and to simulate night time temperatures, the concrete came out of a state of compression, briefly through a stress free state, and into a state of tension. The SMO mix was the worst case mix in this series of tests, because it went into a state of tension at only 16 hours after mixing and even with the rise in temperature of the next day, the SMO concrete never recovered. Because the SMO set quickly, it did develop a high amount of tensile strength capacity and did not crack within the 72 hours even when held at 3°C, despite the early onset of tension. It was cooled beyond the 3°C to -2°C, to induce cracking. Following the

temperature reduction that puts the concrete into a state of tension, is another temperature rise that force the concrete back into a state of compression before the cooling is initiated. What was observed at this stage was that only mixtures CA and C went from the state of tension back into a state of compression for this short duration of time. CNA and CHA concretes never went back into compression during this second temperature rise and as a result, the concrete continued to develop more and more tension which ultimately resulted in a crack. It has been observed that, the earlier that the concrete goes into tension, the more likely for a crack to occur. This is evident when comparing the two CNA test results, one went into tension earlier than the other, and it also cracked earlier. Mixture CA barely went into a state of compression, but because of stress relaxation, it was able to alleviate some of the tensile stress and it did not crack. The tensile strength of mixture CNA was the lowest at 1 day from the cylinder testing, and just barely out performed CA at 3 days. Although the tensile strength of CA was not as high as CNA on the third day, it was able to relax some of the tensile stress preventing it from cracking. The early development of the tensile strength could be a product of the internal temperature differences between the mixtures. The ones without accelerator have slower development of elastic modulus because the setting is delayed. Since there are admixtures delaying setting, and cooler temperatures are developed as a result, the mixture CNA will have the highest potential to crack when temperature changes in the environment cause thermal deformations to occur.

Mixture CHA contained the least amount of accelerator and it too, cracked. This mixture did not return to compression during the second temperature rise, it is apparent that there was some stress relaxation taking place but the amount of tensile stresses exceeded the tensile capacity of the concrete resulting in a crack. In the cracking frame, mixture CHA went into a high degree of compression, most likely from thermal expansion and the fact that setting was

somewhat slower than the CA mixture. Once setting was established, the mixture quickly began to shrink. The rate and magnitude that CHA shrank at was comparable to that of CA in the free shrinkage frame isothermal experiment. In the varying temperature experiments, CHA concrete was the second highest shrinking concrete, and had a faster rate of shrinkage than CNA did between hours 10 and 20.

If there were a way to slow the temperature spike during heat of hydration and extend out the length of time that the concrete remains in compression, there would be improved odds against cracking. The accelerator will speed early chemical reactions, but too much will lead to shorter heat of hydration times and vastly increased autogenous shrinkage.

The timing of this stress state transition seems to be controlled by the temperature developed in the first temperature rise, the amount of accelerator and the amount of compression that the concrete is under. Longer time in compression will postpone this transition point from compression to tension and will allow the concrete to develop more tensile capacity. Higher compression, takes longer to be alleviated in mixes with higher doses, and tension is delayed, allowing for higher tensile strength development. This can be good because the concrete will develop a higher tensile strength as it ages as a defense against cracking, when drying shrinkage kicks in.

There could be techniques implemented to keep the temperature moderately high in the early age just after placement to allow hardening but to not allow the heat generation period to be short lived. One benefit would be that moderate temperature rise will still allow the concrete to harden in sufficient time, but will keep it in a compressive stress state for as long as possible. Early high heat has been shown to increase autogenous shrinkage, and if this shrinkage can be curbed, the concrete will have better odds against cracking. Altering the concrete placement time

and temperature will change the timing of when the heat generation period occurs versus when the daily temperature cycles occur, changing the stresses development. Lowering the placement temperature can facilitate this by slowing hydration slightly.

Inaccurate dosing of accelerator and the lack of accounting for the amount of water in the accelerator can be a significant source of error which can lead to lower tensile strengths which can increase cracking risk. In the case of the SMO mixture, the water in the additional accelerator was not compensated for and the concrete had a high risk for cracking as a result. The SMO concrete went into tension in only 16 hours after mixing and there were higher tensile stresses developed throughout the early age. There was some stress relaxation, but ultimately the concrete did crack.

Table 13 Table for comparing results from cracking frame tests

Parameter		SW C	SW CNA	SW CNA	SW CHA	SW CA	SW SMO
T_{Ci} =	°C	24	24.9	24.9	24.5	24.4	23.6
$\sigma_{maxCompression}$ =	psi	-214.8	-173.7	-190.4	-274.9	-265.8	-244
$t\sigma_{maxCompression}$ =	hours	10	10	10.3	9.5	7.5	6.3
T_{max} =	°C	52.5	51.7	51.8	51.6	54.8	59.1
t_{Tmax} =	hours	10.4	11.6	11.5	11.6	9.5	8.5
T_{zs} =	°C	40.1	43.5	45.4	38.2	43.2	49.7
t_{zs} =	hours	35.1	20.2	18.8	35.9	19.5	16.2
σ_{48} =	psi	167.2	241.6	247.1	197.5	189.4	238.6
T_{48} =	°C	26.7	25.6	25.6	25.2	25.2	25.6
$t\sigma_{max\ Tension}$ =	hours	70	63	60.9	67.5	69	70.6
$\sigma_{maxTension}$ =	psi	347.9	362.2	352.2	350.1	341.3	411.8
T_{cr} =	°C	6.4	11.2	13.3	6.7	5.5	4.1
ΔT_{cr} =	°C	NC	32.4	32.1	36.8	NC	45.6

Testing on isothermal frees shrinkage frame specimens was performed to determine the amount of free shrinkage for unrestrained strain measurements to have some baseline on autogenous shrinkage to compare to. The experimental comparison between mixes was to measure the sensitivity to cracking. From the free shrinkage data collected on the varying temperature tests, the thermal strain can be compared with the temperature changes, which were quite different from the isothermal free shrinkage strains.

CHAPTER 5: CONCLUSIONS AND RECOMMENDATIONS

Different reasons were identified for higher cracking potential of replacement slabs when using calcium chloride accelerators. The mixtures were getting too hot and shrinking substantially leading to cracking. The amount of restraint on the slabs was enough to allow them to crack. In the field, accelerators are added to the concrete in the concrete mixing trucks when they arrive on site. The dosage of accelerators should be pre-determined by the engineer before the raw materials are added to the truck, and not estimated on the jobsite after the mix water has been already added. A specific dosage is required for a specific mixture but field conditions may allow the engineer to deviate from that protocol. An overdose could occur due to: operator error, faulty measuring devices, or to speed up early opening to traffic.

If the concrete in the truck has started to stiffen up and has a low slump value before the accelerator has been added, extra accelerator might be added to the truck, creating a mixture like SMO. Before the accelerator is added, and slump is still low, more accelerators might be added to attain a certain slump for workability. This should be a rare occurrence, but it could be a strong possibility for why slabs are cracking. Regulations on rejecting a concrete delivery are in place for concretes that are less than a few hours old, and it is the determinations of the engineer to make a rejection. If additional accelerator is added to the concrete, there will be consequences. Inaccurate dosing or over dosing of accelerator is problematic because the accelerator is water based and extra water will be introduced to the mixture from an overdose in accelerator. Extra water in the concrete mixture will compromise performance in terms of water-cement ratio (w/c). The chloride based accelerator used in this research contains approximately 61% water, when the

concrete is being batched, this 61% water by volume is accounted for and adjustments are made to the mix water. If this water is not adjusted for when extra accelerator is added, there will be a change in the concretes w/c just like the SMO mixture. A higher water to cement ratio will result in a shift in tensile and compressive strength development. A delay in tensile strength development could lead to a higher risk of cracking because if the concrete is under any restraint, the tensile strength could be exceeded and cracking would result.

Autogenous shrinkage is an important factor in the risk of cracking of the concretes studied here, because of the low w/c, increased temperatures, and the use of the accelerator. High temperatures coupled with high accelerator doses cause more chemical shrinkage because the reactions are consume available water at a high rate in the first few hours. The rapid heat generated from the cement chemistry reactions causes some early expansion, but shrinkage still occurs and when the temperature finally starts to subside and cooling begins, tension will set in and if restrained, cracking potential will increase.

The SMO concrete had additional accelerator added beyond the amount in CA and no adjustments were made to the mix water to offset the intentional additional water that the accelerator provided. This mixture, when tested in the cracking frame went into tension in only 16 hours after mixing and there were higher tensile stresses developed throughout the early age. The extra water added, provided plenty of water for hydration but at the same time the extra accelerator promoted more shrinkage. There was some stress relaxation, but ultimately the concrete did crack within 74 hours.

From the cracking frame experiments, when the mechanical property development is delayed like in CHA and CNA, there is more risk potential for cracking. The accelerator will force faster hardening, but the retarder admixture delays the hardening, together they

compromise the ultimate performance. Mixture C also had a delay in the strength development but because it did not contain any admixtures, the strength gain was not compromised. As was seen in cylinder testing, the C mixture's mechanical properties surpassed all those in other mixes by the 3rd day of curing/testing. It was expected that C would perform well, and it did.

Higher dosage of accelerator did cause more shrinkage in the free shrinkage frame at 23°C. Developing strength early provides the ability to resist cracking and the best case scenario is to have the majority of the shrinking happened in the first 12 hours. Additionally, the higher dose mixtures had experienced more stress relaxation in the later hours, which also helped to resist cracking.

The weaker mixture was the SMO, which had an overdose of accelerator, and those with less accelerator like CHA and CNA. The conclusion is that the dosage amount needs to be compensated for with water adjustments and the manufacturer recommended dose should be used. It is important to note that adding non-accelerating liquid admixtures can increase workability of a mixture, but it can also effect and damage strength potential. The retarding water reducer used should not be used alone for these high performance concretes or without a high amount of accelerator to offset the delayed setting time and delayed heat generation period. Mixture CHA and CNA are good examples of low or no accelerator mixtures that cracked in the cracking frame experiments.

The SMO mixture was the mixture that poses the most potential to crack, both in concrete works software and through experimentation. It is weakened by the additional water that is added when the too much accelerator is added, and it generates more heat from the additional accelerator being present. The additional heat generation creates a higher heat differential for the young concrete during the heat of hydration temperature generation. It is apparent that there is a

lot of potential for mixtures like SMO to be made accidentally in the field. If materials do not arrive on time or if batching varies too much, a weaker SMO mixture could result simply from the workability required be able to place the concrete.

Proper dosing, reducing the heat differential, and reducing restraint through better construction practices have all been proven to be effective means of combatting early age cracking in HPCs tested at 23°C Proper dosing, reducing the heat differential, and reducing restraint through better construction practices have all been proven to dowel alignment and proper greasing of dowels and form walls is as equally important as proper base preparation. Bond breakers such as plastic sheeting should be used between the base and the new concrete to reduce the restraint cause by friction from self-weight.

Efforts should be made to better regiment batching and stronger guidelines should be in place to ensure quality concrete is being made to a strict standard. If temperature of the environment is not the expected normal temperature, minor adjustments to the dosage could be made to reduce the temperature differential. Finally, sources of restraint should be reduced as much as possible such that the concrete can naturally shrink. Prompt curing also needs to be implemented as soon as possible and should remain in place as long as possible.

Future experiments should be conducted to determine if the same results and trends occur when the materials are warmed to 38°C or hotter because this hotter temperature is more representative of the field slabs. The fact is that the slabs in the fields are susceptible to changing conditions that cannot be duplicated in the laboratory. Wind, the effect of the sun, and slab drying, warping and curling can only be experienced in the field. Testing using actual slabs, dowels and curing compounds or blankets could provide unmatched results to better understand the risks and effects of mix design using accelerator.

REFERENCES

[1] T. J. Van Dam, K. R. Peterson, L. L. Sutter, A. Panguluri, J. Sytsma, N. Buch, R. Kowli, and P. Desaraju, "Final Report for Portland Cement Concrete for Pavement Rehabilitation Prepared for :," vol. 76, no. June 2005, 2005.

[2] B. J. J. Shidelert, "Calcium Chloride in Concrete", no. 48, pp. 537–559, 1952.

[3] H. Hedlund and G. Westman, "Autogenous Shrinkage of Concrete" *Proc. Int. Work. organised by JCI (Japanese Concr. Institute)*, vol. 23, p. p. 339, 1999.

[4] Caltrans, "CHAPTER 8 Full Depth Concrete Repair" vol. II, pp. 1–19, 2008.

[5] K. Manokhoon, "Evaluation of Concrete Mixes for Slab Replacement using the Maturity Method and Accelerated Pavement Testing" pp. 1–237, 2007.

[6] R. W. Lenz, "Pavement Design Guide," *Tx DOT*, 2011. [Online]. Available: http://onlinemanuals.txdot.gov/txdotmanuals/pdm/manual_notice.htm.

[7] P. Taylor, S. Kosmatka, and G. Voigt, "Integrated Materials and Construction Practices for Concrete Pavement," *A State-of-the-Practice Man. HIF-07*, 2007.

[8] ACPA, "Guidelines for full depth repairs," Skokie, IL, 1995.

[9] D. F. Brautigam and V. Y. Tillander, "Standard specifications for road and bridge construction," *FDOT Stand. Specif. B.*, 2013.

[10] G. Webb, "Personal Communication," Tampa, FL, 2013.

[11] Caltrans, "SLAB REPLACEMENT GUIDELINES," 2004.

[12] FDOT, "Standard Specifications For Road And Bridge Construction," 2010.

[13] C. Dar Hao and M. Won, "Field Performance Monitoring Of Repair Treatments On Joint Concrete Pavements," *J. Perform. Constr. Facil.*, 2007.

[14] J. MEADOWS, "Early-Age Cracking Of Mass Concrete Structures," 2007.

[15] ACI 318, *Concrete Buidling code and commentary*. 2011.

[16] G. T. Halvorsen and A. G. Bishara, “Joints in Concrete Construction,” vol. 95, no. Reapproved, pp. 1–44, 2001.

[17] A. Nazef, J. Greene, H. Lee, T. Byron, and B. Choubane, “State of Florida Department of Transportation Portland Cement Concrete Pavement Specifications : State of the Practice,” 2011.

[18] J. P. E. Floyd, “Standard Specifcations Construction Of Transportation Systems,” 2013.

[19] ACPA, *Guidelinees For Full Depth Repairs*. Skokie, IL, 2013.

[20] P. K. Mehta and P. J. M. Monteiro, *Concrete, Microstructure, Properties, and Materials*. McGraw Hill, 2006.

[21] ACI Committee 231, *Early-Age Cracking: Causes, Measurement, and Mitigation (ACI 231R-2010)*. Farmington Hills, MI: American Concrete Institute, 2010.

[22] ACI, “ACI 207R-07, Report on thermal and volume change effects on Cracking of Mass Concrete.pdf.” 2007.

[23] T. R. Naik and Y. Chun, “Wisconsin Highway Research Program Reducing Shrinkage Cracking of Structural Concrete Through the Use of Admixtures,” 2006.

[24] A. M. Neville, *Properties of Concrete*, 4th ed. Harlow, England: Pearson Education Limited, 2006.

[25] S. Mindess, J. F. Young, and D. Darwin, *Concrete*, 2nd ed. Upper Saddle River, NJ: Prentice Hall, 2003.

[26] D. P. Bentz, K. K. Hansen, H. D. Madsen, F. Vallée, and E. J. Griesel, “Drying/Hydration in Cement Pastes during Curing,” *Mater. Struct.*, vol. 34, pp. 557–565, 2001.

[27] P. Lura, K. van Breugel, and I. Maruyama, “Effect of curing temperature and type of cement on early-age shrinkage of high-performance concrete,” *Cem. Concr. Res.*, vol. 31, no. 12, pp. 1867–1872, Dec. 2001.

[28] O. M. Jensen and P. F. Hansen, “Autogenous deformation and RH-change in perspective,” *Cem. Concr. Res.*, vol. 31, no. 12, pp. 1859–1865, Dec. 2001.

[29] T. Lu and E. Koenders, “Modeling and analyzing autogenous shrinkage of hardening cement paste 1 Introduction 2 Theoretical basis,” vol. 2, no. May, pp. 155–162, 2014.

[30] S. Slatnick, K. A. Riding, K. J. Folliard, M. C. G. Juenger, and A. K. Schindler, “Evaluation of Autogenous Deformation of Concrete at Early Ages,” no. 108, pp. 21–28, 2011.

[31] E. E. Holt, “Early Age Autogenous Shrinkage Of Concrete,” *Tech. Res. Cent. Finl.*, vol. 446, 2001.

[32] K. Riding, D. a. Silva, and K. Scrivener, “Early Age Strength Enhancement Of Blended Cement Systems by CaCl2 and diethanol-isopropanolamine,” *Cem. Concr. Res.*, vol. 40, no. 6, pp. 935–946, Jun. 2010.

[33] J.F Young, “Powder Technology,” p. 173, 1974.

[34] A.K. Suryavanshi, S. J.D., and L. S.B., “Pore Size Distribution Of Opc & Srpc Mortars In Presence Of Chlorides,” *Pergamon*, vol. 25, no. 5, pp. 980–988, 1995.

[35] G. Thielen and W. Hintzen, “Investigation Of Concrete Behaviour Under Restraint With A Temperature Stress Testing Machine,” *RILEM Rep.*, pp. 145–152, 1994.

[36] J. WHIGHAM, “Evaluation Of Restraint Stresses And Cracking In Early-Age Concrete With The Rigid Cracking Frame,” 2005.

[37] J. Nam, S. Kim, and M. C. Won, “Measurement and Analysis of Early-Age Environmental Loading,” pp. 79–90, 2006.

[38] B. McCullough and R. O. Rasmussen, “Fast-Track Paving: Concrete Temperature Control And Traffic Opening Criteria For Bonded Concrete Overlays,” *Task G, Final Report, FHWA,* October, 1999.

[39] B. J. Zhang and V. C. Li, “Influence of Supporting Base Characteristics On Shrinkage - Induced Stresses In Concrete Pavements,” no. December, pp. 455–462, 2001.

[40] M. Wesevich, “Stabilized Subbase Friction for Concrete Pavements.” 1987.

[41] JCI, “Report of Committe On Autogenous Shrinkage of Concrete,” *Japanese Concr. Inst.*, 2002.

[42] S. Hagiwara, S. Nakamura, M. Y., T. Uenishi, T. Okihashi, and M. Kono, “Mechanical Properties and creep behavior of high strength concrete in aerly age,” *Control Crack. Early Age Concr.*, pp. 265–274, 2002.

[43] H. Mihashi and J. P. D. B. Leite, “State-of-the-Art Report on Control of Cracking in Early Age Concrete,” *J. Adv. Concr. Technol.*, vol. 2, no. 2, pp. 141–154, 2004.

[44] Cusson and Hoogeveen, “Measuring Early Age Coefficient Of Thermal Expansion In High Performance Concrete.pdf,” 2006.

[45] Emanuel and Hulsey, “Prediction Of Thermal Coefficient Of Expansion of Concrete,” 1977.

[46] J. L. Meadows and G. E. Ramey, “Early Age Cracking In Mass Concrete Structures.”

[47] ASTM International, “ASTM C114-10 - Standard Test Methods for Chemical Analysis of Hydraulic Cement,” in *Book of Standards Volume: 04.01*, 2010.

[48] ASTM International, “ASTM C 150/C150M Standard Specification for Portland Cement,” pp. 1–10, 2009.

[49] P. E. Stutzmanl, “Powder Diffraction Analysis of Hydraulic Cements: ASTM Rietveld Round Robin Results on Precision,” *ICDD Adv. X-Ray Anal.*, vol. 48, no. 1, pp. 33–38, 2005.

[50] P. E. Stutzmanl, “Guide for X-Ray Powder Diffraction Analysis of Portland Cement and Clinker,” Gaithersburg, MD, 1996.

[51] Y. Leng, *Materials Characterization: Introduction to Microscopic and Spectroscopic Methods*. Singapore: J. Wiley & Sons, 2008, pp. 45–79.

[52] A. Maqsood and K. Iqbal, “Materials Characterization by Non-Destructive Methods,” *J. Pakistan Mater. Soc.*, vol. 4, no. 1, pp. 31–38, 2010.

[53] ASTM Standard C204 2011, *Standard Test Method for Fineness of Hydraulic Cement by Air Permeability Apparatus*. West Conshohocken, Pa.: ASTM International, 2012.

[54] HORIBA Instruments, *LA-950 Instructional Manual*. Irvine, CA, 2001.

[55] HORIBA Instruments, “A Guidebook to Particle Size Analysis,” 2012. .

[56] “Why Switch from Blaine to PSD?,” *Malvern.com*. .

[57] ASTM International, “Standard Test Method for Density (Specific Gravity), and Absorption of Coarse Aggregate,” *Astm Int. c127-07*, pp. 1–6, 2007.

[58] ASTM International, “Standard Test Method for Density, Relative Density (Specific Gravity), and Absorption of Fine Aggregate,” *Astm Int. c128-07*.

[59] ASTM International, “Standard Practice for Estimating Concrete Strength by the Maturity Method,” *ASTM C 1074-04*, pp. 1–9, 2004.

[60] ASTM International, “Standard Test Method for Time of Setting of Concrete Mixtures by Penetration Resistance,” *ASTM C403-08*, pp. 1–7, 2008.

[61] ASTM International, “Standard Test Method for Temperature of Freshly Mixed Hydraulic-Cement Concrete,” *ASTM C1064-11*, pp. 1–3, 2011.

[62] ASTM International, “Standard Test Method for Slump of Hydraulic-Cement Concrete,” *ASTM C 143-10a*, pp. 1–4, 2010.

[63] ASTM International, “Standard Test Method for Density (Unit Weight), Yield, and Air Content (Gravimetric) of Concrete,” *ASTM C 138-12*, pp. 1–4, 2012.

[64] ASTM International, “Standard Test Method for Air Content of Freshly Mixed Concrete by the Pressure Method,” *ASTM C231-10*, 2010.

[65] ASTM International, “standard specification for compressive strength of cylindrical concrete specimens,” *ASTM C39-12*, pp. 1–7, 2012.

[66] ASTM International, “Standard Test Method for Static Modulus of Elasticity and Poisson’s Ratio of Concrete in Compression1,” *ASTM C 469-10*, pp. 1–5, 2010.

[67] ASTM International, “Standard Practice for Use of Unbonded Caps in Determination of Compressive Strength of Hardened Concrete Cylinders1,” *ASTM C 1231-10a*, pp. 1–5, 2010.

[68] K. A. Riding, J. L. Poole, A. K. Schindler, M. C. G. Juenger, and K. J. Folliard, “Quantification of Effects of Fly Ash Type on Concrete Early-Age Cracking,” no. 105, pp. 149–155, 2009.

[69] K. Riding, *Early age concrete thermal stress measurement and modeling*. ProQuest 2007.

[70] G. Le Saout, V. Kocaba, and K. Scrivener, “Application of Rietveld method to the analysis of anhydrous cement,” *Cem. Concr. Res.*, vol. 2, no. 41, pp. 133–148, 2011.

[71] N. J. Carino and H. S. Lew, “THE MATURITY METHOD : FROM THEORY TO NOTE : The Maturity Method : From Theory to Application 1,” 2001.

[72] J. L. Poole, M. Asce, K. A. Riding, M. C. G. Juenger, K. J. Folliard, and A. K. Schindler, “Effect of Chemical Admixtures on Apparent Activation Energy of Cementitious Systems,” Journal of Materials in Civil Engineering, no. 23. December, pp. 1654–1661, 2011.

[73] Bien-Aime. A., “Effect of cement Chemistry and Properties on Activation Energy,” 2013.

[74] V. M. Sounthararajan and a. Sivakumar, “The Effect of Accelerators and Mix Constituents on the High Early Strength Concrete Properties,” *ISRN Civ. Eng.*, vol. 2012Article ID 103534, pp. 1–7, 2012.

APPENDICES

Appendix A Free Shrinkage Frame

This appendices section will present the construction of the Free Shrinkage Frame as well as the required materials.

A.1 Construction of the Free Shrinkage Frame

There are several different materials required to build a free shrinkage frame and some professional machine shop work will be required. The frame chassis needs to be made from Invar 36 Steel Bars 1-1/2 inch diameter of solid Invar 36 Alloy bar welded together using Invar welding sticks. Approximately 10 lineal feet of solid 1-1/2 inch diameter bar should be purchased. Invar welding rods are to fasten the Invar bars together with welds of the identical material. Approximately 8 square feet of stainless steel plate ¾ inches thick will be needed. Aluminum solid square bar of dimensions 1-1/2 inch x 3/16 inch was used to make small aluminum squares to embed into fresh concrete to give the concrete something to bond to. Sensitive small deformation measuring LCP-8Ts with threaded ends (Linear Current Potentiometers) were used to measure strain from the ends of the concrete frame. Thin 1/8th inch diameter extremely straight Invar rods were used to connect the LCPs to the aluminum plates in the concrete. Two rigid thermocouples approximately 1/8th inch diameter at least 6 inches long are needed to get concrete core temperature. One sheet of ¾ inch plywood was used to build the insulated formwork box exterior. Approximately 2 inch thick dense foam insulation board or similar with an R value of 13 or better. Various copper fittings to make the many turns required to traverse the formwork and 50 feet of ½ inch rigid copper piping type L like that in Figure One sheet of 3 ft x 5 ft 20 gage polished copper plate.

Figure A.1 The copper piping that circulates the coolant fluid. The pipes are numerous and as tight as can be to maximize surface area

A high efficiency heating/cooling circulating bath capable of circulating 50/50 ethylene glycol and water, and capable of accuracy up to 0.1 °C is recommended. Required is : a data logger, capable of collecting data from multiple strain gauges and thermocouples with USB or RS-232 connectivity. Several feet of thermocouple wire and high resolution insulated three strand shielded wire for connecting the LCPs. Adjustable feet for leveling the frame are essential as well. Plastic sheeting is an important consumable component of the free shrinkage frame along with foil tape and silicone. A combination of lubricants can be used to reduce friction, petroleum Jelly and WD-40 have worked best for this project.

A.2 Stainless Steel Fabrication and Assembly

All component of the free shrinkage frame were constructed from Grade 316 stainless steel plates that were 3/4 inch thick. Stainless steel was chosen for its superior corrosion resistance and low expansion. The frame consists of 4 stainless steel plates and 3 alignment brackets for fastening points to the plywood, these components can be seen in Figure A.2. The main component of the frame is the 2 large outside fixed plates fitted with four alignment studs

per side, which allow the smaller inner movable plates to travel back and forth along a fixed linear path with the turn of a screw as seen in Figure A.3.

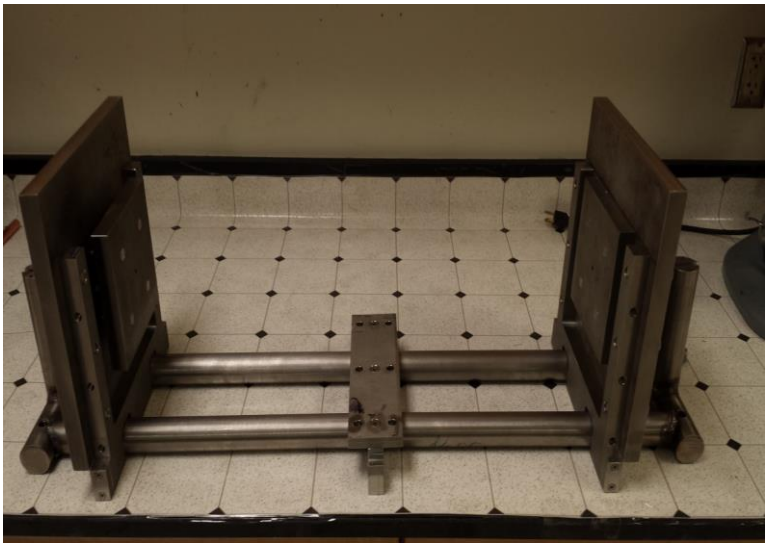

Figure A.2 Invar steel alloy frame rails and stainless steel plate components of free shrinkage frame

The plates are drilled in a manner that allows the movable plates to travel along the same center axis that deformation measurements are taken. The 4 plates are centrally drilled and it is at this location that the connecting rod that is embedded in the concrete passes through the frame and is connected to the LCPs.

Cabinet grade plywood was selected for the construction mostly because it is free of knots and defects which was important for durability. The actual formwork in contact with the concrete is made from a single folded thin copper plate folded and bent using a bending brake. Rigid copper tubing was soldered together to maximize the surface area in contact with the polished copper formwork. Several fittings were used to traverse the formwork. A layout of the copper tubing for the lower half of the box can be seen in Figure A.6.

Figure A.3 Movable 6 inch x 6 inch x ¾ inch thick stainless steel movable plate with bolts that drive the plate in and out for free shrinkage frame

Figure A.4 Image showing the 4 alignment studs

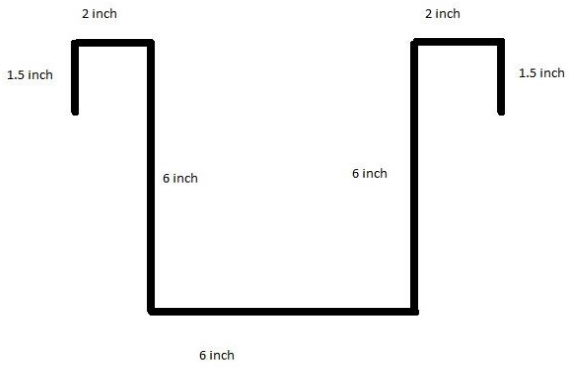

Figure A.5 Thin profile view of what copper plate looks like

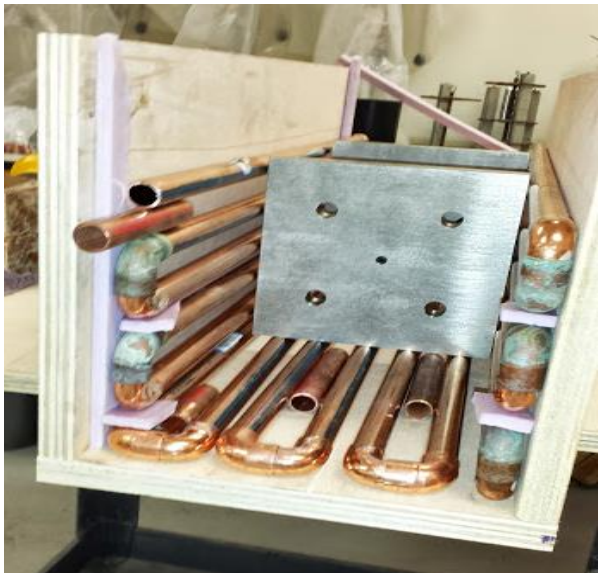

Figure A.6 Copper piping layout before soldering to ensure correct position of pipes relative to the movable plate and sheet copper formwork

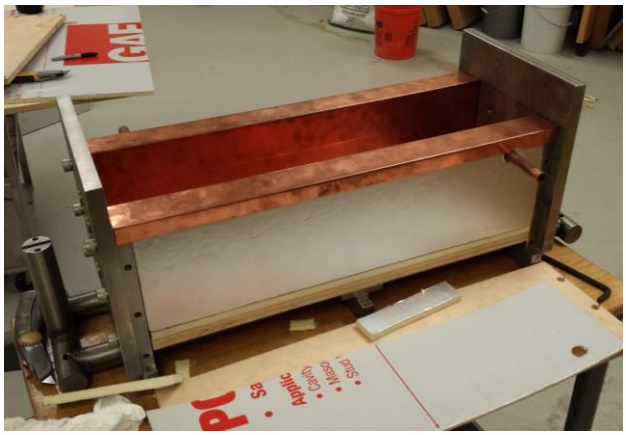

Figure A.7 Copper sheet form work in place on the free shrinkage frame after the ½ inch tubing was installed

Backing the copper plate is the copper tubing which is circulating the fluid that regulates the temperature in the concrete. Copper pipes in the frame are connected to the circulating bath through flexible hoses that connect via quick connect fittings which heats and cools the concrete specimen and is controlled by a computer. The lid to the frame also has the same 2 inch thick insulation and an even tighter arrangement of copper pipes. There is also a polished smooth

copper plate in the lid to more evenly distribute the change in temperature. The lid is pictured in Figure A.8. Buckles were installed on both the top and the bottom of the wooden box so the lid could be snapped onto the bottom box compressing a gasket and sealing the box as seen in Figure A.9.

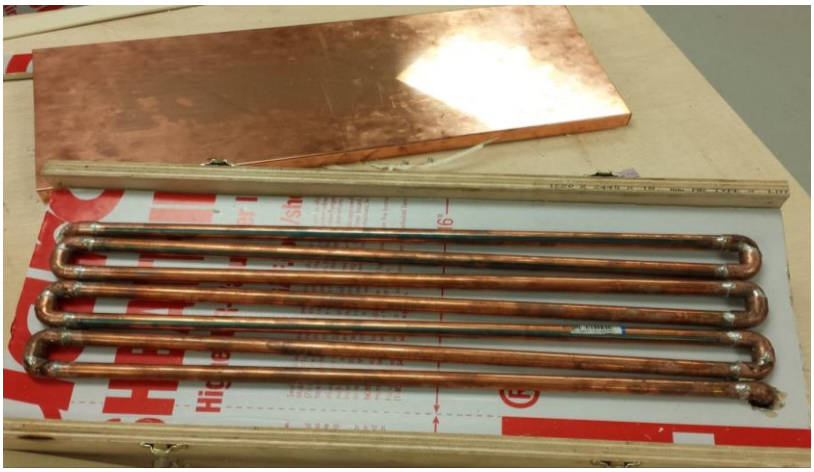

Figure A.8 Pipe layout and copper plate before finalizing the construction of the free shrinkage frame lid

Figure A.9 Finishing touches of the construction of the free shrinkage frame. This includes a drain for easy emptying of the frame and latches for a good seal during operation

Appendix B Rigid Cracking Frame Construction

There are a total of 4 strain gauges oriented at 90 degrees from each other arranged around the circumference of each Invar bar, with 4 rosette gages per side, for taking the strain measurements from both bars to generate an average strain measurement.

The cracking frame was constructed from ½ inch thick steel plates welded together to construct a water chamber. The steel work including tapping and drilling was all prepared by the USF machine shop. The bolts used to assemble the frame connecting the Invar to the cross heads required high torque for tightening and were grade 8 steel bolts and nuts.

Polished copper sheeting was cut and folded to serve as the temperature conducting formwork used to cool and heat the concrete when necessary. The copper was carefully fastened to reduce sharp edges and provide the easiest transition from the steel jaws to the copper plating as seen in Figure B.1.

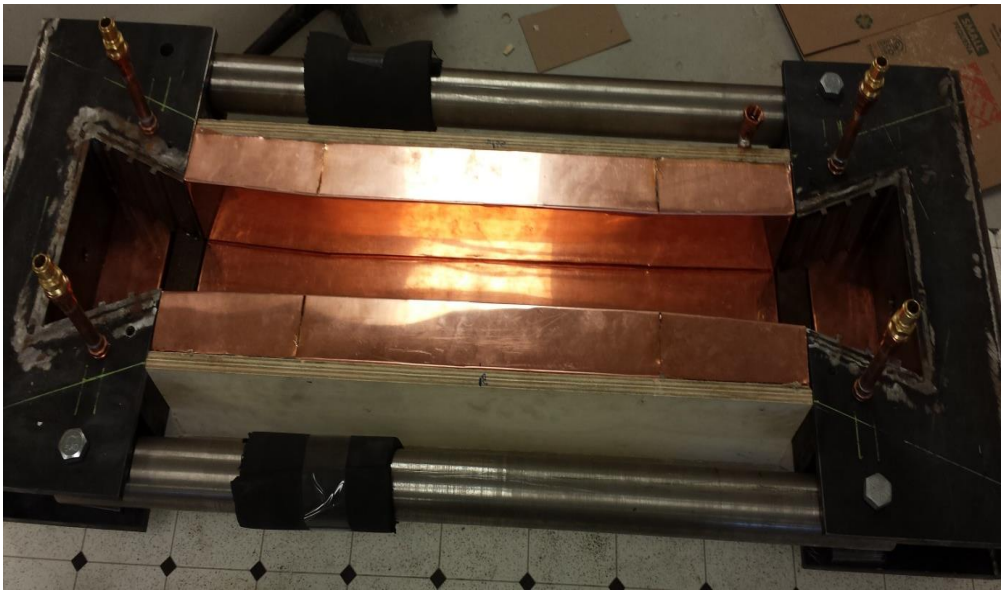

Figure B.1 Cracking frame under construction

Brass hose fittings were utilized to create quick disconnect points in 6 locations of the frame to allow for easier assembly and disassembly. A matrix of copper lines were fabricated and soldered to make the cooling system as efficient as possible. Dense foam boards were used to achieve better than an R-13 insulating value. A circulating bath was used to flow tempered fluid through the form work as pictured in Figure B.3. The exterior box structure was constructed from ¾ inch sanded plywood. There is a drain at the lowest point in the lower box, designed to drain the system between experiments. Plastic sheeting is used to line the formwork for easy form removals. Silicone rubber sealant is used to seal up the frame after the plastic has been placed. The concrete in the frame is also covered with plastic and is sealed up using silicone and tape to create a water proof seal. Attention to detail should be practiced when sealing the frame, it is essential to seal all possible spots where air can be exchanged for a successful experiment.

The frame is designed to have a smaller necked down cross section that has a cross sectional area of 16 square inches which is approximately 4 in x 4 in. The reduction in area is inended to induced cracking in the concrete where cross section is smallest. The concrete does not always crack in this location. When the concrete cracks in other locations it is most likeley from stress concentrations that develop from sharp corners in the frames, the teeth, or the jaws. The teeth can become knicked when removing the concrete from the crossheads between tests. A stong suggestion is to file and smooth the teeth between every test such that burrs can be removed. Careful removal of the last 10 % of concrete from the frame can be the most difficult. Hand tools should be used to get the teeth clean, followed by a metal file and a wire brush. Any bent teeth can be or lead to sources of stress for the concrete. Figure B.2 is a photo of a crack occuring in the center of the frame.

Figure B.2 Close up on the center cracked concrete

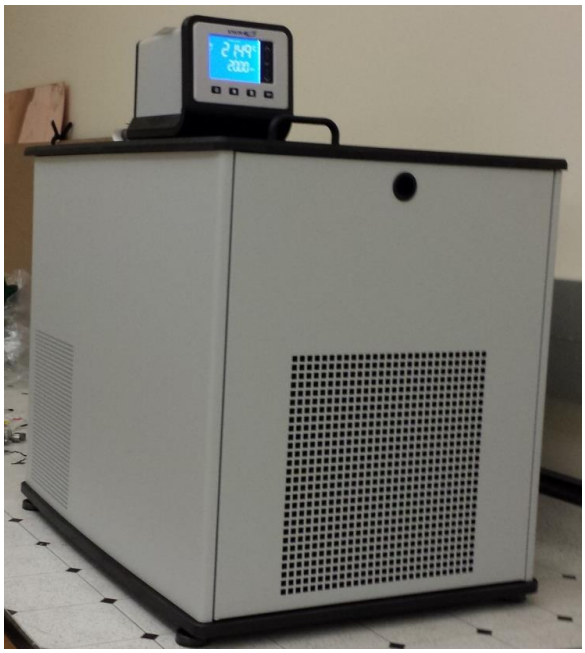

Figure B.3 VWR Circulating bath with advanced digital control head utilized in free shrinkage and rigid cracking frame experiments

Appendix C Cracking Frame Schematics

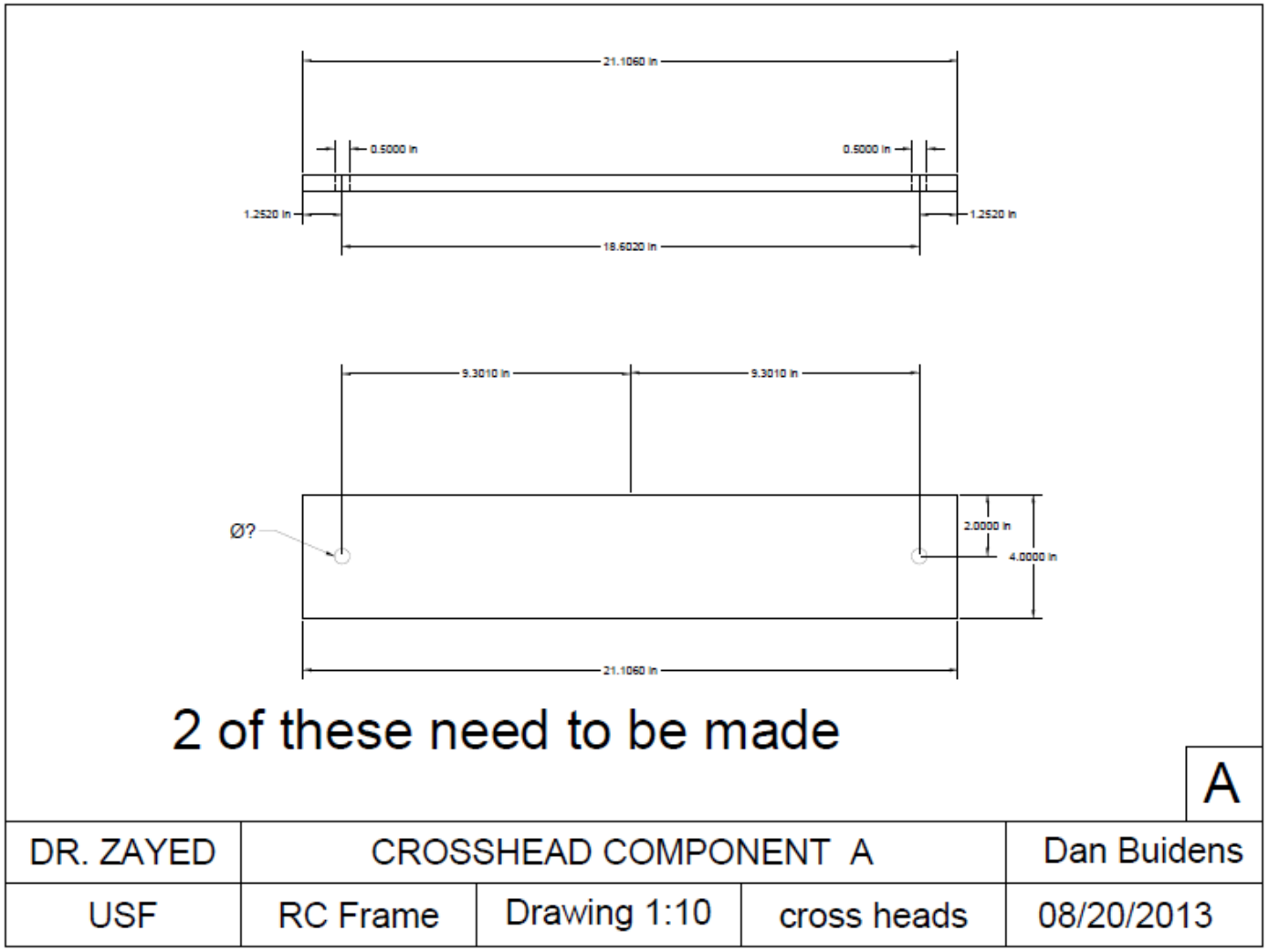

Figure C.1 Shop drawings for cracking frame parts 1:9

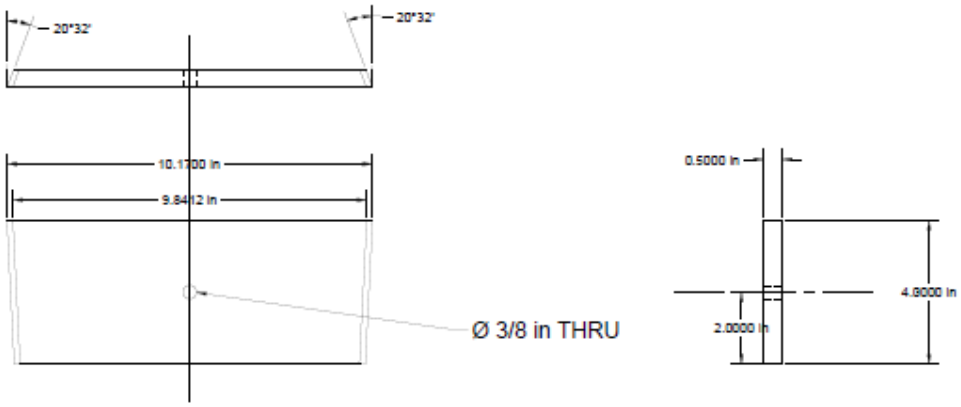

2 of these need
to be made

B

DR. ZAYED	CROSSHEAD COMPONENT B			Dan Buidens
USF	RC Frame	Drawing 2:10	cross heads	08/20/2013

Figure C.2 Shop drawings for cracking frame parts 2:9

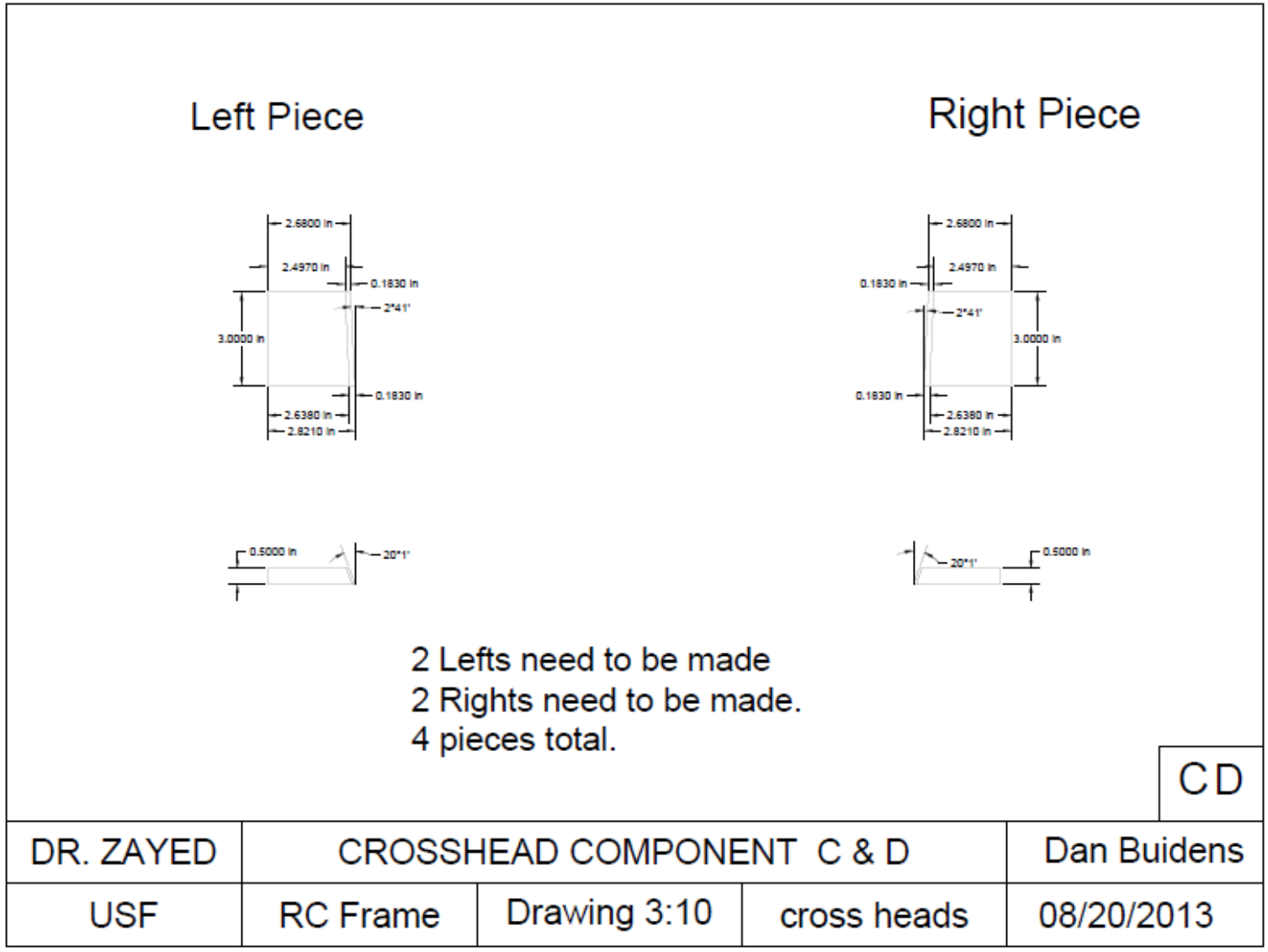

Figure C.3 Shop drawings for cracking frame parts 3:9

4 of these need to be made.

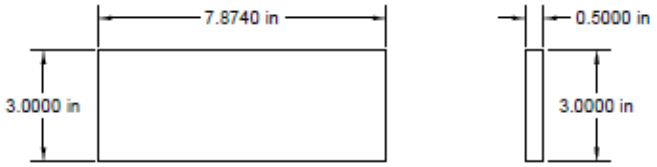

E

DR. ZAYED	CROSSHEAD COMPONENT E			Dan Buidens
USF	RC Frame	Drawing 4:10	cross heads	08/20/2013

Figure C.4 Shop drawings for cracking frame parts 4:9

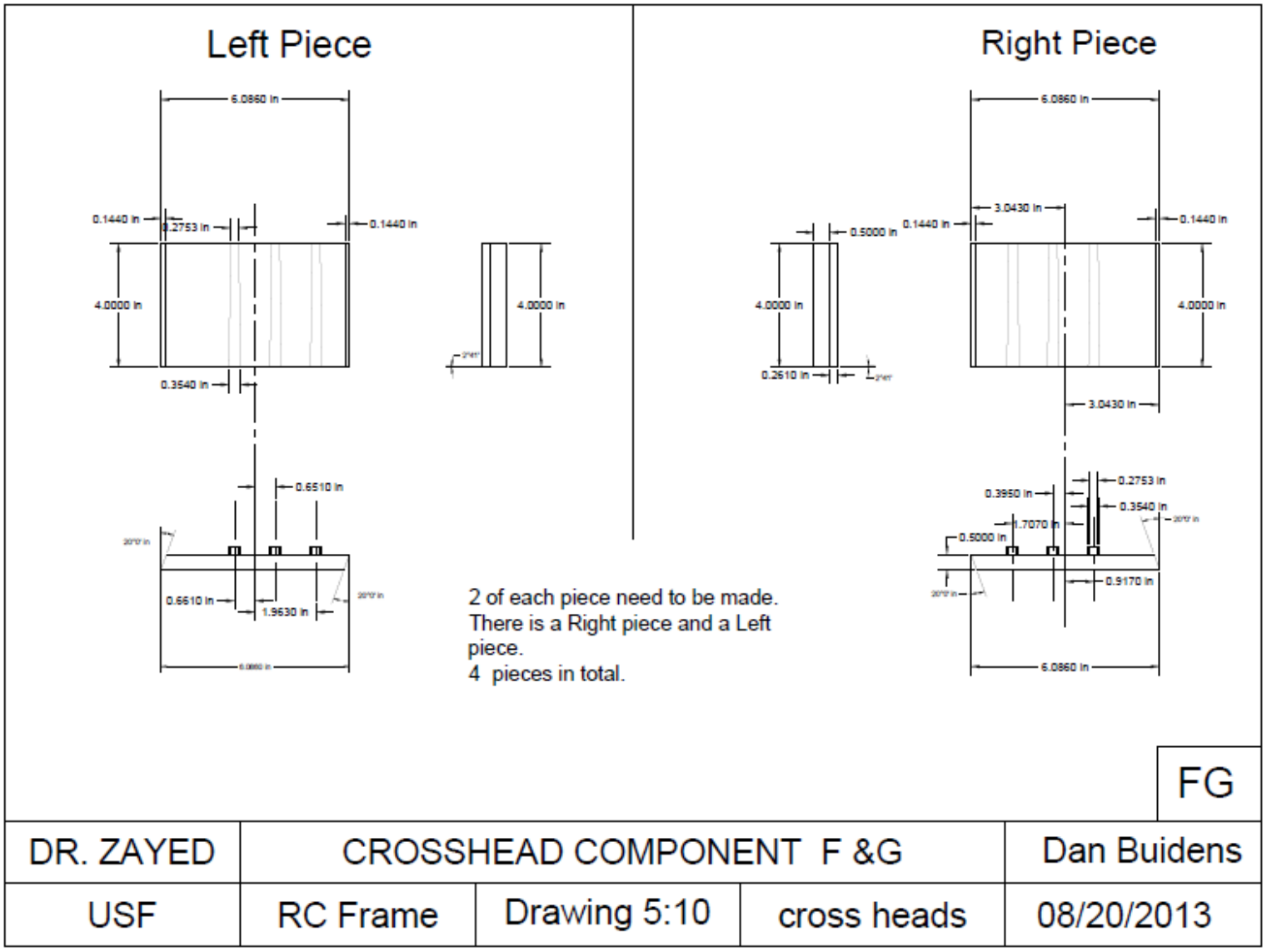

Figure C.5 Shop drawings for cracking frame parts 5:9

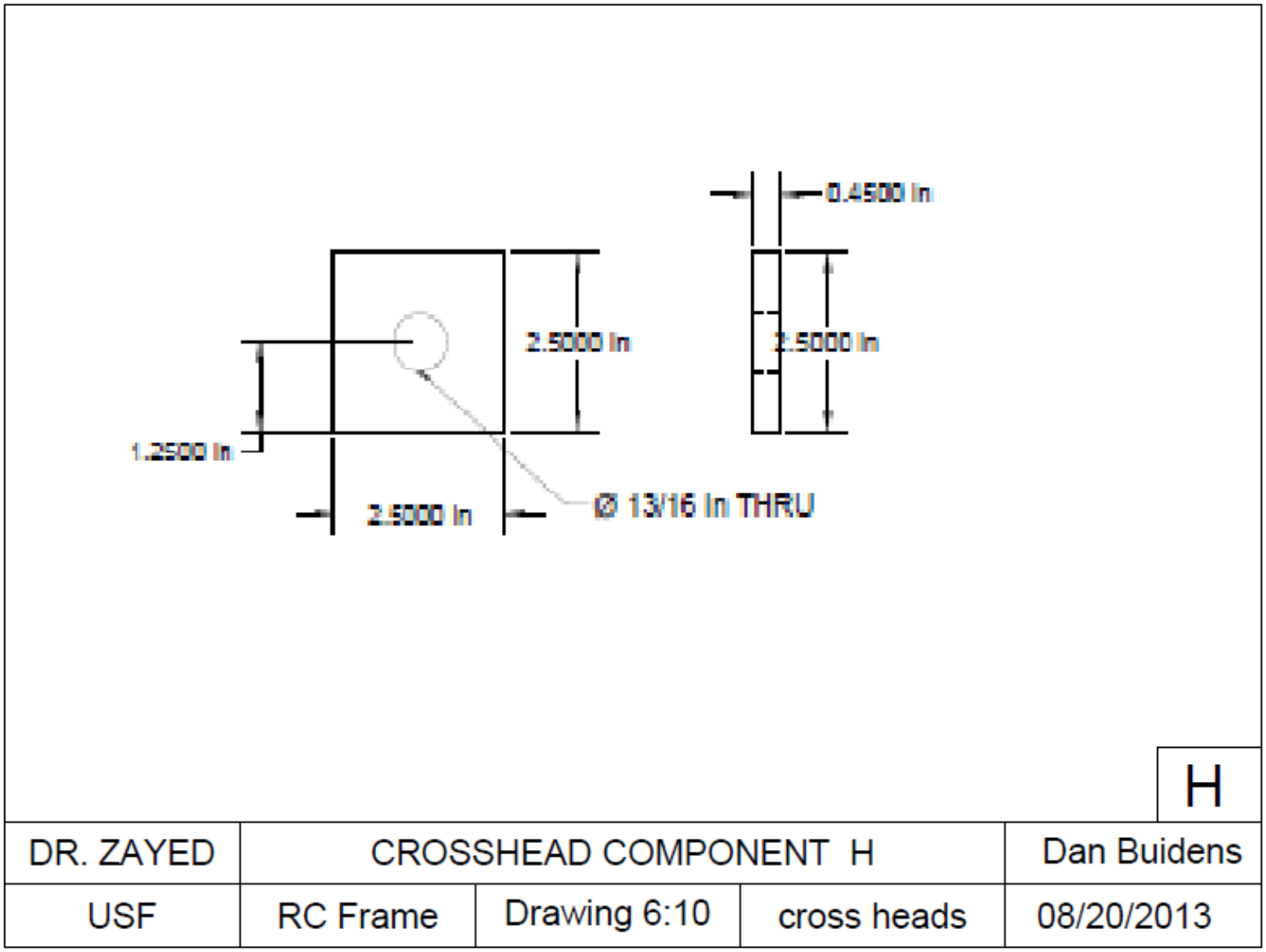

Figure C.6 Shop drawings for cracking frame parts 6:9

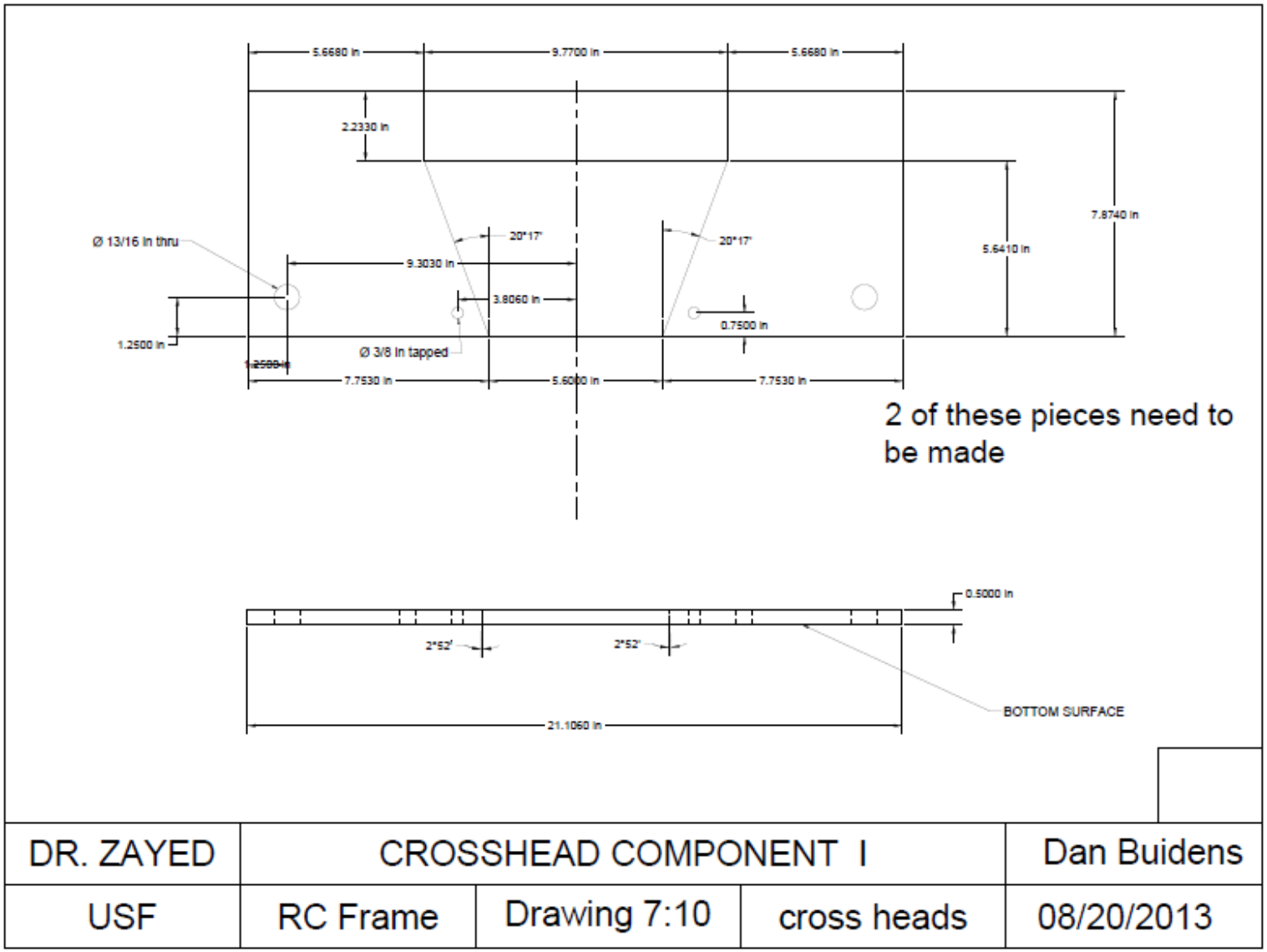

Figure C.7 Shop drawings for cracking frame parts 7:9

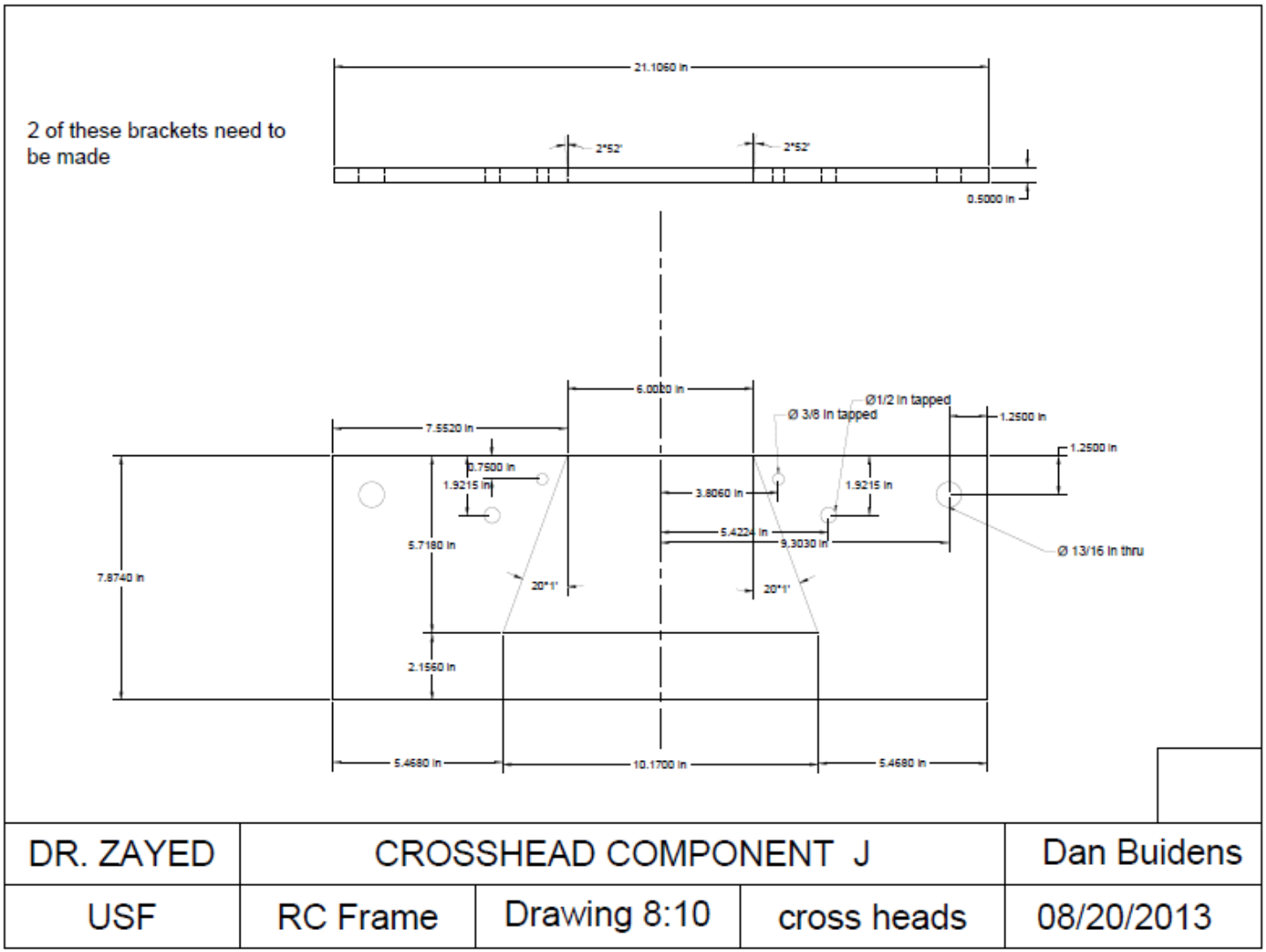

Figure C.8 Shop drawings for cracking frame parts 8:9

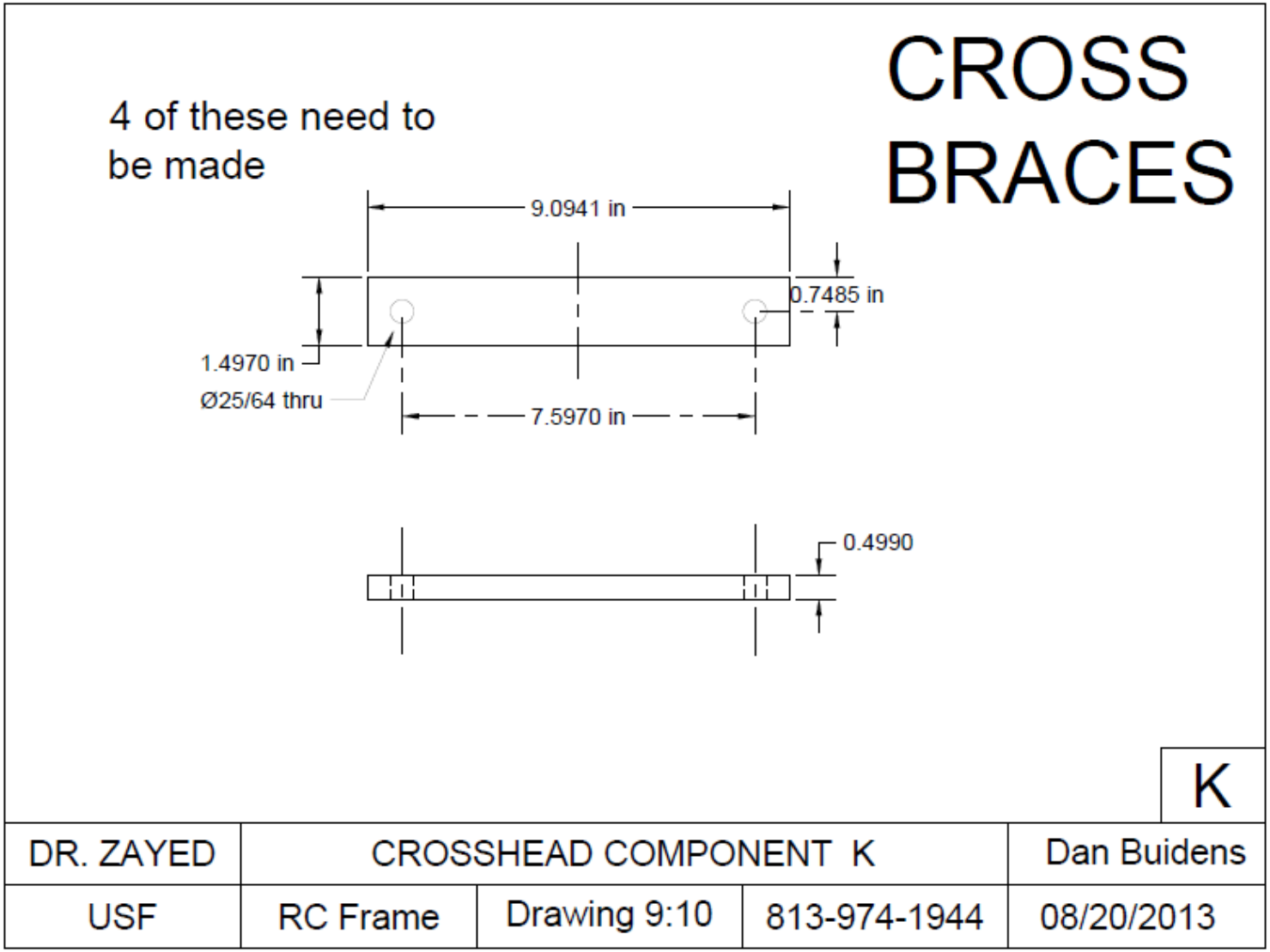

Figure C.9 Shop drawings for cracking frame parts 9:9

Appendix D Hyperbolic and Exponential Plots, Apparent Activation Energy

The following plots were used to determine the apparent activation energy by plotting the natural log of the k value against the reciprocal of the absolute temperature in Kelvin.

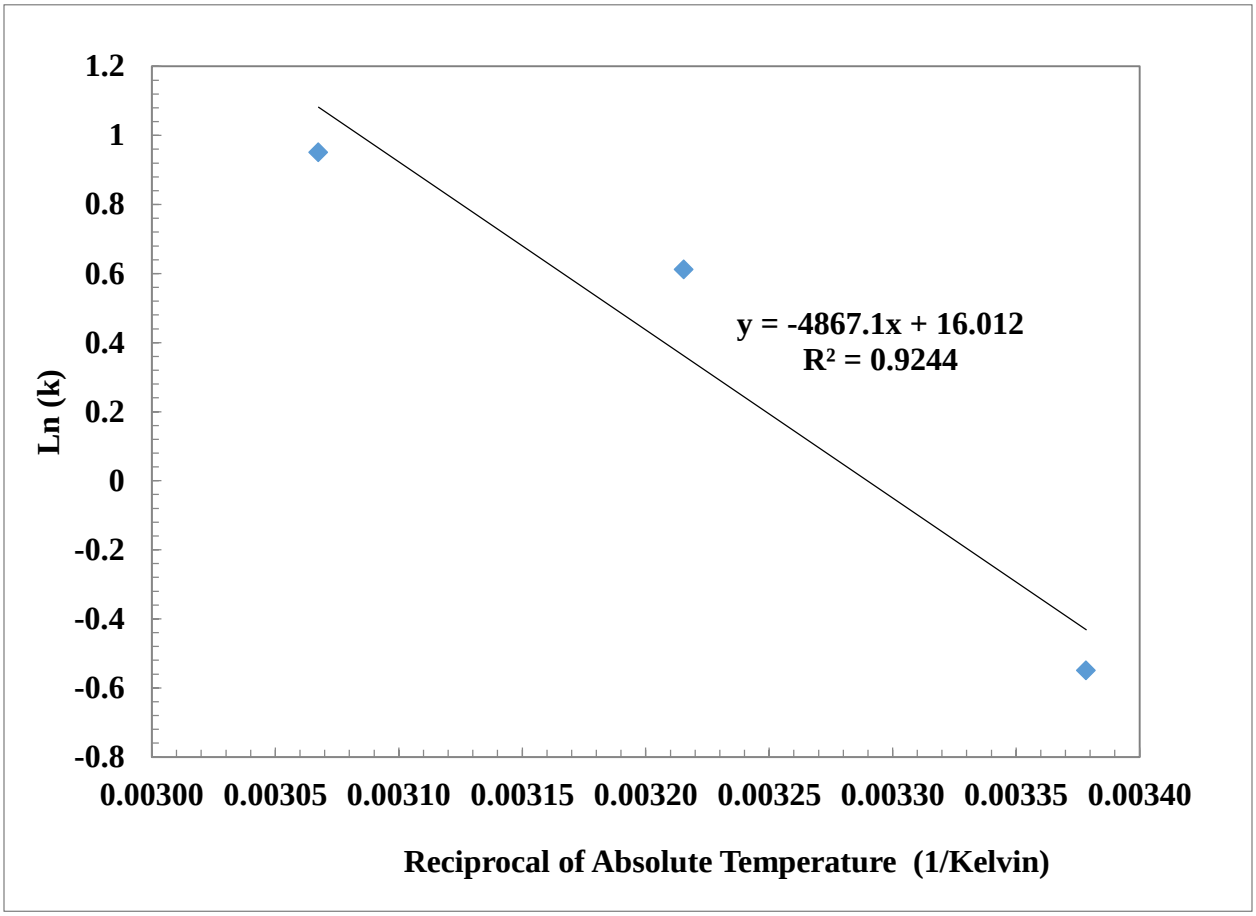

Figure D.1 Plot of k values versus temperature for hyperbolic function for C mortar cubes at 23°C, 38°C, and 53°C isothermal curing

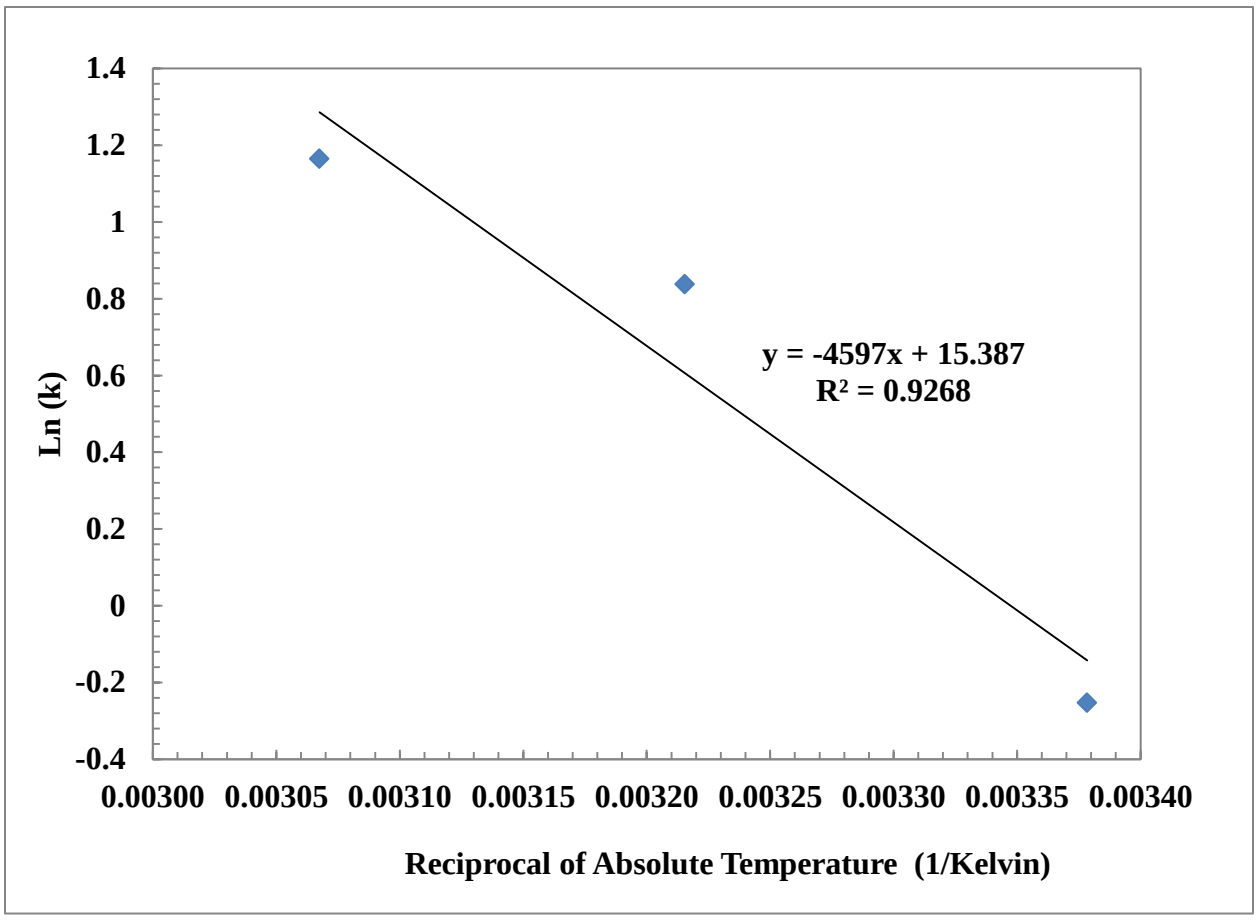

Figure D.2 Plot of k values versus temperature for the exponential function for C mortar cubes at 23°C, 38°C, and 53°C isothermal curing

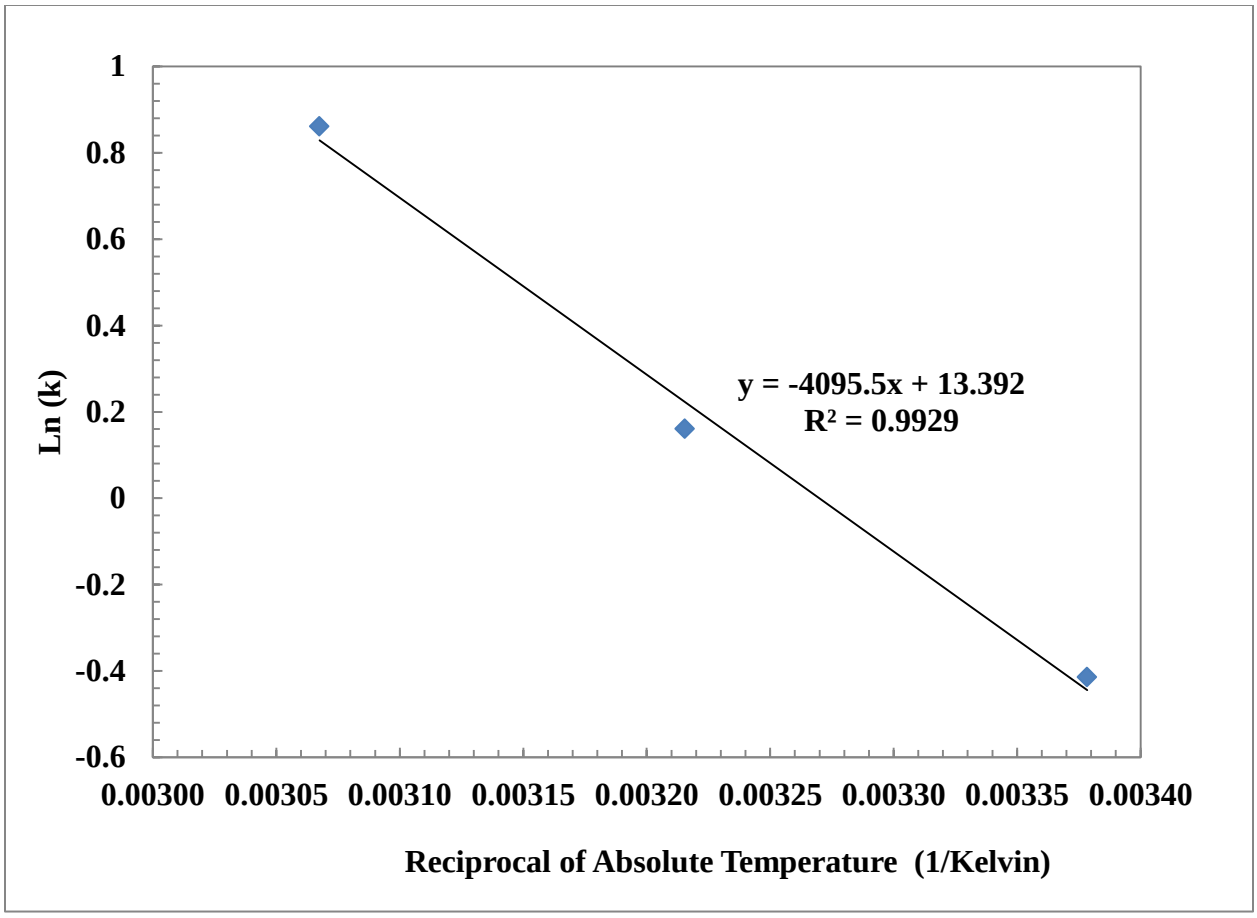

Figure D.3 Plot of k values versus temperature for hyperbolic function for CNA mortar cubes at 23°C, 38°C, and 53°C isothermal curing

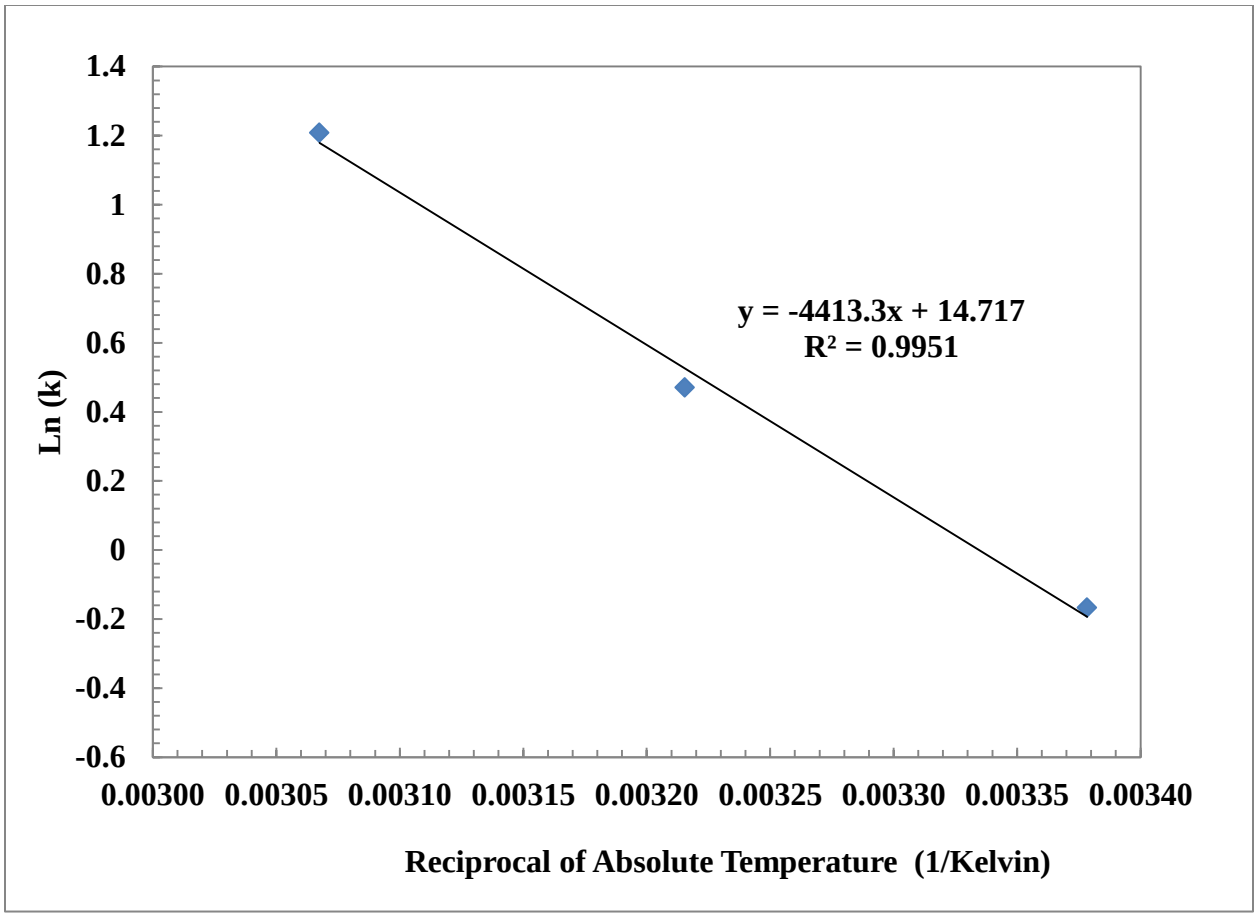

Figure D.4 Plot of k values versus temperature for exponential function for CNA mortar cubes at 23°C, 38°C, and 53°C isothermal curing

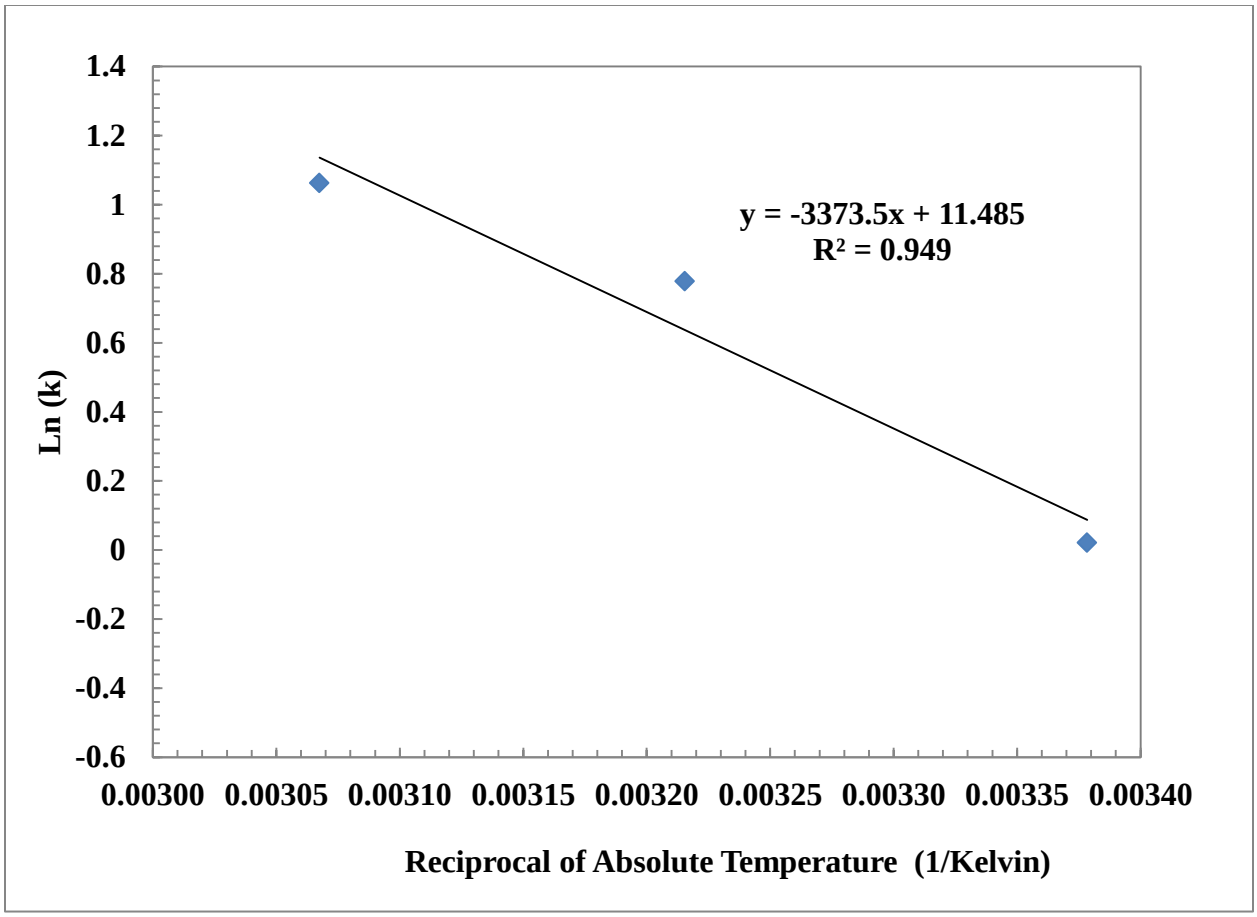

Figure D.5 Plot of k values versus temperature for hyperbolic function for CHA mortar cubes at 23°C, 38°C, and 53°C isothermal curing

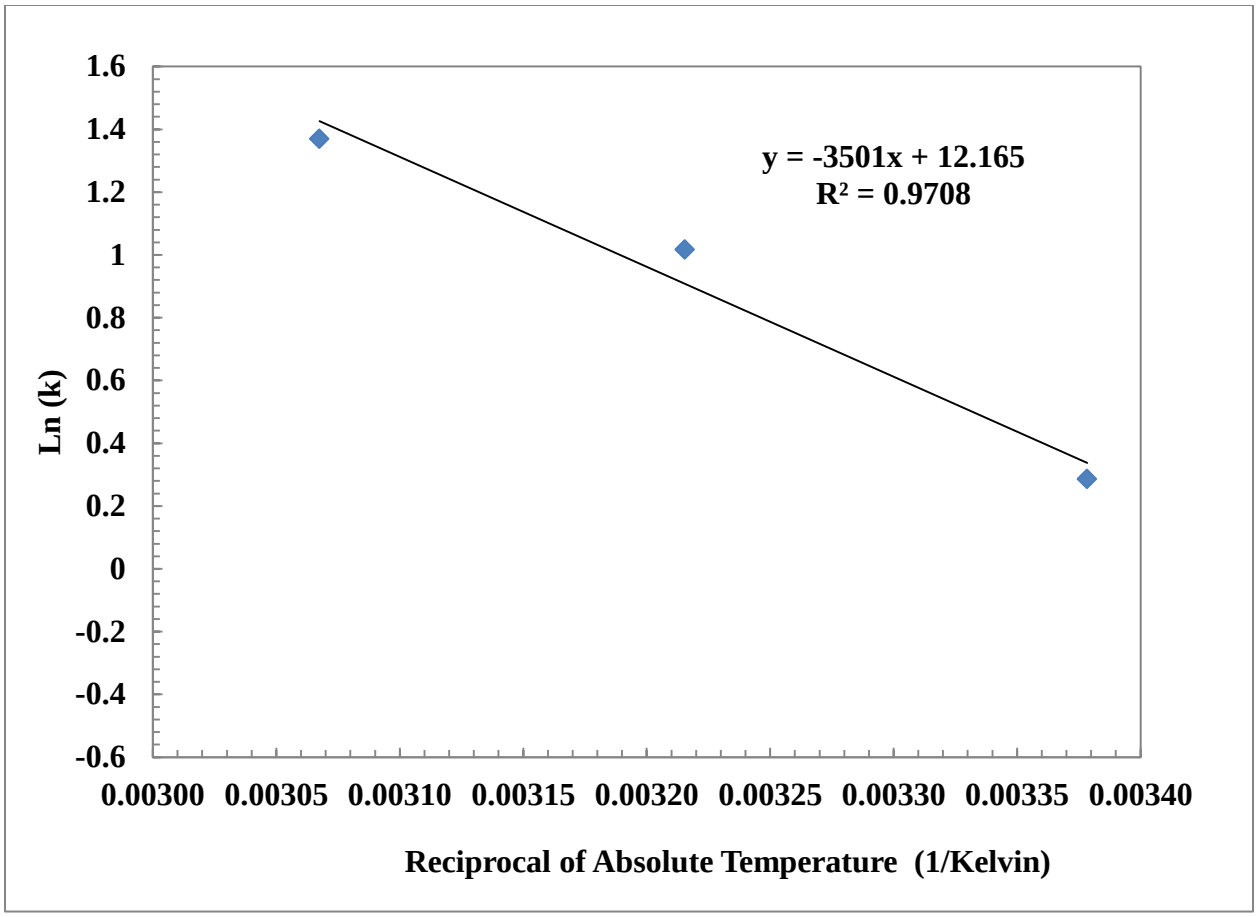

Figure D.6 Plot of k values versus temperature for the exponential function for CHA mortar cubes at 23°C, 38°C, and 53°C isothermal curing

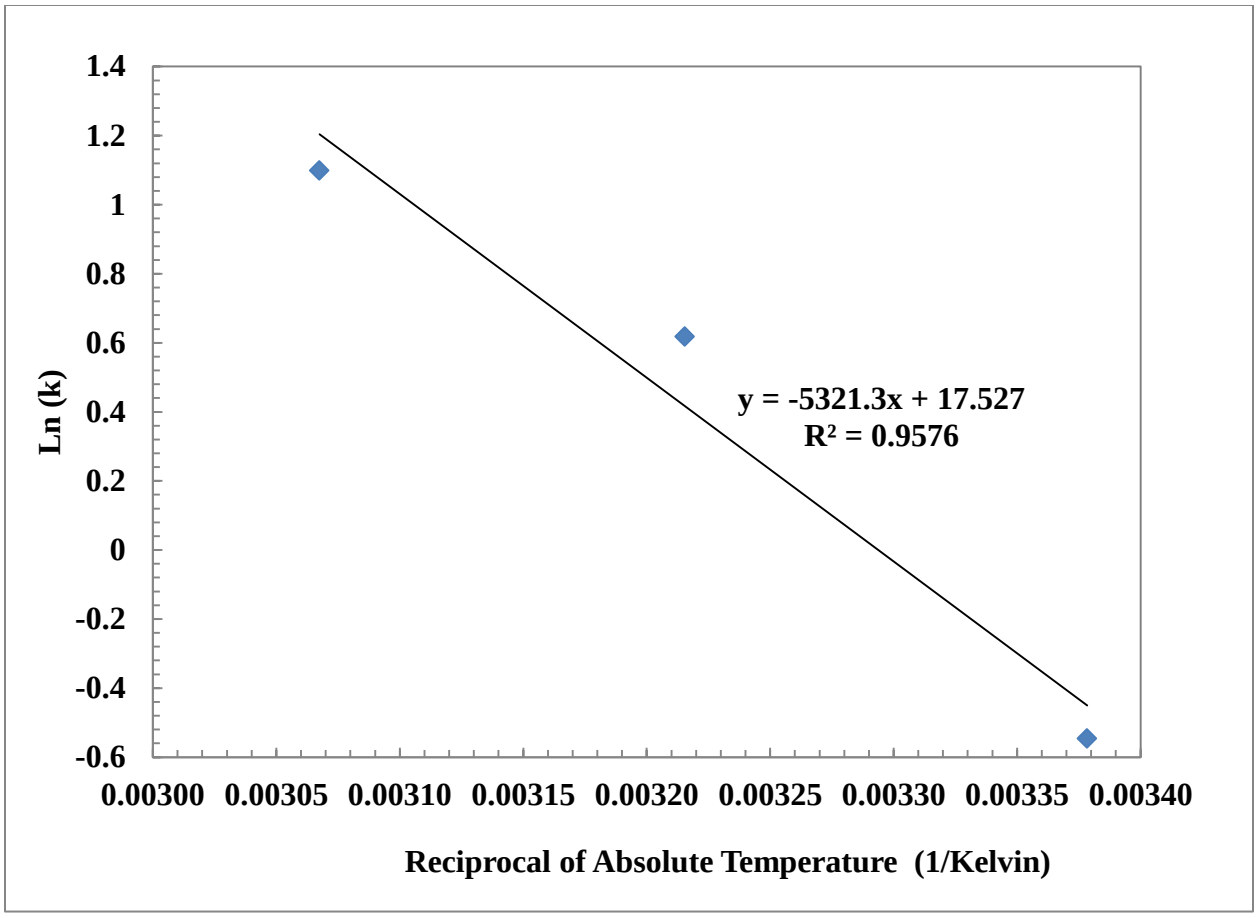

Figure D.7 Plot of k values versus temperature for hyperbolic function for CA mortar cubes at 23°C, 38°C, and 53°C isothermal curing

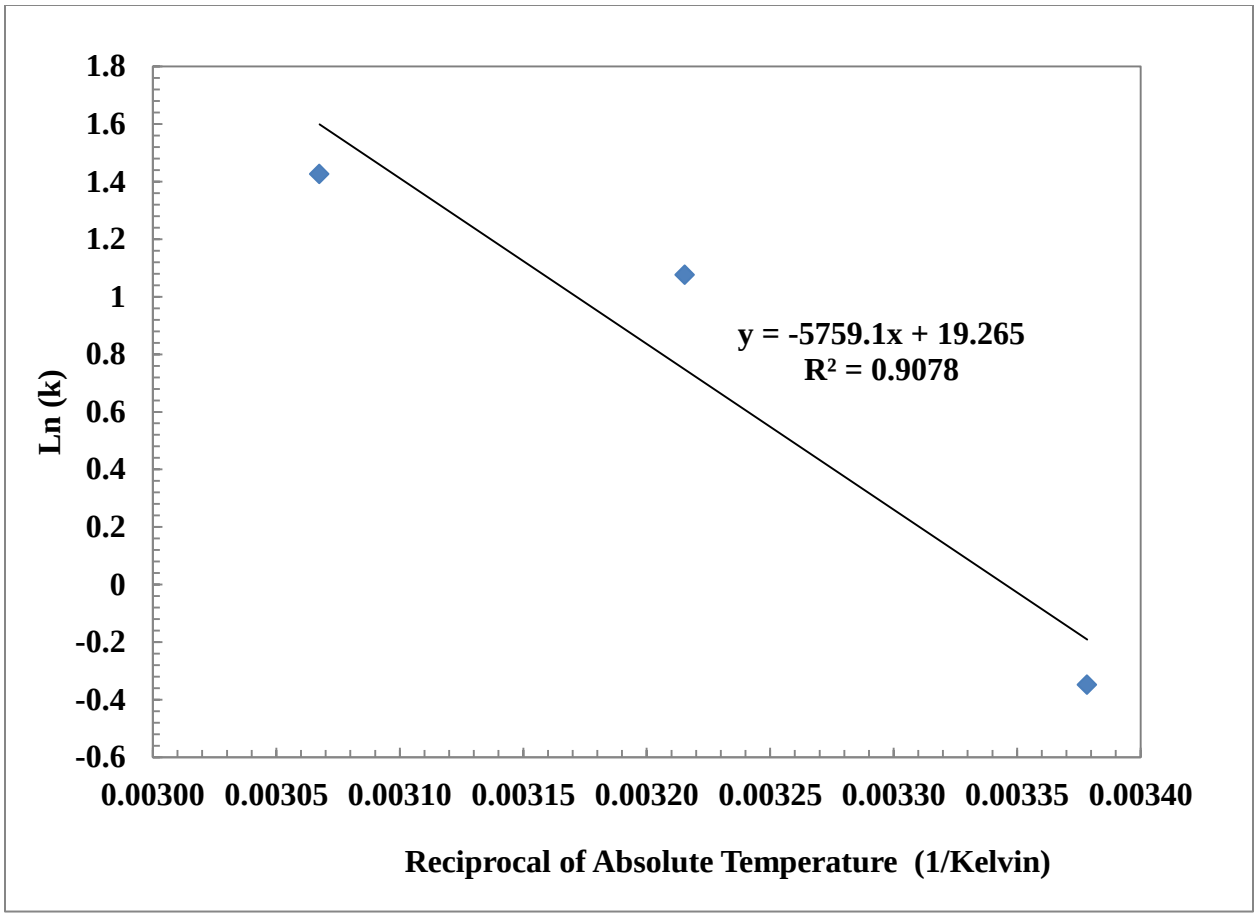

Figure D.8 Plot of k values versus temperature for exponential function for C mortar cubes at 23°C, 38°C, and 53°C isothermal curing